NTNU
Norwegian University of
Science and Technology

Modeling and validation of passive techniques for stabilizing indoor environment in buildings

A case study of the Viking Ship Museum in
Norway

Stian Wirak

Civil and Environmental Engineering
Submission date: June 2018
Supervisor: Mohamed Hamdy Hassan Mohamed, IBM

Norwegian University of Science and Technology
Department of Civil and Environmental Engineering

NORWEGIAN UNITVERSITY OF SCIENCE AND TECHNOLOGY
DEPARTMENT OF CIVIL AND ENVIRONMENTAL ENGINEERING

Report Title:	Date: 07.06.2018		
Modeling and validation of passive techniques for stabilizing indoor environment in buildings - A case study of the Viking Ship Museum in Norway.	Number of pages (incl. appendicies): **114**		
	Master Thesis	**X**	Project work
Name: Stian Wirak			
Professor in charge/supervisor: Mohamed Hamdy			
Other external professional contacts/supervisors: Stig Geving			

Abstract:
This thesis investigates how Phase Change Material (PCM) and moisture buffering can stabilize the indoor environment by using a case study of the new Viking Ship museum in Norway.

The simulations have been carried out in IDA ICE, and the models for simulating PCM (i.e. PCM model) and moisture buffering (i.e. HMwall model) have first been tested. The HMwall model was found to only be valid when simulating concrete and has not been used in the case study. The PCM model was found valid and has been implemented in the case study.

The case study of PCM showed that temperature fluctuations could be reduced by 2.56%. The highest reduction of energy consumption was found to be 0.27% and the reduction of peak energy demand for fuel heating to be 0.26%.

The main reason for such low effect from PCM is that the PCM was implemented at the surfaces of a heavy weight building with high thermal mass. Due to low thermal conductivity in the PCMs, the energy was not absorbed and released fast enough to affect the indoor environment significantly. The highest measured change in enthalpy for the PCMs during 24 hours was found to be about 29 kJ/kg, which is about 16% of the potential of 183 kJ/kg.

Keywords:

| 1. Validation |
| 2. Passive stabilization of indoor environment |
| 3. IDA ICE |
| 4. Building performance simulation |

Stian Wirak

Preface

This thesis marks the finish of five years of studying at NTNU. The journey has been long, interesting, valuable, fun and exhausting. It has been five years consisting of a master's degree, two kids, an own company and three different jobs. Early in the study program, I realized I wanted to focus on energy and building physics. This thesis sums up a lot of the knowledge I have gained throughout the last five years. I am looking forward to closing this chapter in life and start on the next one.

I want to thank several persons for helping me through all these years, and most of all my wife, Mia Julie, and two kids, Pernille and Annika. I also want to thank my father and grandfather for encourage me to follow their footsteps in building engineering.

During my master thesis, I have received a lot of help from several persons. I want to thank professor Mohamed Hamdy for being my supervisor, for discussions, for encourage me, challenge me and help me through the semester. I want to thank professor Stig Geving for keeping his door open, helping me and show that he believes in me both through the study and at work at Sweco. Thank you Sweco for giving me the flexibility at work so I could focus on my thesis when I had to. Professor Arild Gustavsen, professor Bjørn Petter Jelle, Rebecca Lundqvist, Tor Atle Skramdal, Gaurav Chaudhary and Rickard Tällberg deserves to be mentioned as they have helped me through discussions and by sharing information. I want to thank NTNU for sponsor a course in IDA-ICE in Stockholm and Patrik Skogqvist at EQUA for helping me with understanding IDA-ICE and to reply to all my emails. Finally, I want to thank Henrik Kyte Assmann for proofreading this thesis.

Trondheim, 07.06.2018

Stian Wirak

Summary

This thesis investigates how Phase Change Material (PCM) and moisture buffering can stabilize the indoor environment by using a case study of the new Viking Ship museum at Bygdøy outside of Oslo. The museum stores a cultural heritage that is well preserved and needs to be taken care of in the new museum as well. Fluctuations of temperature and relative humidity can damage the artifacts, so the indoor environment needs to be planned carefully. PCM is a technology which uses latent heat (melting and solidifies) to store and release energy and can therefore be used to stabilize the fluctuations of temperature within the building. Moisture buffering is a phenomenon where materials absorb and release humidity from the surrounding air. Moisture buffering can therefore be used to stabilize the fluctuations of relative humidity within the building. Three research questions have been formulated for this thesis:

1. Does IDA ICE provide valid models for simulating the effects of moisture buffering and PCM?

2. Can moisture buffering and PCM improve the indoor environment in the Viking Ship Museum?

3. Can moisture buffering and PCM reduce the total energy consumption and peak energy demands for HVAC in the Viking Ship Museum?

IDA ICE by EQUA AB was selected as the simulation tool and EQUA provided models for both simulating PCM (i.e. PCM model) and moisture buffering (i.e. HMwall model). The validity of both these models has been tested in this thesis, in addition to a review on validation done by others. The PCM model was found to be valid, while the HMwall model was found to have limitations in the validity. The validation tests show that the HMwall model has limitations when simulating other materials than concrete (e.g. insulation). The HMwall model was therefore found not valid to simulate moisture buffering in the case study.

The case study has been divided in a single zone case study and a whole building case study. The single zone case study investigates how PCM can affect the indoor environment in one of the exhibition rooms and the HVAC systems was made constant to isolate the effect from PCM. Seven different PCMs were implemented and evaluated. The results from a simulated week in the summer showed that when PCM was implemented internally on the surface of the concrete, the average mean air temperature decreased with about 1°C, but the temperature fluctuations increased.

The whole building case study was in difference to the single zone case study im-

plemented with sensor-controlled HVAC systems. Two different PCMs were implemented into one of the exhibition rooms, and the stabilization effect on the indoor environment, along with the energy consumption and peak energy demand, was investigated. The results showed that by implementing PCM, the energy consumption for HVAC could be reduced with 0.27% and the peak energy demand for fuel heating by 0.26%. The highest reduction of temperature fluctuations was found in the summer simulation, where one of the PCMs managed to reduce the Temperature Stabilization index (TS) by 2.56%.

The main reason for such low effect from PCM is that the PCM was implemented in a concrete building with high thermal mass and the implementation reduced the exposed surfaces of concrete. In addition, the thermal conductivity of PCM is low compared to concrete, which implies that concrete manages to store and release heat to the indoor environment faster than PCM. The PCMs were found to only use an average of about 6% of the potential daily energy storage. The results showed that only about 11 kJ/kg was stored or released as an average during 24 hours, while the implemented PCMs had a potential of storing or releasing 183 kJ/kg. The highest change in enthalpy during 24 hours was found to be about 29 kJ/kg, which is 16% of the potential of the implemented PCMs.

Sammendrag

Denne masteroppgaven tar for seg hvordan faseendringsmaterialer (PCM) og fuktbufring kan stabilisere inneklimaet i det nye Vikingskipshuset på Bygdøy utenfor Oslo. Museet inneholder en kulturarv som er godt bevart og som må bevares i det nye museet som skal bygges. Svingninger i relativ fuktighet og temperatur kan skade gjenstandene, så inneklimaet må planlegges nøye. PCM er en teknologi som bruker latent varme (den smelter og fryser) for å absorbere og avgi energi. PCM kan derfor benyttes for å stabilisere svingningene i temperatur inne i bygget. Fuktbufring er et fenomen hvor materialer absorberer og avgir fukt til lufta rundt. Fuktbufring kan derfor benyttes for å stabilisere svingningene av relativ fuktighet inne i museet. Tre forskningsspørsmål har blitt formulert:

1. Har IDA ICE valide modeller for å simulere effekten av fuktbufring og PCM?

2. Kan fuktbufring og PCM forbedre inneklimaet i Vikingskipshuset?

3. Kan fuktbufring og PCM redusere energiforbruket og effektbehovet for ventilasjon, varme og kjøling i Vikingskipshuset?

IDA ICE, av EQUA AB, ble valgt som simuleringsverktøy for denne masteroppgaven. EQUA hadde modeller for å både simulere fuktbufring (HMwall modell) og PCM (PCM modell). Validiteten til begge disse modellene har blitt testet i denne masteroppgaven, i tillegg til at valideringer gjort av andre er presentert. PCM modellen ble funnet å være valid, mens HMwall modellen ble funnet å ha begrensninger i validiteten. Valideringen viste at HMwall modellen hadde begrensinger når andre materialer enn betong ble simulert. HMwall modellen ble, grunnet den begrensede validitien, ikke benyttet til å simulere fuktbufringen i Vikingskipshuset.

Dette casestudiet tar for seg både en modell av en enkelt sone, og en modell av hele bygget. Enkeltsonemodellen tar for seg hvordan PCM can påvirke inneklimaet ved å bli implementert i et av utstillingsrommene. I denne modellen er ventilasjon, varme og kjøling gjort konstante slik at det eneste som påvirker inneklimaet er implementeringen av PCM. Totalt ble det simulert syv ulike PCM materialer og simuleringen tok for seg en uke på sommeren. Resultatet viste at implementeringen av PCM reduserte den gjennomsnitlige lufttemperaturen med 1°C, men det økte temperatursvingningene.

Modellen av hele bygget hadde i motsetning til enkeltsonemodellen ventilasjon, varme og kjøling som var sensor-styrt og to ulike PCM materialer ble simulert i ett av utstillingsrommene. Denne modellen gav resultater for inneklimaet, energiforbruket og effektbehov. Resultatet viste at implementeringen av PCM kunne

redusere energiforbruket til ventilasjon, varme og kjøling med 0.27% og effektbehovet for varme med 0.26%. Her ble det også funnet en reduksjon av svingningene i temperaturen (TS) med 2.56%.

Hovedårsaken til at implementeringen av PCM gav så liten effekt er at det ble lagt inn på overflaten av veggene i et betongbygg med høy termisk masse. Implementeringen meførte da mindre eksponert betong som har god varmelagring. I tillegg er den termiske konduktiviteten til PCM lav sammenlignet med betong. Dette medfører at betong klarer å absorbere varme og energi raskere fra omgivelsene, sammenlignet med PCM. Fra en årssimuleringen ble det funnet at entalpiendringen i PCM materialet i løpet av 24 timer hadde et gjennomsnitt på 11 kJ/kg, noe som kun er rundt 6% potensialet til PCM materialet som har en latent varmelagring på 183 kJ/kg. Den høyeste entalpiendringen i løpet av 24 timer ble funnet å være omtrent 29 kJ/kg, noe som utgjør 16% av potensialet.

Abbreviation

Abbreviation	Explanation
CAV	Constant Air Volume
EMPD	Effective Moisture Penetration Depth
HVAC	Heating, Ventilation and Air Conditioning
PCM	Phase Change Material
MBV	Moisture Buffer Value
NRMSE	Normalized Root Mean Square Error
RH	Relative Humidity
RHS	Relative Humidity Stabilization index
RMSE	Root Mean Square Error
STB	Solar Test Boxes
TS	Temperature Stabilization index
VAV	Variable Air Volume

Contents

List of Figures

xiii

List of Tables

1 — Introduction

1.1 Background

Building designs are getting more complex every year due to an increased demand to fulfill environmental, social and economically requirements. The European Union (EU) committed in 2009 to limit the rise in the average global temperature, compared to pre-industrial level, to 2°C (Eurostat, 2017). By the Paris Agreement, this commitment was strengthened to a limitation of 1.5°C, and by the Europe 2020 strategy three objectives was formed (European Commission, 2014):

- Reducing GHG (greenhouse gas) emissions by at least 20% compared with 1990 levels

- Increasing the share of renewable energy in final energy consumption to 20%

- Moving towards a 20% increase in energy efficiency

According to OECD/IEA (2015), 53% of all electricity consumption, and 32% of all energy consumption was consumed by buildings globally in 2012. About 38% of the global buildings energy consumption was for heating, cooling and lighting, and the development is according to OECD/IEA (2015) evaluated to be "not on track" in order to limit the temperature rise as committed in the Paris Agreement.

In combination with these increased demands concerning energy consumption, the demands to fulfill strict indoor environmentally requirements also increase. The indoor environment is dependent on several parameters and Bluyssen (2009) relates the parameters into four basic factors; thermal comfort, lighting quality, acoustical quality and air quality, as shown in figure 1.1. For this thesis, only air quality and thermal comfort are relevant. Thermal comfort is defined as *"the condition of mind which expresses satisfaction with the surrounding thermal environment"* (ASHRAE, 2017), and the most well-known parameter for thermal comfort is the mean air temperature, or the operative temperature.

In addition to the requirements from the human beings in the building, some building categories also have demands regarding the objects within the building, the usage of the building or the building body in itself. One of these building categories are museums, where the work against degradation of the artifacts have a great focus.
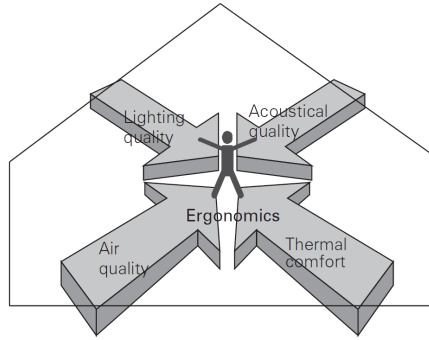
Figure 1.1: Environmental factors that affect the indoor environment (Bluyssen, 2009)

ASHRAE Technical Committee 9.8 et al. (2010) describes a total of eight threats to collections, which can be listed in in a decreasing order of seriousness:

- Light

- **Relative humidity**

- **Temperature**

- Air pollution

- **Pest infestation**

- Shock and vibration

- Natural emergencies

- Theft, vandalism and misplacing objects

The bold threats are the ones that are relevant for this thesis. Even though pest infestation is dependent on RH and temperature, it is listed as a separate threat due to the fact that objects can be damaged by RH and temperature without pest infestation. Fluctuation of RH and temperature can make material both shrink and stiffen, and needs to be taken into consideration (ASHRAE Technical Committee 9.8 et al., 2010). Thomson (1986) implies that several substances (such as wood) contracts and are likely to warp and split due to low moisture content. Many other organic products (such as paper, leather, etc.) are easier to break with a lower moisture content, due to a decrease in their flexibility. Thomson (1986) concludes that the RH should not be allowed to drop below 40%, but preferably stay above 45% in order to prevent physical damages. These physical damages are less likely to occur in very humid conditions, but it is in a humid environment mould and fungi occur. According to Geving (2017), there are four main conditions for biological activity which can lead to pest infestation: nutrition, moisture, temperature and

time (see figure 1.2). As both time and nutrition (e.g. wood) usually are present in a museum, the moisture content and the temperature are the two main factors that can be affected and controlled in order to prevent degradation.
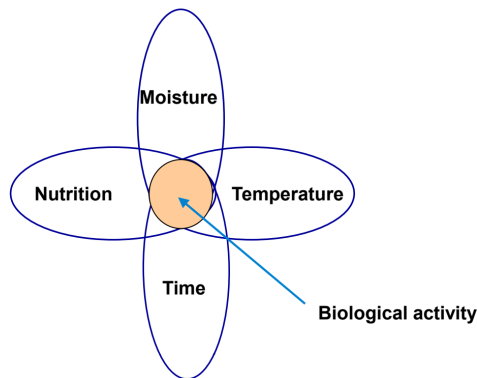
Figure 1.2: Necessary conditions for biological activity (Geving, 2017)

There are numerous different mold species that can occur under the right conditions, and some of them are shown in figure 1.3. The figure shows that mold can occur in quite a large temperature range, and that the optimum temperature for most of the species lies in the temperature range that is expected to be found within a building.
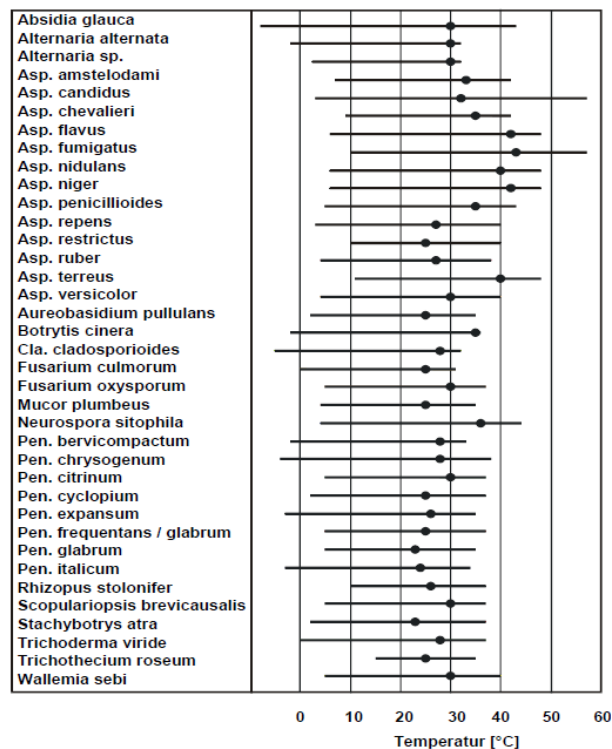
Figure 1.3: Optimum temperature and temperature range for growth of different mold species (Geving, 2017)

When looking closer into one of the species, an isopleth diagram can be made to show the necessary conditions for mold to grow. An isopleth diagram for one of the

species (Aspergillus restrictus) is shown in figure 1.4. The diagram to the left show the amount of days it takes for the specie to start to grow under certain conditions, and the diagram to the right shows how fast the mold grows (in mm each day) after the germination. As seen in the figures, RH above 70% in normal indoor temperature makes foundation for mold growth. The limit at about 70% is also the same limit Thomson (1986) suggest for a museum in order to prevent mould growth. Thomson (1986) implies that the danger occurs above 70% RH and suggests putting the upper limit to 65% RH.
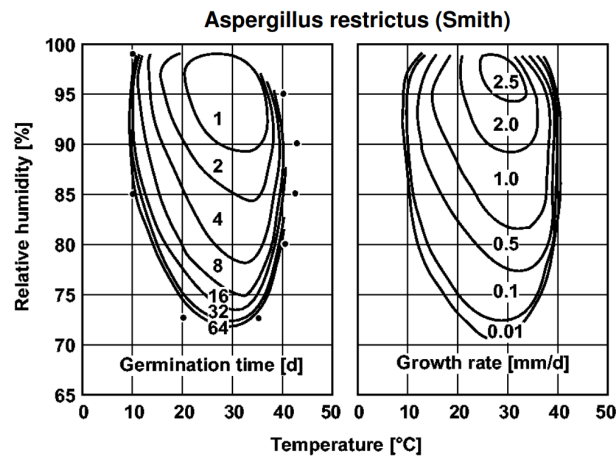
Figure 1.4: Development of Aspergillus restrictus related to RH and time (Krus and Sedlbauer, 2008)

The indoor temperature and RH are highly connected to the outdoor conditions, in addition to indoor heating, cooling and moisture gain. SINTEF Byggforsk (2005) has published some figures to illustrate this in Norwegian climate, which can be seen in figure 1.5. Figure 1.5a shows that the outdoor RH in general is around 70-80%, while the indoor RH varies during the year. The fluctuations of the RH indoor (fig 1.5b) are due to the cold winters in Norway. The cold winter air has a low water content, and when this air ventilated into the building and heated up, the relative humidity gets low. This phenomenon occurs as warm air can store more water than cold air, which makes RH dependent om both water content and temperature. For instance, air at 25°C can store a water content of 23.04 g/m^3 at 100% RH, while air at 0°C only stores $4.84g/m^3$ at 100% RH (Thue, 2014). Figure 1.5b shows that the RH indoor can exceed 80% with a relative high moisture gain during the summer, and the RH can be below 20% during the winter with low moisture gain.

The relation between RH and temperature makes it important to plan for both factors before the construction of a building takes place. If the temperature turns out to be lower than planned for, a result could be a higher RH than planned for. The stabilization of the indoor environment within the Viking Ship Museum in Oslo
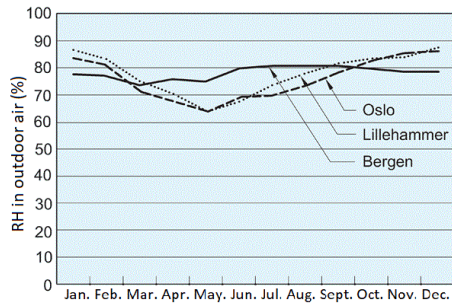
(a) Monthly average RH in the outdoor
air for three different cities in Norway
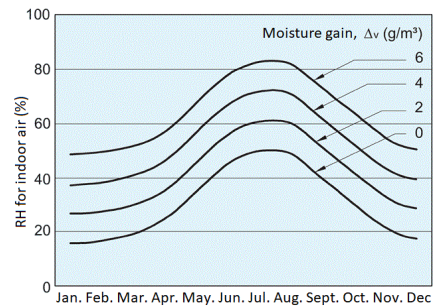
(b) Monthly average RH indoor (at
21°C) in Trondheim, Norway

Figure 1.5: Monthly average values for indoor and outdoor RH in Norway
(SINTEF Byggforsk, 2005)

is the background for this thesis.

1.2   The Viking Ship Museum

The Viking Ship Museum at Bygdøy, outside of Oslo in Norway, is used as a case
study for this thesis. The first wing of the museum was finished in 1926 and two
more were added in 1932 (UiO, n.d.[a]). The last wing of the museum was finished
in 1957, and the result can be seen in figure 1.6. In 2016, the museum had a
total amount of 510 139 visitors, and it stores 2 268 306 different historical objects
according to UiO (n.d.[b]).
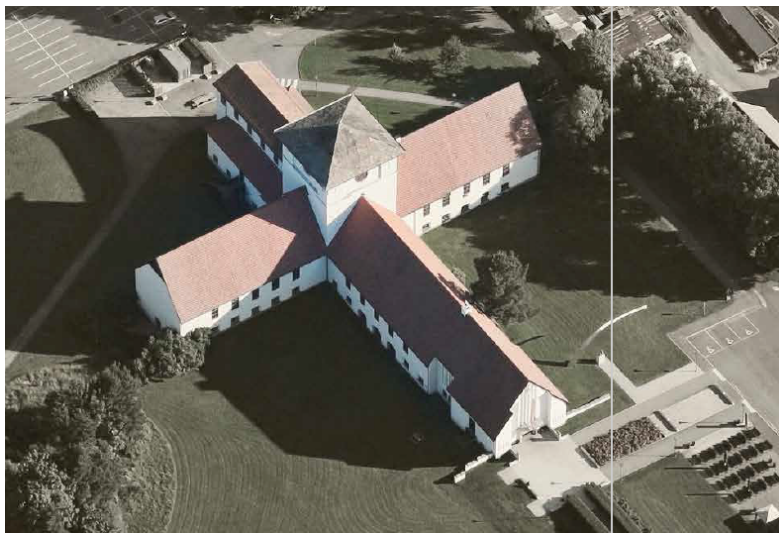
Figure 1.6: Illustration of the existing Viking Ship Museum (UiO, n.d.[c])

Within the collections, the museum stores three different Viking ships. The world's
best preserved Viking ship, "Gokstad", the first excavated Viking ship, "Tune", and

5

a Viking ship with exceptional woodwork, "Oseberg", are among the artifacts in the museum and can be seen in figure 1.7 (UiO, n.d.[c]).

<div align="center">

(a) The "Gokstad" ship   (b) The "Tune" ship   (c) The "Oseberg" ship

Figure 1.7: Images of the three Viking ships stores at the Viking Ship Museum (UiO, n.d.[c])

</div>

In 2015 there was held an architectural competition to design a new concept for the Viking Ship Museum. AART architects was announced the winner, and Hjellnes Consult AS was selected as the consultants for the project (Statsbygg, n.d.). The construction of the new Viking Ship Museum is planned to start in year 2020 and to be finished around 2022/2023 (Statsbygg, 2017). The new design for the building can be seen in figure 1.8.

<div align="center">

Figure 1.8: Overview of the design of the new Viking Ship Museum (Statsbygg, n.d.)

</div>

As the museum stores a cultural heritage that is well preserved, the indoor environment needs to be planned for carefully. The indoor environment needs to satisfy the employees and visitors, the artifacts in the museum needs to be preserved, while the energy demand needs to be as low as possible.

During the autumn semester of 2017, Rebecca Celine Lundqvist was engaged by Hjellnes Consult to investigate how to stabilize the indoor environment in the Viking Ship Museum (Lundqvist, 2018). She received files used in the project and made a model in IDA-ICE in order to simulate the indoor environment. Hjellnes Consult informed that the early stage estimations of the museums ventilation system resulted in a high ventilation rate and large systems. The indoor environment can theoretically be stabilized by using a large and powerful ventilation system, but this requires a lot of energy. There was a need for other techniques in order to handle the fluctuations of temperature and RH in the museum.

1.3   Literature Review

Both the indoor temperature and RH are expected to have both seasonal and daily fluctuations. By choosing materials for the building carefully, it is possible to damp these fluctuations passively. Passive implies that it does not need to be controlled or need energy to function. All buildings store some heat and moisture whether it is planned for or not, but in many cases, it can be hard to take into account in the design phase. During this literature review, both moisture buffering and PCM has been studied, and the findings will be presented in this chapter.

1.3.1   Moisture buffering

Fluctuations of the relative humidity can, as mentioned in the introduction, affect both the building and what is inside the building in several ways. For buildings with no specific need for humidity-control, the indoor relative humidity is often a direct result of the outdoor conditions, the HVAC systems, along with the internal moisture production. Some building categories, such as museums, have the need for additional measures in order to keep the humidity at an acceptable level. By using building materials that absorb moisture from the surrounding air, the fluctuations in RH can be reduced. This concept is called moisture buffering and will be presented in this chapter.

Calculation techniques

Materials can absorb humidity and water in several different ways. The absorption of water as liquid (e.g. contact with a water pool) will not be presented in this thesis, as it is the water storage of moisture from humid air that is relevant for

the museum. The amount of moisture absorbed in a material, based on the RH in the surrounding air, can be presented as a sorption isotherm, as in figure 1.9. The figures illustrate the theory that with an increased RH in the surrounding air, the water content in the material increases (i.e. the material absorb moisture from the air). Both figure 1.9a and 1.9b show that the relationship between RH and water content is different if the RH is increasing or decreasing. This phenomenon is called hysteresis and shows that the water content before the change in RH has influence on the equlibrium. Thue (2014) states that this effect could occur because the water during absorption needs to "push away" oxygen and nitrogen molecules that are bound to the surfaces in the material, which requires energy. Both at low and high humidity, the water content increases quite fast compared to the gradient at RH around 50%. Thue (2014) describes the phenomenon to occur due to strong forces in a dry material, and due to capillary suction when the RH is high. Thue (2014) points out that the curves are representative up to about 98% RH, and that the capillary suction will dominate when the RF goes beyond this limit.

(a) Concrete with $\rho = 1830 kg/m^3$ (b) Mineral wool with $\rho = 18 kg/m^3$
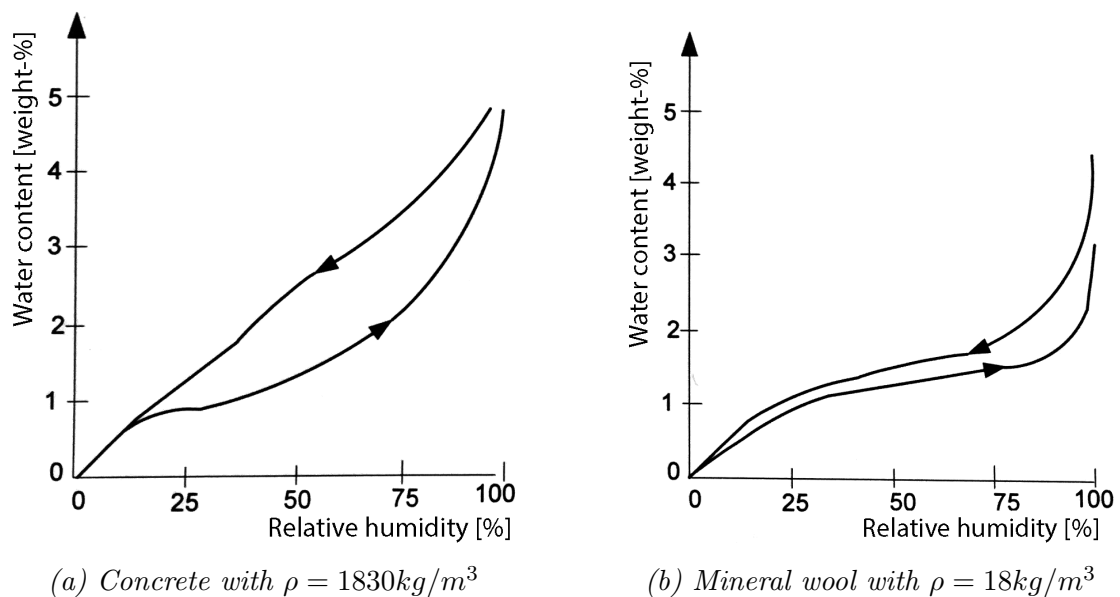
Figure 1.9: Sorption isotherms for concrete and mineral wool, freely translated from Thue (2014)

The heat and moisture transfer through a multi-layer building envelope in steady-state conditions can easily be calculated by the Glaser method, which is described in EN ISO 13788 (Standard Norge, 2012). However, the calculation in a non-steady environment can be severe. Künzel (1995) developed a method to calculate both one and two-dimensional heat and moisture transport. One of the objects was to be able to make accurate calculations by using simple parameters. Even though the calculations had to neglect some effects (e.g. gravity), the results have been used in a great extent by other researchers. The findings have also been used in

the development of EN 15026 (Standard Norge, 2007), which is highly referred to and has a benchmark test for simulation tools. The object of this thesis is not to validate or develop these equations further, so one should look to Künzel (1995) or EN ISO 13788 to see further information about the equations.

In addition to the equations used for calculating the moisture transfer, there have also been several studies on how to define the moisture buffer properties. In 2003 there was a workshop seminar at the Technical University of Denmark arranged by NORDTEST, attracting 30 academics and some manufactures and consultants. One of the activities of the workshop was the following:

- *To establish a robust **definition** of the moisture buffer property of materials and material systems used in the indoor environment.* (Rode et al., 2005)

In difference to Künzel (1995), the process was more practical and not only directed against the simulation of the materials. Rode et al. (2005) describes the moisture buffer phenomena with a scheme as shown in figure 1.10.
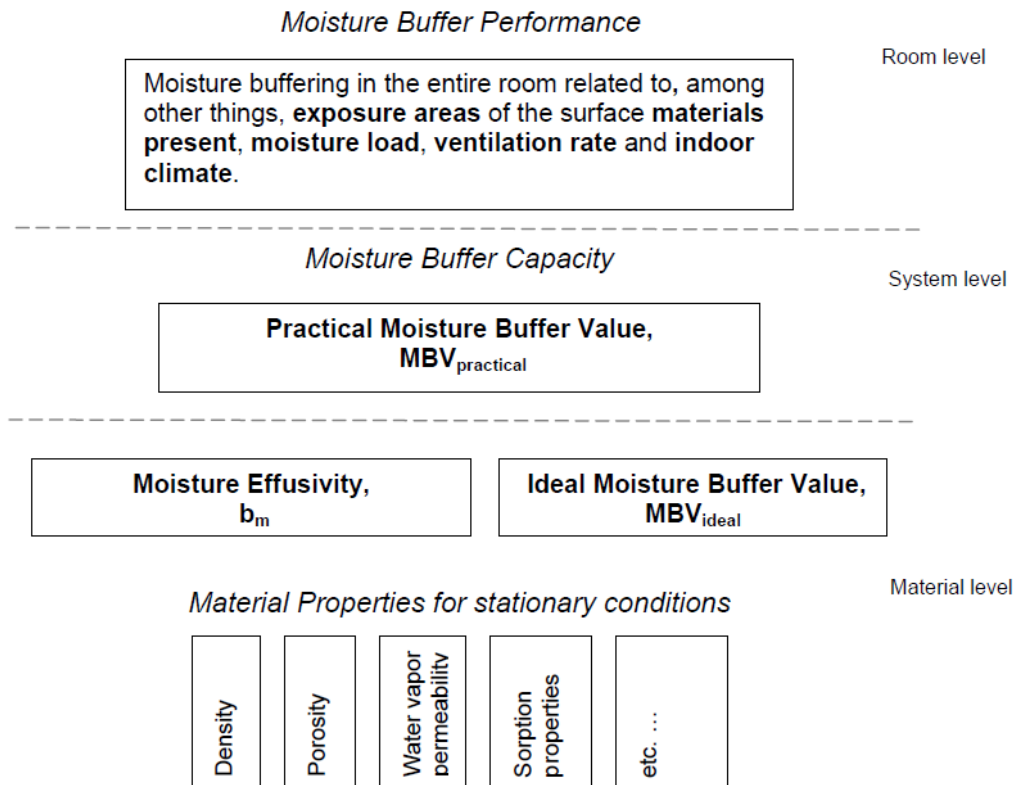
Figure 1.10: Moisture buffer phenomena definition scheme for three descriptive levels (Rode et al., 2005)

At the material level in figure 1.10 the properties of the materials are defined. These parameters are used to define the moisture effusivity (b_m) and the ideal moisture buffer value (MBV_{ideal}). The moisture effusivity is a theoretical value to express in

9

which rate a material absorb moisture by an increased surface humidity. The theory is based upon the analogy of thermal effusivity.

An issue for the quantification of MBV both by calculations and by simulation is that material parameters need to be implemented. These parameters (e.g. vapor permeability) are tested under various conditions, and often under steady state conditions, according to Rode et al. (2005). Some of these parameters are not constant in all conditions, and as a result, there can be uncertainties in the input values.

The MBV_{ideal} only includes the material parameters and can be calculated theoretically. The $MBV_{practical}$ on the other hand includes the air film resistance, the thickness of the material and surface coatings, so Rode et al. (2005) turn to experimental set-up for calculating this value. The $MBV_{practical}$ of eight different materials can be seen in figure 1.11. The thin vertical lines in the figure show the standard deviations of the tests. The figure shows that concrete has the lowest $MBV_{practical}$ of all the tested materials, while spruce board has the highest value.
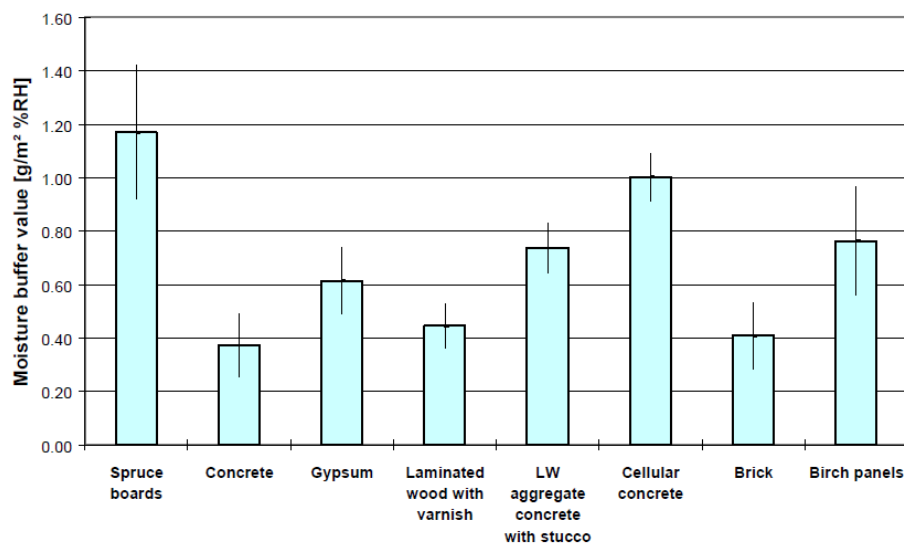
Figure 1.11: Calculated average MBV$_{practical}$ for eight different materials (Rode et al., 2005)

Even though the MBV_{ideal} describes much of the moisture buffering potential of the material, it is also important to evaluate the penetration depth. The MBV_{ideal} will not be representative if the penetration depth exceeds the thickness of the material. The Effective Moisture Penetration Depth (EMPD) can be used for quantification of the penetration depth, and the EMPD for concrete is shown in figure 1.12. The figure shows that about 5 cm of the concrete is affected by the daily fluctuations.

Abadie and Mendonça (2009) has taken the concept of EMPD further and tried to
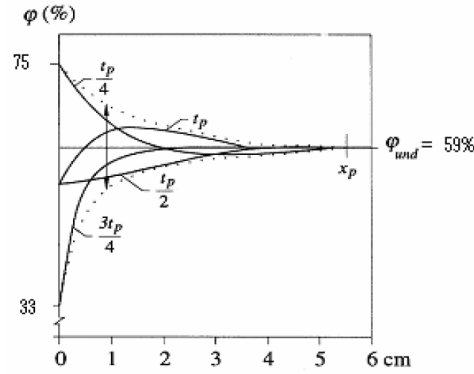
Figure 1.12: The EMPD in concrete from daily fluctuations of RH (Rode et al., 2005)

evaluate the links between the material characterization and simulation. The report refers to Peukuri (2003) for the surface resistance of a concrete wall and compares the EMPD for a concrete with and without the surface resistance. It is important to specify that the surface resistance is not a layer of coating (e.g. paint), but the boundary surface resistance. The results show a small reduction of the amplitudes of the fluctuations, but just a small effect of the penetration depth. The results for concrete can be seen in figure 1.13.
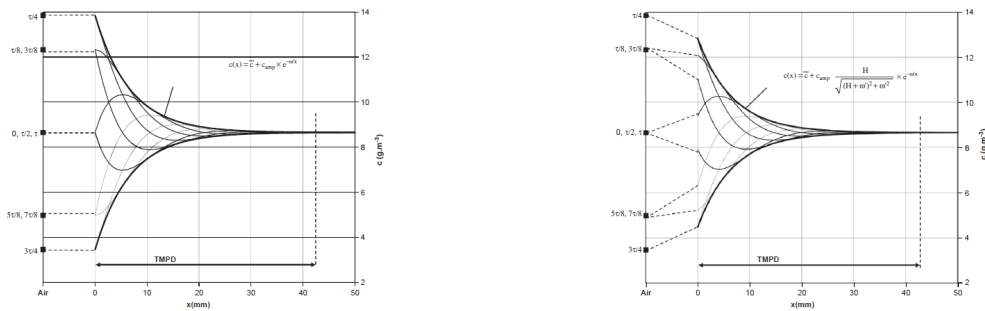
(a) EMPD with no surface resistance

(b) EMPD with surface resistance

Figure 1.13: EMPD for concrete, comparison with and without surface resistance (Abadie and Mendonça, 2009)

In a building, there will be both external walls exposed to the indoor environment on one side, and internal walls which are exposed at both sides. By looking at the penetration depth at an internal wall of concrete, it can be illustrated as in figure 1.14. The illustration shows that if the concrete wall is twice the EMPD (approximately 80 mm total), there will be no extra dampening effect of the indoor humidity by making the walls thicker. It is important to specify that this does not imply that the center of the wall does not absorb moisture if the surrounding humidity changes for a long period of time, but it will not be affected by the daily fluctuations.

11
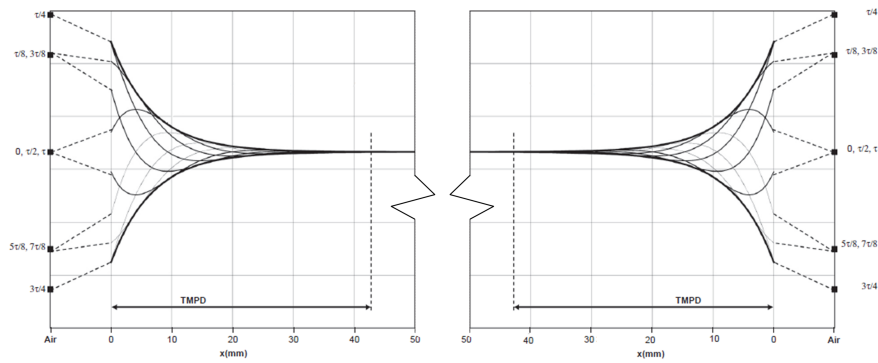
Figure 1.14: The penetration depth when exposed to both sides, developed from Abadie and Mendonça (2009)

1.3.2 Phase Change Material

In order to be able to discuss the opportunities by using PCM, its basic concept needs to be presented. Phase Change Material (PCM) is for many a new technology and can be hard to understand. PCM is a material that goes through a phase change at a given temperature, which results in absorption or release of energy. Most PCM products on the marked are micro encapsulated within other materials and can therefore be hard to visualize. The most common known PCM is used in hand warmers as seen in figure 1.15.

Figure 1.15: Image of melted and solidified hand warmers with PCM (Pawar, n.d.)

When the PCM is activated, the bag of PCM immediately goes through a phase change and releases energy. The PCM used in such hand warmers usually needs to be boiled to melt and will solidify when activated again, i.e. it is not activated based on the surrounding temperature. The PCMs used in buildings does not release the energy in the same way (i.e. becomes warm), but have a given temperature when the phase change occurs, and the cycle will go repeatedly without the need for activation or boiling. The moisture buffering described in chapter 1.3.1 can reduce

the fluctuations of humidity, while PCM can be used to reduce the fluctuations of temperature.

The physics of PCM

When a material is exposed to a change in temperature, the material will store or release heat from the surrounding environment. When the temperature of a material increases, it is described as an increasing enthalpy. The enthalpy is according to ASHRAE (2017) defined as "*the sum of the internal energy of a system, plus the product of the pressure volume work done on the system*". This thesis will neither be focusing on the change of volume nor pressure. The amount of heat stored and released is related to the material properties and is described as the heat capacity, $c[J/(kg{\cdot}K)]$. The specific heat capacity is the amount of heat one kilo of a substance stores when the temperature increases by one degree. A simple drawing of the concept of heat storage in a building can be seen in figure 1.16.
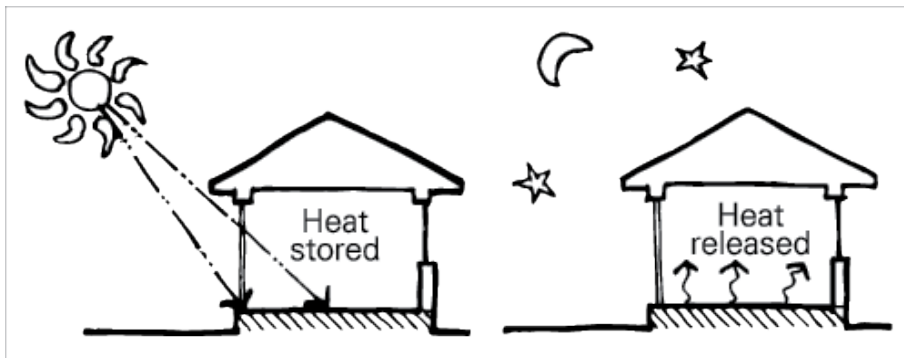
Figure 1.16: Illustration of heat storage in buildings (Reardon, 2013)

PCM uses the concept of latent heat to store and damp the fluctuations of temperature within a system (Fleischer, 2015). Latent heat is the heat stored or released during a phase change. This phase change could be from solid to liquid state, liquid to vapor or vice versa. As an illustration of the concept, the change of enthalpy for water has been illustrated in figure 1.17. Values both for the heat capacities and the latent heat storage are found from Thue (2014) and Britannica (n.d.). Be aware that in reality, the heat capacity may not be constant throughout the different phases, but is presented like that in the figure. As seen in figure 1.17, the energy needed to heat the material through a phase change is large compared to the heat needed to heat a material within the same phase. The phase change between solid and liquid is called heat of fusion, while the change between liquid and vapor is called heat of vapor. The phase change used in building materials is the change from solid to liquid and vice versa. Even though the heat of vapor might require even more

energy than the heat of fusion, vapor is hard to control and is often resulting in a great change of volume.
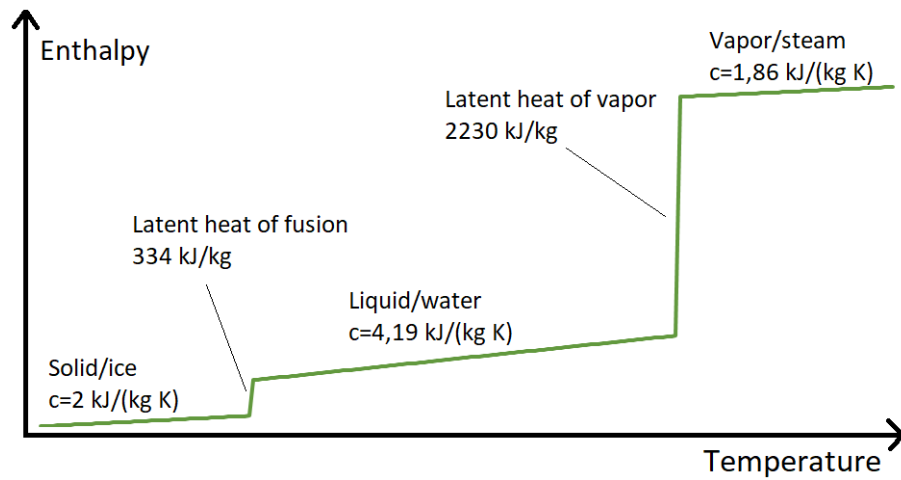
Figure 1.17: Illustration of the stored energy in water, values from Thue (2014) and Britannica (n.d.)

In PCM, the melting temperature can be modified based on the product used, and one can achieve a melting temperature within the temperature range expected to find in buildings. If PCM with a melting temperature at 28°C is implemented in a building, the material will start to melt when the indoor temperature exceeds this limit. The material will then be able to store heat through the phase change, limiting the indoor temperature to continue to increase. On the other hand, when the surrounding temperature drops, the PCM will solidify and release the energy to the surrounding air.

Hysteresis

An important property of PCM is that it melts and solidifies during a temperature range. When heating a cube of PCM, the entire cube will not melt at the same time, and the cube will not solidify at the same time. In addition, the melting and solidifying temperatures can be different, which results in what is called hysteresis. Rubitherm SP24 can be used to illustrate the concept and can be seen in figure 1.18.

Figure 1.18 shows that even though the main enthalpy change during heating (i.e. melting) happens at 24°C, there is latent heat storage at other temperatures as well. The same happens for the change during cooling (i.e. solidifying). The peak enthalpy change happens at 22°C, but the figure also shows a high change of enthalpy both at 21 and 23°C.

To illustrate the total accumulated enthalpy of the material, the enthalpy can be
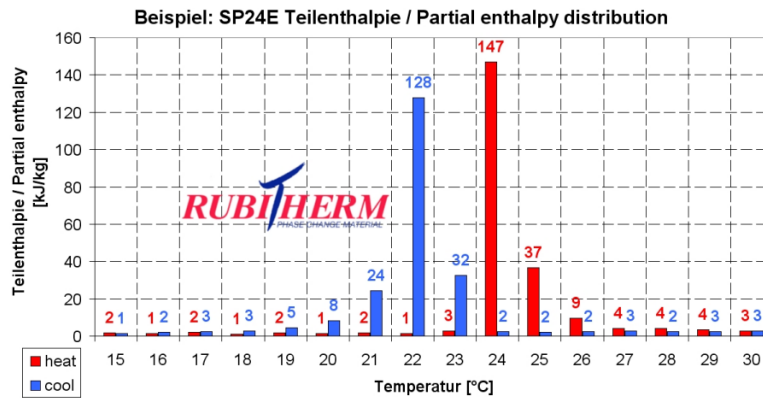
Figure 1.18: Partial enthalpy change of Rubitherm SP24 (Rubitherm Technologies GmbH, n.d.[a])

summed up and be presented as in figure 1.19. Be aware that the enthalpy is relative to 15°C and does not illustrate the absolute total enthalpy.
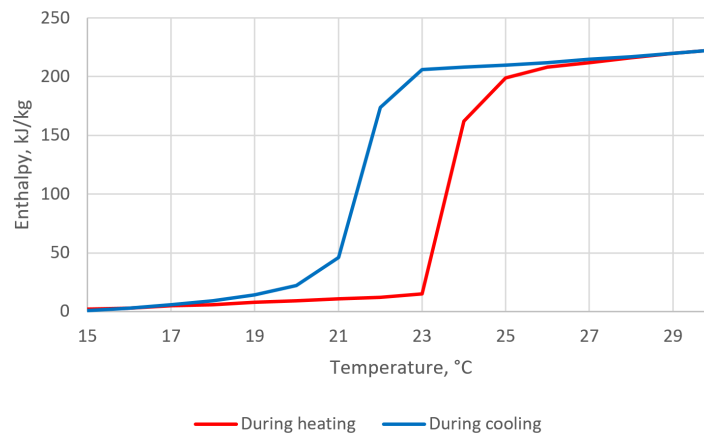
Figure 1.19: Accumulated enthalpy of Rubitherm SP24, data from Rubitherm Technologies GmbH (n.d.[a])

Figure 1.19 shows clearly that the change of enthalpy does not happen at the same time for heating and cooling. This phenomenon will not be hard to simulate if the material completely melts before the temperature drops and it completely solidifies again, but the physics can be hard to understand and describe if the process stops before complete melting/solidification. The problem can be described by using three different figures as shown in figure 1.20.

If a cube of PCM with the properties of Rubitherm SP24 is heated to 24°C and the heating stops, the material will be in a state that is illustrated in figure 1.20b. If the temperature drops to 23°C, it will not solidify according to the technical data from Rubitherm Technologies GmbH (n.d.[a]), but it will neither reach complete melting. How the enthalpy is changing within this range and how to calculate it correctly has

15

(a) Complete solid   (b) Partial solid/liquid   (c) Complete liquid
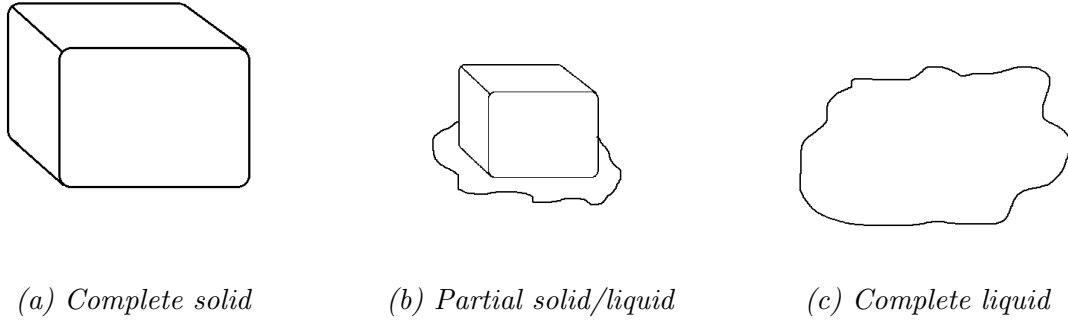
Figure 1.20: Illustration of the melting process of a cube

not been found during this study, as the material tends to both melt and solidify at the same time. However, IDA-ICE uses a constant heat capacity for the PCM in this state, which will be described further in chapter 2.3.1.

Kalnæs and Jelle (2015) made a review of manufacturers and properties of commercial PCMs where both melting and solidifying temperatures was presented. For instance, the study showed that Rubitherm RT 18 HC both melted and solidified between 17-19°C, while Rubitherm SP 24 melted between 24-25°C and solidified between 23-21°C. This implies that it is possible to choose a PCM both with desired melting temperature, and with a desired level of hysteresis. This could be useful if the building for instance has nighttime cooling and it is desired to let the temperature to drop a few degrees before the energy is released.

PCM in buildings

Even though PCM is highly described in literature, there is limited amount of buildings with PCM installed. Garathun (2014) has made an article for *Teknisk Ukeblad* (a technical magazine published in Norway), where she states that the building industry in Norway is the industry that spends least money on developing new technology compared to the number of employees. The building industry is by many seen as conservative and it is hard for new technology to make its way into the marked.

Schröder and Gawron (1981) investigated the properties needed in PCMs to develop efficient and reliable products. Some of the properties was:

– **High storage capacity**. The higher heat capacity, the higher effect of the PCM.

– **High thermal conductivity.** If the conductivity is too low, the thickness of the PCM will achieve a great variance of the temperature. Only parts of the

material will melt/solidify and the potential of the PCM will not be used.

– **Melting point suitable for the usage.** As the melting point can be modified, it is importance to use a product with the correct melting point. During a study of PCM glazing systems, Goia et al. (2013) stated that wrong selection of melting temperature could affect the comfort in a negative way, which again could lead to increased energy consumption.

The properties of a PCM are related to the substance used within the PCM, and are often divided into organic, inorganic and eutectic. This thesis will not go deeper into all differences between the PCMs but present the advantages and disadvantages of the three material groups. Jelle and Kalnæs (2017) has made a summarized table of the advantages and disadvantages, which are based on several research articles. The summarized table from Jelle and Kalnæs (2017) is redrawn in table 1.1, and has been extended with some information from Rathod and Banerjee (2013).

	Advantages	**Drawbacks**
Organic	- No supercooling - Recyclable - No phase segregation - Low vapor pressure - Large temperature range - Compatible with conventional construction materials - Chemically stable - High heat of fusion	- Flammable - Low thermal conductivity - Low thermal conductivity - Low volumetric latent heat
Inorganic	- High volumetric latent heat - Low cost - Non-flammable - Sharp phase change - Higher thermal conductivity than organic PCMs	- Corrosive to metals - Phase segregation - Congruent melting - High volumetric change - Supercooling
Eutectic	- Sharp melting points - No phase segregation - High thermal conductivity - Properties can be tailored to match specific requirements	- Limited data on thermophysical - High cost

Table 1.1: *Advantages and drawbacks for PCMs, redrawn from Jelle and Kalnæs (2017) and extended with Rathod and Banerjee (2013)*

The conductivity of the PCMs is one of the properties that is varying. Jelle and Kalnæs (2017) states that organic PCMs often have a conductivity around 0.15-0.2 W/mK, while inorganic salts have a conductivity around 0.5 W/mK. Evola et al. (2013) found in a study of PCM boards that the tested products only used 45% of the potential during a summer simulation. The PCMs used in the study by Evola et al. (2013) had a conductivity of 2.7 W/mK, which is remarkably higher than the PCMs described by Jelle and Kalnæs (2017).

In a review about PCM related to energy performance, Zhu et al. (2009) presented four different application categories of how to use PCM in buildings. In addition to the four categories described by Zhu et al. (2009), Jelle and Kalnæs (2017) extend the usage to also include thermal comfort control. All five application categories are listed below.

- Free cooling

- Active building systems

- Peak load shifting

- Passive building systems

- Thermal comfort control

Both the free cooling systems and the active building systems includes the usage of a larger technical system. The free cooling systems found in literature are related to ventilation, while the active building systems are related to e.g. heat pumps, floor heating systems or solar systems. These techniques will not be described further, as the developing of these systems exceeds the limits of this thesis. See Souayfane et al. (2016) for an overview.

The peak load shifting, the passive building system and the thermal comfort control are quite similar when it comes to how the PCM is implemented, but the goal of the techniques is different. Ideally, all three application goals can be achieved if the system is designed optimal. The peak load shifting, as illustrated in figure 1.21, can be used to postpone the peak temperature in the building, and thereby also postpone the load on the ventilation system. Halford and Boehm (2007) states that one of the advantages with such a delay can result in a peak temperature later in the evening when the outside ambient temperature is lower, which will ease the cooling of the building. In addition, it can ease the electrical grid by distributing the need for energy throughout the day.

The concept behind using PCM as a passive building system is to prevent over-heating during daytime and reduce the need for heating during nighttime (Jelle and
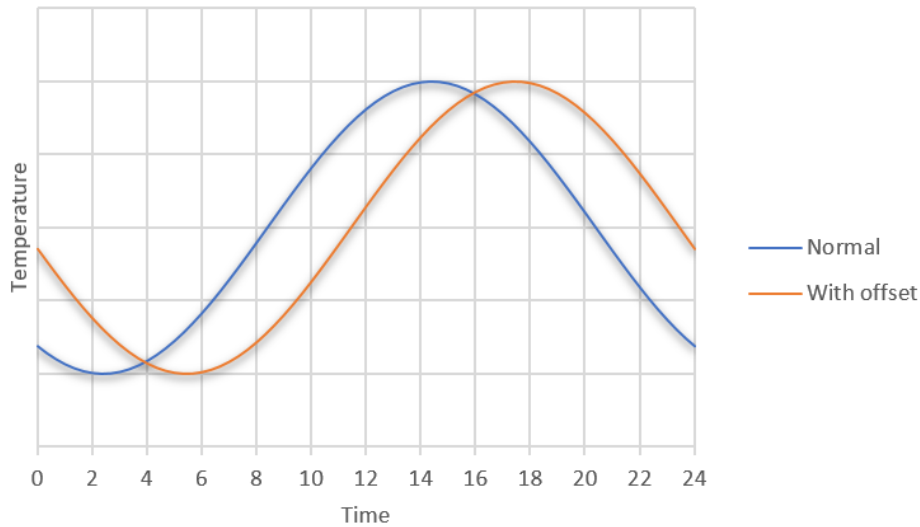
Figure 1.21: Illustration of the temperature fluctuations with a peak offset

Kalnæs, 2017). By using thermal mass, the building will need more time to be heated and cooled, which will result in a dampening effect of the temperature fluctuations. An illustration of the wanted dampening effect can be seen in figure 1.22. The dampening effect is dependent on the thermal mass of the building, along with an additional effect from PCM. Jelle and Kalnæs (2017) states that the use of PCM is especially beneficial when the constructions are built of lightweight materials. The dampening effect does not only result in saved energy, but also by reducing the peak loads. Halford and Boehm (2007) found 11-15% reduction in the peak cooling load by implementing a layer of PCM in between two insulating layers in a heavy mass building, and 19-57% reduction in a lightweight building. Consequentially the HVAC systems can be reduced in size and effect.
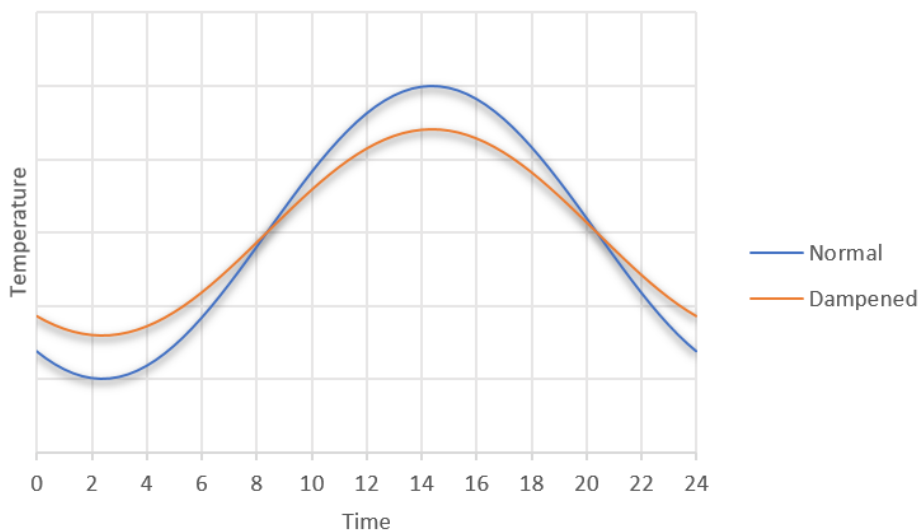
Figure 1.22: Illustration of the temperature fluctuations with dampening effect

When it comes to the thermal comfort control, it is the same concept as described for the passive building system and peak load shifting. By implementing PCM, the temperature will be held more stable throughout the day which will improve the thermal comfort. PCM within the surrounding surfaces will also stabilize the surface temperature and reduce the thermal discomfort from radiative heat (Jelle and Kalnæs, 2017).

In reality, the use of thermal mass and PCM will result in a combination of figure 1.21 and figure 1.22. A combination of the two can be seen in figure 1.23, which is a redrawn version of a figure by Tate (2016). The potential energy savings that are illustrated in figure 1.23 are dependent on several parameters (e.g. night time temperature).
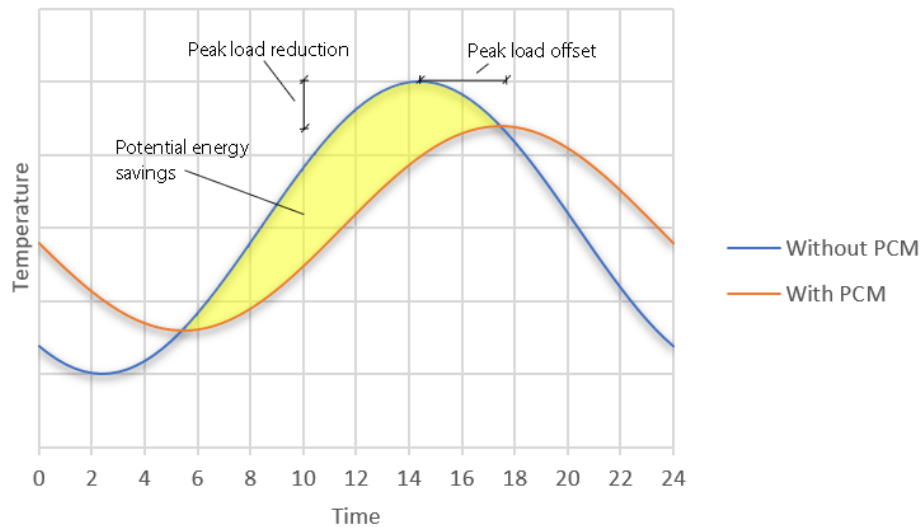
Figure 1.23: Illustration of the temperature fluctuations with both peak offset and dampening effect, redrawn from Tate (2016)

During a study on how PCM affected the energy consumption in several locations across the United States, Han and Taylor (2016) simulated the implementation of PCM internally on external walls. The study used a wall consisted of gypsum, lightweight concrete, insulation and brick wall, described from the inside and out-wards. The PCM was then added internally on the walls, and six different PCMs were tested in four different cities. The results showed that PCM could reduce the total energy consumption for heating and cooling with 1.3-17.0%.

Becker (2014) has also done similar tests, where both lightweight and heavyweight buildings were simulated. He concluded that by implementing PCM internally on walls, the energy consumption in lightweight buildings could be reduced by up to 57%. However, in heavyweight constructions, the PCM only improved the thermal comfort, but not the energy consumption.

20

PCM has been used in several different projects and is, for instance, stated to be used successfully in an office building outside of Zurich in Switzerland. The building has been implemented with GLASSXcrystal, which is a glazing system by GLASSX with internal PCM from Rubitherm (GLASSX AG, 2005). In a video posted by GLASSX, they state that the building does not need either heating or cooling to provide comfortable indoor temperatures for the employees (GLASSX AG, n.d.[b]). The sun is directly heating the PCM, which stores the energy within the window and releases it when the indoor temperature is low. The building can be seen in figure 1.24, where the white windows are the GLASSXcrystal glazing system.

Figure 1.24: Image of an office building in Zurich with PCM in the windows (GLASSX AG, n.d.[a])

1.4 This thesis

This thesis has been given the title "Modeling and validation of passive techniques for stabilizing the indoor environment". This title implies that the techniques selected have been both modelled and validated as a part of this thesis. "Passive techniques" implies that the implemented materials and technologies does not require energy or need to be controlled to function. "Stabilizing the indoor environment" implies that the object of studying the techniques have been to dampen fluctuations of temperature and relative humidity in the building. By using the moisture buffering properties of building materials to absorb and release moisture, the relative humidity indoor can be stabilized. Similarly, by using the latent heat capacity of PCM to store and release heat/energy, the indoor temperature can be stabilized. The Viking Ship Museum has been used as a case study for the thesis as it is a building that requires stable indoor environment.

1.4.1 Research questions

The following research questions have been developed.

1. Does IDA ICE provide valid models for simulating the effects of moisture buffering and PCM?

2. Can moisture buffering and PCM improve the indoor environment in the Viking Ship Museum?

3. Can moisture buffering and PCM reduce the total energy consumption and peak energy demands for HVAC in the Viking Ship Museum?

1.4.2 Limitations

There are several limitations in this thesis, and it is first of all limited to time. In the beginning of the semester, it was an object to investigate four different techniques: moisture buffering, PCM, smart windows and double skin facades. Due to the limitation of time, only moisture buffering and PCM was selected, which are the two techniques that are implemented internally in the zones.

The work done in this thesis are limited to only be carrying out simulations in IDA ICE, by EQUA AB. Other software's has been investigated (e.g. COMSOL multiphysics), but both due to limitations in time and because it has been a desire to fully understand IDA ICE, other software's have not been used.

The Viking Ship Museum is planned to be built with concrete and this thesis are investigating how moisture buffering and PCM can affect the indoor environment, energy consumption and peak energy demand in this specific building. This implies that there has not been carried out case studies of the effect from moisture buffering and PCM in the museum with other building materials (e.g. wood).

The Viking Ship Museum is located in Norway and has only been simulated in with a climate file for Oslo in Norway. The findings in this thesis does therefore only claim to be valid for climates comparable to Oslo.

1.4.3 Structure of this thesis

Chapter 2 (Methodology) presents the how the different models has been built. This chapter will both present arguments for the selections done, and the process of making the models.

Chapter 2.2 (Validation of the HMwall model) and chapter 2.3 (Validation of the PCM model) presents the validations of the software models used to investigate moisture buffering effect and PCM, respectively. These validations have been used to evaluate whether the models can be used in the case study and the chapters will therefore also present the results, discussion and conclusion related to the validations.

Chapter 2.4 (Single zone case study of PCM) presents the process of carrying out the single zone model of the "Gokstad" exhibition room. This model uses fixed values for the HVAC systems in order to isolate the effect on the indoor environment from the implementation of PCM.

Chapter 2.5 (Whole building case study with PCM) presents the implementation of PCM in the "Gokstad" exhibition when the zone is interfering with other zones and it has sensor-controlled HVAC systems. This model is used for investigation of the effect on the indoor environment, along with energy consumption and peak energy demand for HVAC by implementing PCM.

Chapter 3 (Results) presents the results from both the case studies described in chapter 2.4 and 2.5. The results are presented as a comparison between the models with and without PCM.

Chapter 4 (Discussion) presents the discussions related to the three research questions presented. This chapter will discuss how the findings in the literature review match the findings in this thesis and answer the research questions.

Chapter 4.2 (Validation) discusses the overall outcome of the validations of the HMwall and PCM model.

Chapter 4.3 (Stabilization effect) discusses the effect on the indoor environment by taking moisture buffering and PCM into account. The discussion uses results from the single zone and the whole building case study, along with some results from the validations.

Chapter 4.4 (Energy consumption and peak energy demand) discusses how the implementation of PCM in the Viking Ship Museum affects the energy consumption and peak energy demand for HVAC. The discussion is based on the results from the whole building case study in chapter 2.5.

Chapter 5 (Conclusion) concludes on the three research questions presented.

Chapter 6 (Further Work) will describe work related to this thesis that could be investigated further.

2 ⸺ Methodology

2.1 Brief

When selecting software for this thesis, several factors was important to evaluate.

- Is the software suited for the task?

    - Does it provide data for both energy and indoor environment?

    - Do the software have models for moisture buffering and PCM?

- Is knowledge of the software valuable when the thesis is finished?

- Are help available when trouble in the simulation occur?

IDA Indoor Climate and Energy (IDA ICE) by EQUA AB was selected, which is a trusted software used for study both the indoor climate and energy consumption of an entire building (EQUA Simulation AB, n.d.[b]). Knowledge about the software has a great value when the thesis is finished, as it is used by many consultants in Norway and the rest of the world. IDA ICE has models for implementing both moisture buffering and PCM, even though both the models are still in beta mode. The moisture buffering model is called HMwall (Heat and Moisture wall) in IDA ICE, and will be described as "HMwall model" further. In addition, IDA ICE is not a black-box software, which makes it possible to understand how the software works. EQUA AB is located in Stockholm, Sweden, where courses are held every third month. They provide help through email, though a forum online and they also give the option to send the entire model to them for help.

Validation of the model has been necessary for the thesis, as both functions are in beta mode in IDA ICE. There has been found validations of both the HMwall and PCM model done by EQUA AB and Cornaro et al. (2017) respectively. In addition, both models have been tested within this thesis. The process can be seen in figure 2.1, along with the chapters related to the different simulations.

As seen in figure 2.1, the moisture buffering of concrete was found ineffective, and the HMwall model was found to have limitations in the validity. This will be further described in chapter 2.2. The PCM on the other hand was found valid (chapter 2.3), and has been investigated further in both chapter 2.4 and 2.5.
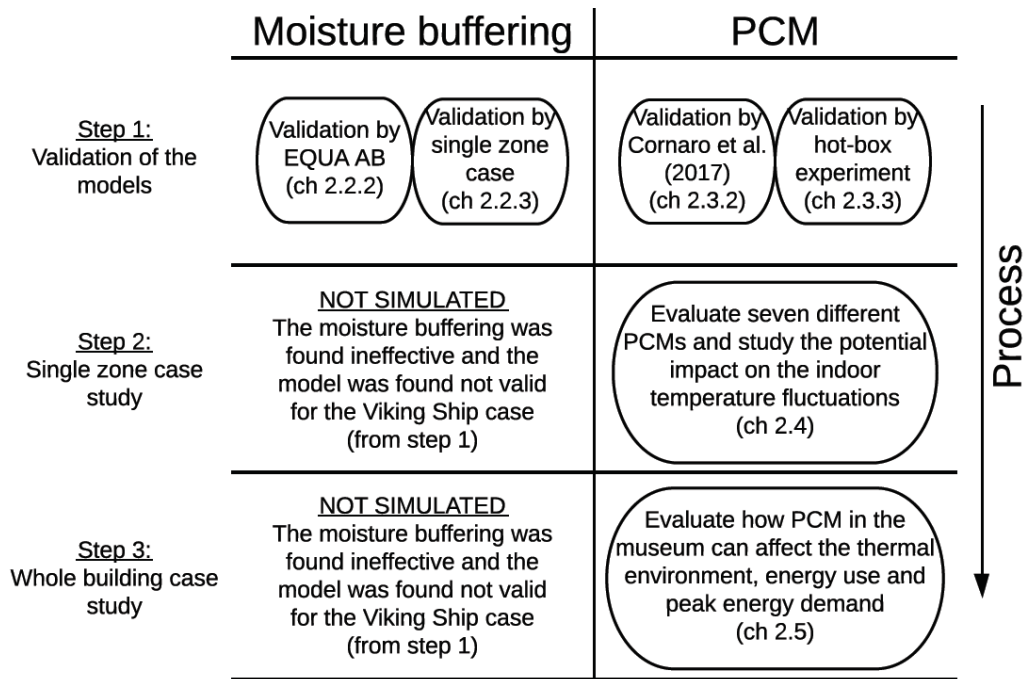
Figure 2.1: The structure of the methodology in this thesis

During the research done in this thesis, several different models in IDA ICE have been used. Figure 2.2 shows which models in IDA ICE that have consequences for other models in this study. The geometry of the building was received from Rebecca Lundqvist, which had this as a part of her thesis in the autumn semester of 2017. Her model has been used as a foundation both for the single zone model of the "Gokstad" exhibition room (in chapter 2.4), and for the whole building simulation (in chapter 2.5).
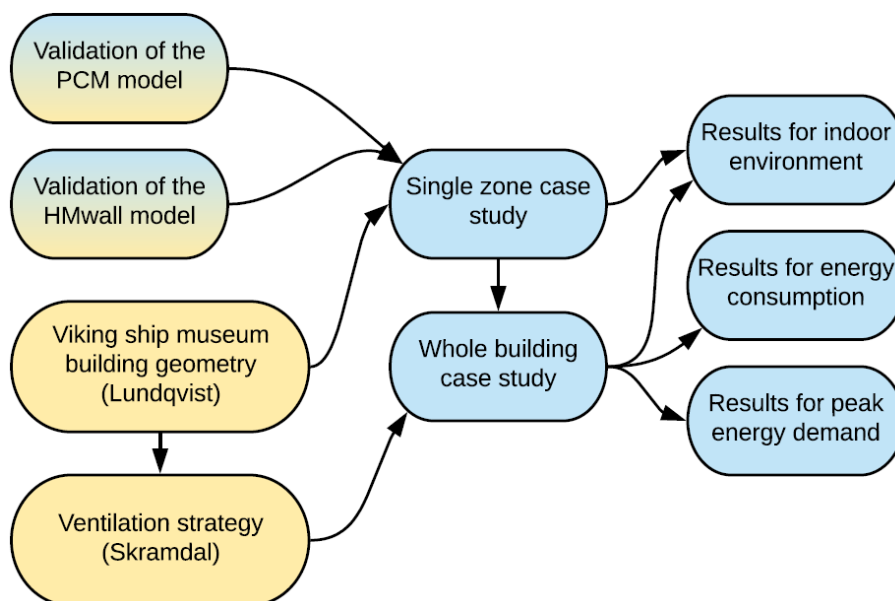
Figure 2.2: Flowchart of how models have been shared and revised

Parallel with this thesis, Tor Atle Skramdal was working on the ventilation system of the Viking Ship Museum as a part of his thesis. His model was received in order to evaluate how PCM and moisture buffering could affect the energy consumption and peak energy demand for HVAC. The yellow color in figure 2.2 represent work done by other, while the blue color represent work done as a part of this thesis.

2.2 Validation of the HMwall model

As IDA ICE is used for simulation in this thesis, it is necessary to understand how the program handles moisture buffering in the building materials. The general answer for how the program handles this effect is that it does not. The RH calculated in the zones in IDA ICE is based upon the outdoor conditions (e.g. temperature, RH), the indoor temperature, indoor moisture production, ventilation and infiltration. However, EQUA has made a model that takes this into account. This is an add-in in IDA ICE called HMwall and can be received from EQUA by request, along with a description file (EQUA Simulation AB, n.d.[a]). The HMwall model calculates the heat and moisture transfer in 1D through the wall. This add-in is, according to Patrik Skogqvist at EQUA, in beta (or might even alpha) stage, and needs to be handled carefully.

2.2.1 Implementation of the HMwall model in IDA ICE

The HMwall model needs to be added in schematic view in IDA ICE. When the add-in is installed, it is possible to replace the existing walls with moisture buffering walls. The wall needs to be connected to the measured indoor and outdoor relative humidity and specific material parameters needs to be implemented. A print screen of how it looks in schematic view can be seen in figure 2.3, and the process of changing the wall to a HMwall is listed below.

1. Replace the existing wall

2. Connect the wall to indoor and outdoor RH

   – The indoor RH is given as a value between 0 and 1, while the external RH is given as percentage (i.e. from 0 to 100). To be able to compare these values, the outdoor RH needs to be multiplied with a factor of 0.01.

3. Give the wall some initial values (e.g. water content).

- There are too many unknowns for the software to solve all equations without these initial values.

4. Specify material parameters (as seen in figure 2.4)

5. Log variables necessary to be sure the wall is acting as intended

  - This could for instance be water content or RH in wall layers

6. Repeat for all walls that needs to be replaced
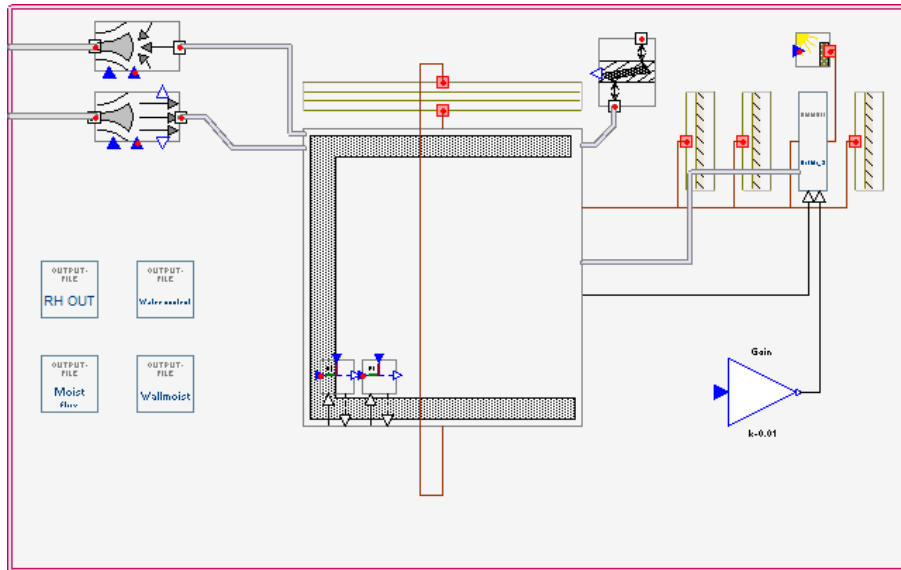
Figure 2.3: Schematic view in IDA ICE when an existing wall is replaced by a HMwall, print screen from IDA ICE

For the standard wall in IDA ICE, only thermal conductivity, specific heat capacity and density are needed as parameters for the materials. Figure 2.4 shows that the implementation of the HMwall model requires several extra parameters for the materials. When first give a total amount of layers in the wall (NLAYERS), it is possible to implement all the parameters for the number of layers selected. EQUA turns to Masea (n.d.) for information about the different parameters, which is a trusted database where Fraunhofer-Gesellschaft are among the actors.

Name	Value	Start	Unit	Connected to	Logged to	Description
N	2		items			Total number of nodes
NLAYERS	2		items			number of layers
SUBMODE	1		items			Subdivision mode: 0 uniform, 1 tighter at be...
NM1	1		items			Number of intevals n-1
A	80.15		m2			wall area
T0	20.0		°C			Initial temperature
PHI0	0.5					Initial relative humidity in the wall
L[1:2]	{0.5 0.283}		m			layer thickness
LAMBDA0[1:2]	{1.94 0.04}		W/(m K)			layer heat conductivity
RHO[1:2]	{2104.0 3...		kg/m3			layer density
CP[1:2]	{776.0 15...		J/(kg K)			layer specific heat capacity
WF[1:2]	{144.0 27...		kg/m3			Free water saturation
W80[1:2]	{101.0 30...					Equilibrium water content at 80% rel hum
BLAM[1:2]	{8.0 4.0}					thermal conductivity supplement of wall layers
MUWET[1:2]	{72.0 18.0}					Wet cup vapour diffusion resistance factor
MUDRY[1:2]	{76.1 50.0}					Dry cup vapour diffusion resistance factor
NSUBLAY[1:2]	{1.0 1.0}					number of nodes in Layer i

Figure 2.4: Parameters available to build the moisture buffering wall, print screen from IDA ICE

2.2.2 Similar studies

EQUA AB has started the validation process of the HMwall model, but as mentioned earlier, the model is still a beta version. Three different validation tests have been carried out by EQUA, where there is one test against EN 15026 (Standard Norge, 2007) and two tests against WUFI, which is a trusted software for calculating heat and moisture transfer through materials. The three tests are further on described as:

– EQUA test 1: the validation test against EN 15026

– EQUA test 2: the first validation test against WUFI

– EQUA test 3: the second validation test against WUFI

EQUA test 1

In annex A of the standard 15026, there is a benchmark test for numerical simulation of the hygrothermal effect of building materials. The validation test is concerning the moisture absorption of a homogeneous material that is semi-infinite. Material parameters for concrete have been used for the validation. Initially, the concrete is at steady state with the surrounding environment at 20°C and 50% RH. Instantly, the surrounding conditions are changed to 30°C and 95% RH. The wall is simulated for 7, 30 and 365 days, and the moisture profiles of the material are compared to the results given in EN 15026. The results from the test can be seen in figure 2.5, where the green and red marks represent the tolerance given by the standard, and

the blue lines are the results from IDA ICE. The results show quite accurate results, but EQUA points out that the benchmark test in 15026 has not been finished at this time.
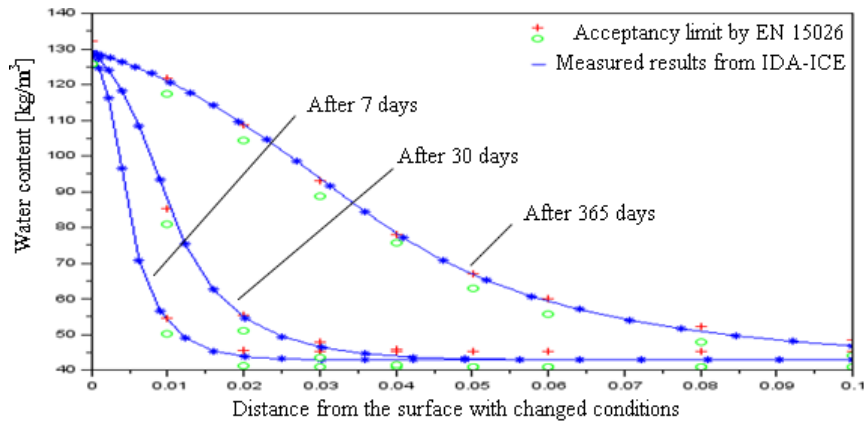
Figure 2.5: Moisture profiles in the wall, comparison of IDA ICE and EN 15026 (EQUA Simulation AB, n.d.[a])

EQUA test 2

The first validation test against WUFI is, in difference to EQUA test 1, concerning how the material dries out over time. The wall was at first at steady state with the surrounding environment at 20°C and 80% RH. The environment was changed instantly to 19°C and 50% RH, and the test was done with four different materials: concrete, brick, gypsum and oak, with a thickness of 20 cm. The results for concrete (figure 2.6) and oak (figure 2.7) are presented further in this chapter.
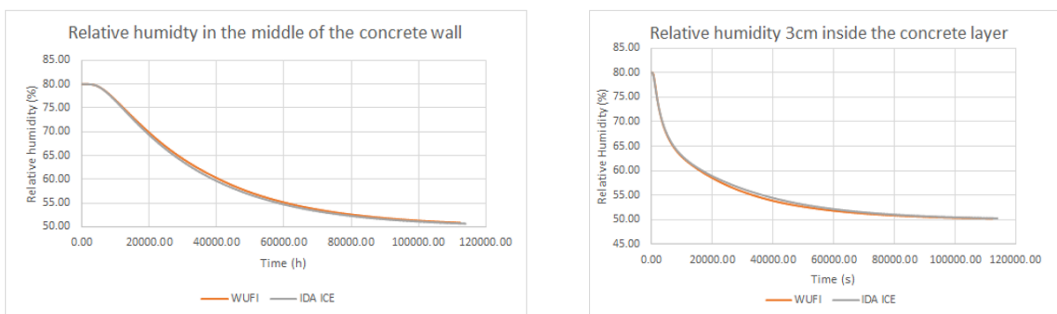
(a) Center of the wall

(b) 3 cm from the surface

Figure 2.6: Evolution over time of the RH in the concrete wall, comparison of IDA ICE and WUFI (EQUA Simulation AB, n.d.[a])

For the concrete wall, the results were proven to be very precise, as shown in figure 2.6. Both in the center of the wall (fig. 2.6a), and at a distance of 3 cm from the surface (fig. 2.6b), the results are overlapping most of the time. Notice that

the figure does not represent the moisture profile as for the test against EN 15026, but it shows how the RH in the wall is changing over time. For the oak wall, the comparison between IDA ICE and WUFI showed different results, as seen in figure 2.7. The results are neither representative at the center (fig. 2.7a) nor at 3 cm from the surface (fig. 2.7b).
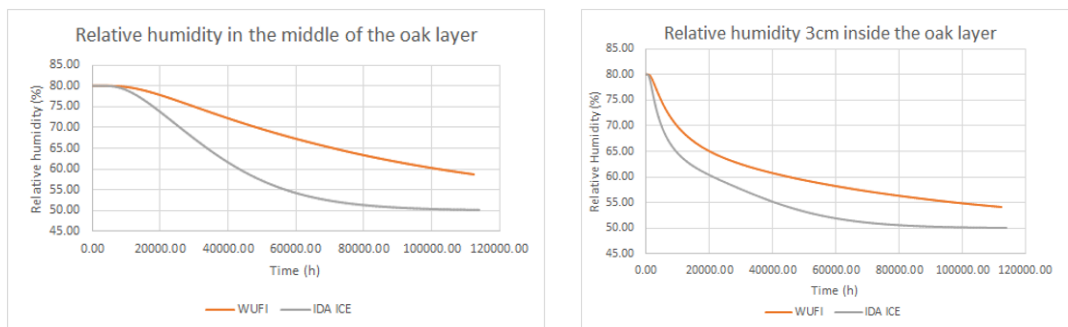
(a) Center of the wall

(b) 3 cm from the surface

Figure 2.7: Evolution over time of the RH in the oak wall, comparison of IDA ICE and WUFI (EQUA Simulation AB, n.d.[a])

During the study of the oak wall, EQUA found some trouble of handling the dry- and wet-cup vapor diffusion factors. When modifying these values for the oak layer, the deviation was decreased significantly. EQUA states that the model needs to be study further. The dry- and wet-cup factor will not be presented and described in this thesis, but they are important to mention as the problem correspond to the mentioned issue Rode et al. (2005) described about input values. Input values are tested with different methods and may not be constant under different conditions. IDA ICE uses a fixed value for these parameters, which was proven to be representative for concrete walls, but not for oak walls.

EQUA test 3

EQUA test 3, which is the second test against WUFI, is in difference to EQUA test 1 and 2 dealing with fluctuations of RH in the boundary conditions. An 20cm thick external concrete wall has been used for the test. The internal side of the wall is exposed to a constant climate at 19°C and 50% RH, while the external side is exposed to a varying climate. The same climate file has been used in both software's, and the result can be seen in figure 2.8.

The comparison shows quite accurate results, but the deviations are larger closer to the external side. As it is the external side that is exposed to the fluctuations, it is also this side that is most interesting to study. EQUA comments that there could
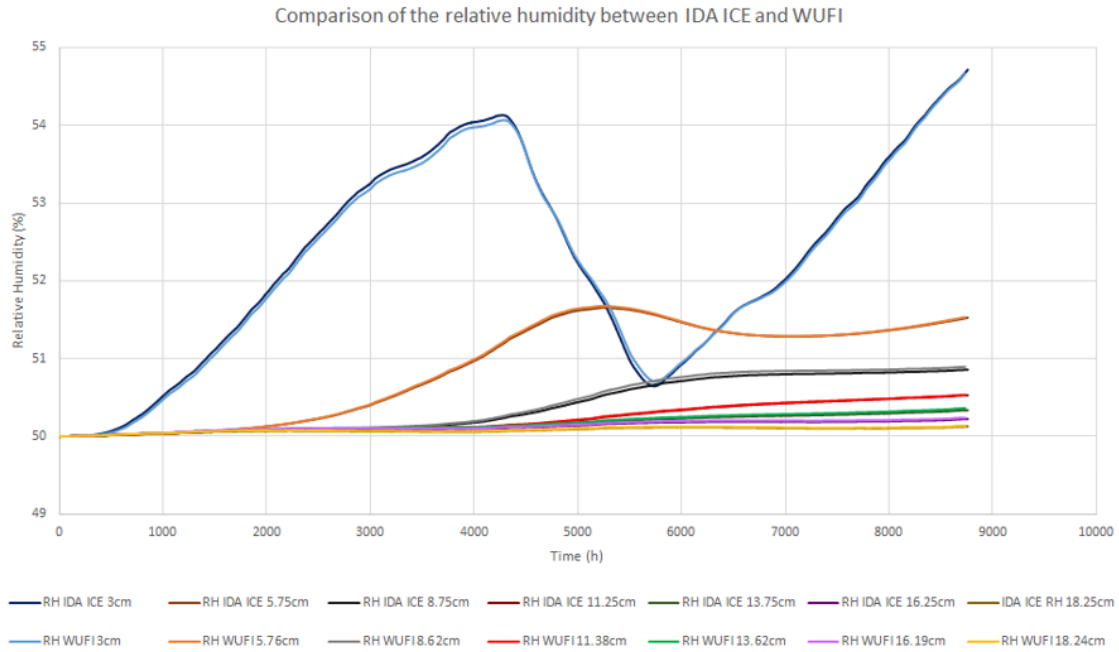
Figure 2.8: Time evolution of RH within an external concrete wall at different distanced from the outside, comparison of IDA ICE and WUFI (EQUA Simulation AB, n.d.[a])

be some problems of how the program handles the boundary conditions, but these problems are yet to be solved.

2.2.3 Validation of moisture buffering effect

The validation done by EQUA focus how the water content within a material is changing and has focused most on how the material is behaving under constant conditions. This validation is important, as the water content within the building materials will affect the RH in the indoor air. Even though, a small study of how the HMwall model is handling the spontaneous response to a change in the RH in a building has been done and will be described further in this chapter. The focus is on how the implementation of the HMwall model is affecting the RH in the internal air. For this study, a small single zone model has been made, and can be seen in figure 2.9.

Built-up of the validation model

The model is made with one external wall and a scheduled moisture production. The moisture production is implemented as equipment with a production rate of

31

- No windows/doors
- No occupants
- No light

- One facade wall
- CAV ventilation at 2 l/(s·m²)
- Moist production of 0.001 g/h from 10-18 every day
- Heater/cooler only in "OneLayer with constant temp"
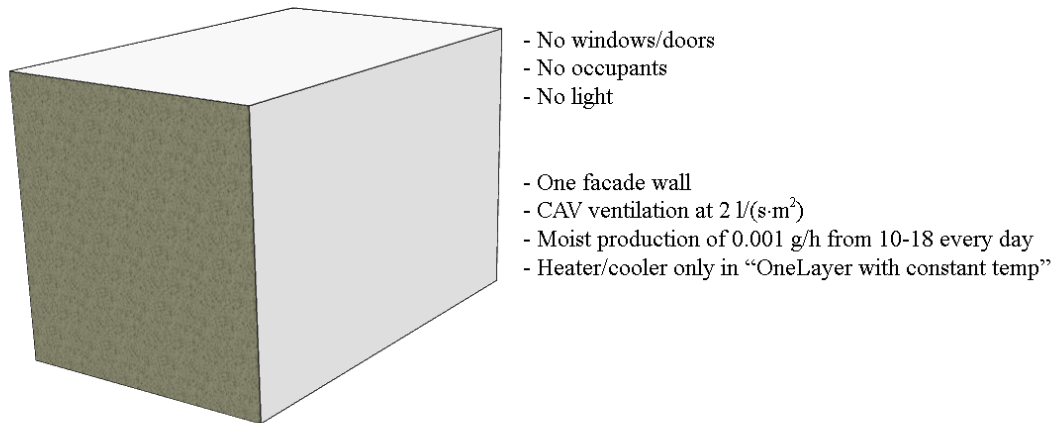
Figure 2.9: Geometry of the single zone model made for evaluating the moisture buffering from the HMwall model

0.001 g/s running from 10-18 every day. The study has been done with six different cases, as shown in figure 2.10.
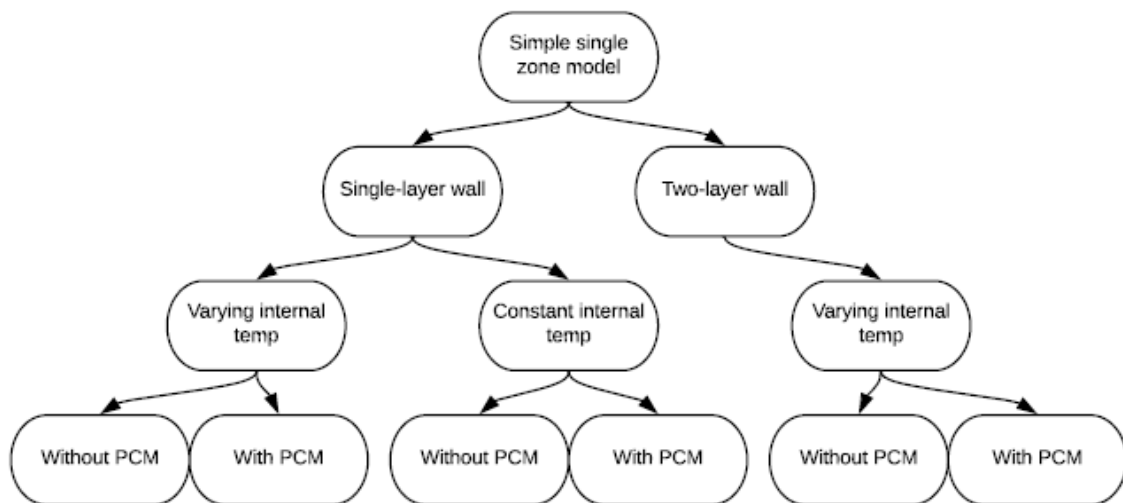
Figure 2.10: Presentation of the six different cases for the moisture buffering validation study

The "Single-layer wall" has an external wall consisting of 15cm concrete, while the "Two-layer wall" also has 15cm external insulation. The basic material parameters can be seen in table 2.1. Be aware that insulation has been implemented with some values that actually makes no sense for the material according to Masea (n.d.). The material properties for insulation are found from the material called "EPS_040.15" in the database. For all the insulating materials (EPS and XPS) in the database, Masea (n.d.) states that some of the properties makes no sense for the material.

These values are marked with "*" in table 2.1. IDA ICE requires to fill inn this information, and the material parameters have been received from EQUA through dialog. This can affect the model, but as it is the concrete that is exposed to the indoor environment, the effect on the moisture buffering effect should be limited. The rest of the values are found from Masea (n.d.).

Table 2.1: Basic material parameters for the fluctuation test of the HMwall model, values from Masea (n.d.)

Material parameter	Concrete	Insulation
Basic parameters		
Heat conductivity	$1.94W/mK$	$0.04W/mK$
Density	$2104kg/m^3$	$30kg/m^3$
Specific heat capacity	$776J/kgK$	$1500J/kgK$
Extra parameters for HMwall		
Free water saturation	$144kg/m^3$	$5kg/m^{3*}$
Water content at 80% RH	$101kg/m^3$	$4kg/m^{3*}$
Vapour diffusion factor (wet cup)	8	4^*
Vapour diffusion factor (dry cup)	72	140^*
Thermal moisture conductivity supplement	76.1	50

*The parameters make no sense for insulation according to Masea (n.d.), but IDA ICE requires values implemented. The implemented values are selected through dialog with EQUA AB

During the simulation it was found necessary to make a model with constant indoor temperature. This was done for the single-layer wall, as seen in figure 2.10. While the models with varying temperature was implemented only with ventilation system, the model with constant temperature had heating/cooling systems. The heating and cooling systems was exaggerated to keep the indoor temperature at 20°C during the entire simulation period. The reason for making this model was due to the fact that RH is dependent on the temperature, and it was found some small differences in the indoor temperature in the other models.

The moisture content within the zone can be traced to understand where the moisture is transferred. There are four different variables or parameters in IDA ICE that can be traced, as listed below.

1. VAPF[i:n] (Vapor flow, term [i]): A variable that track the flow of evaporated water through ventilation in kg/s.

2. VAPFOCC2Z (Vapor flow from occ): A variable that sums up the total vapor production from occupants in kg/s.

3. VAPF_0 (Vapor flow, term_0): A variable for the evaporated water through infiltration in the building.

4. VAPFSRCEQUIP[1:i] (Humidity load): A parameter (i.e. a fixed value by the user) for production of water from equipment.

By implementing the HMwall model, the program also includes the moisture transport through the wall. This variable will be included as a part of VAPF[i:n]. For this study, the ventilation system had one inlet (VAPF[1:3]), one outlet (VAPF[2:3]). The moisture buffering from the HMwall model was then registered as VAPF[3:3].

The models were simulated for one year, with a warm up phase of two years. When the materials were implemented, an initial value for water content had to be sat. The warm up phase is used to stabilize the water content and make it dependent on the surrounding air. In order to quantify the change of the fluctuations several parameters have been used, which are listed below.

- **RHS**: Relative Humidity Stabilization index ($RHS = \sum_{i=1}^{n} |\overline{RH} - RH_i|$)

- **ΔRHS**: Change in RHS compared to the model without the HMwall model [%]

- **$\overline{RH}$**: Average RH [%]

- **RH_{max}**: Highest measured RH [%]

- **RH_{min}**: Lowest measured RH [%]

- **ΔRH**: Total change in RH ($RH_{max} - RH_{min}$) [%]

Results and discussion of the validation

The results from the case with just a concrete layer at the external wall and varying indoor temperatures can be seen in table 2.2. Be aware that the "varying temperature" is seasonal, and does not describe variance between the model with and without the HMwall model. The results show almost no effect from moisture buffering, as ΔRHS is as low as -0.55%. It can also be seen from the results that the model with moisture buffering achieved a lower RH_{min}. When moisture buffering is taken into account, it is not reasonable to achieve lower RH_{min}. The difference is small and can be related to some small differences in the mean air temperature in the two models. These results do not give any reasons to doubt that the HMwall model is handling the moisture buffering wrong, but they show that the effectiveness from moisture buffering of concrete is limited.

Table 2.2: Results for the single-layer model with varying indoor temperature

Case	RHS	ΔRHS	$\overline{RH}$	RH_{max}	RH_{min}	ΔRH
Without HMwall	102350	-	50.60%	90.8%	9.28%	81.52%
With HMwall	101789	-0.55%	50.69%	90.64%	8.99%	81.65%

For the case with two layers in the wall (i.e. concrete and insulation) and varying indoor temperature, the results actually shows a higher RHS with the HMwall model than without. The results are shown in table 2.3. The change in RHS is at 0.10%, i.e. by taking moisture buffering into account, the fluctuations of RH is increasing, according to these results. Independent on the material implemented, it makes no sense to have increased fluctuations when taking the moisture buffering effect into account. This implies that the HMwall model has some limitations, which most likely are related to the insulation. The insulation could not be implemented without giving values that are unreasonable for the material.

Table 2.3: Results for the two-layer model with varying indoor temperature

Case	RHS	ΔRHS	$\overline{RH}$	RH_{max}	RH_{min}	ΔRH
Without HMwall	141853	-	44.88%	91.90%	4.68%	87.22%
With HMwall	142000	+0.10%	44.77%	91.72%	4.66%	87.06%

As mentioned earlier, the two presented cases have seasonal changes, as the temperature is varying based on the external temperature. RH is dependent on the indoor temperature, and it has also been made a model without varying temperature. The moisture production and air flow from ventilation is the same, but the temperature is kept constant at 20°C. This was done in order to minimize the risk of temperature deviations between the cases with and without the HMwall model implemented. The results can be seen in table 2.4.

Table 2.4: Results for the single-layer model with constant indoor temperature

Case	RHS	ΔRHS	$\overline{RH}$	RH_{max}	RH_{min}	ΔRH
Without HMwall	123003	-	36.57%	72.94%	3.48%	69.46%
With HMwall	122987	-0.01%	36.58%	72.94%	3.48%	69.46%

The results show, as for the other cases, almost no changes between the model with and without the HMwall model. The change in RHS is -0.01%, which is low. The values for RH_{max}, RH_{min} and ΔRH are identical. These results confirm that the effect of taking moisture buffer into account is low.

In addition to the comparison of the RH and RHS, the transport of moisture in

the models are of interest. The moisture transport has been tracked for the simulations, and the results for the single-layer case with constant temperature are further presented in this thesis. The variables in the model are presented in figure 2.11. The only moisture transport that is not presented in the figure is the fixed value for moisture production of 0.001 g/s from 10-18 every day, as described earlier.
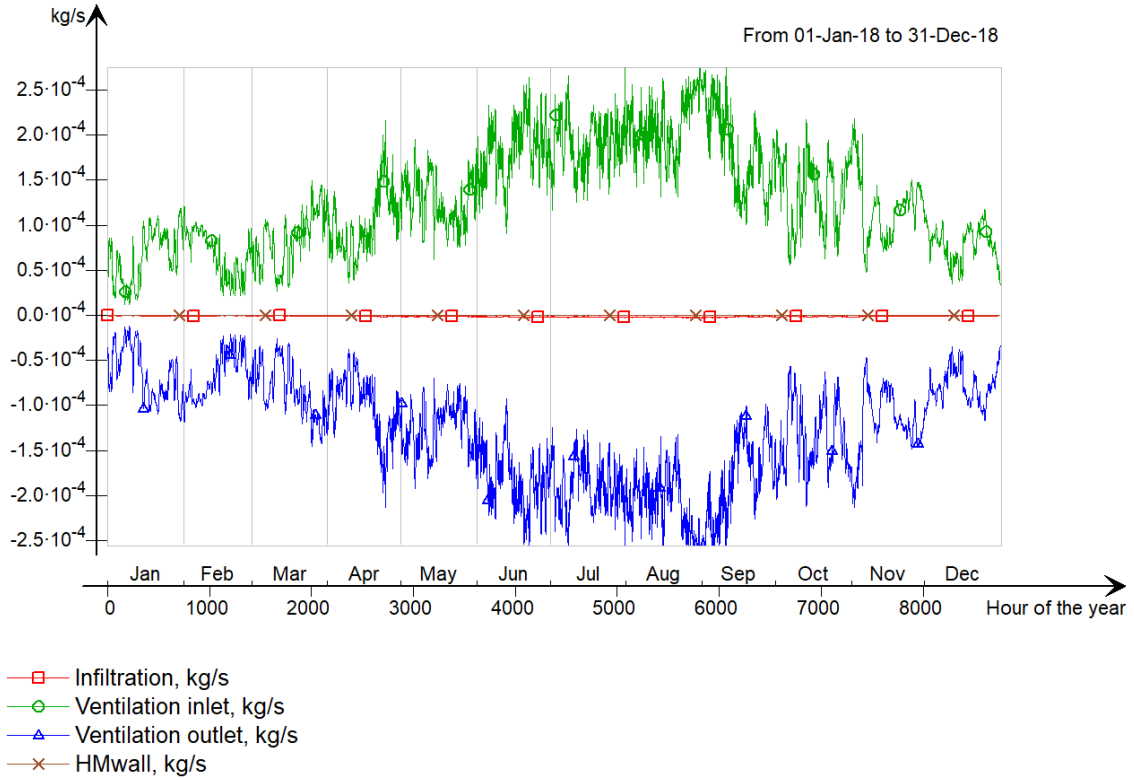
Figure 2.11: Moisture transport in the single-layer model with constant temperature

Figure 2.11 shows that the moisture transport is highest during the summer when the external air is warm and humid. The figure also shows that the moisture transported out of the zone through ventilation is comparable to the moisture transported in by ventilation.

All the moisture transport was exported and summed up. The values were exported with a timestep of 1 hour, which implies that some of the fluctuations can be missed when there are large fluctuations within an hour. The total accumulated moisture flow can be seen in table 2.5. The difference between the total transport in and out of the zone is at 0.061 kg, which is about 0.09% of the total moisture transport. This small difference can be because the results are exported with hourly values, or because there actually can be a change in the total water content in the zone.

It is clear from the values in table 2.5 that there is some moisture transport through the surface of the concrete wall. It is also interesting to see that the total moisture transport through the concrete wall is very low compared to the other sources.

36

Table 2.5: Moisture transport from the different sources in the single-layer model with constant temperature and the HMwall model implemented

Source	Moisture in to the zone	Moisture out of the zone
Infiltration	0.000 kg	0.697 kg
Ventilation inlet	67.727 kg	0.000 kg
Ventilation outlet	0.000 kg	67.213 kg
Equipment	0.219 kg	0.000 kg
Concrete wall	0.008 kg	0.012 kg
Total	68.372 kg	68.310 kg

The concrete wall is built with 8 nodes within the wall, which can be used to track different conditions during the simulated period. All the nodes are evenly distributed in the wall, where node 1 is closest to the internal surface. By this distribution, there is about 17 mm between the nodes as the wall has a total thickness of 150 mm. The results of the RH at the eight nodes and at the surfaces from the single-layer case with constant temperature can be seen in figure 2.12. As seen in the figure, the RH is fluctuating during the entire simulated period. Node 1 and 2 can be described to experience daily fluctuations, which implies that the 34 mm (i.e. 2x17mm) closest to the surface is fluctuating. This is comparable to the expected penetration depth in concrete of about 40 mm, as described in chapter 1.3.1.

EQUA stated in their tests (as described earlier) that the boundary conditions may not be taken into account as they should be. As described in chapter 1.3.1, Abadie and Mendonça (2009) studied the difference between taking the surface resistance into account or not. They found a reduction of the absorbed humidity close to the surface, but no reduction in the penetration depth. If the HMwall model is handling the boundary conditions wrong, the results from Abadie and Mendonça (2009) implies that this can affect the moisture buffering effect. The results from all the validation tests proves that the HMwall model is both storing and releasing humidity, but the effect is very limited. The HMwall model is in an early developing stage, and modifications are yet to be done. The validations done by EQUA proves that the program handles the long-term dry-out of the material, but for now there are limited validation of the way the HMwall model handles fluctuations. Insulation cannot be implemented without being modified with parameters that makes no sense for the material.

Even though it seems like the wall is both transporting and storing moisture, the effect on the RH in the internal air is minimal. The effect was even negative for the two-layer model. These results have been compared to the effect Rebecca Lundqvist
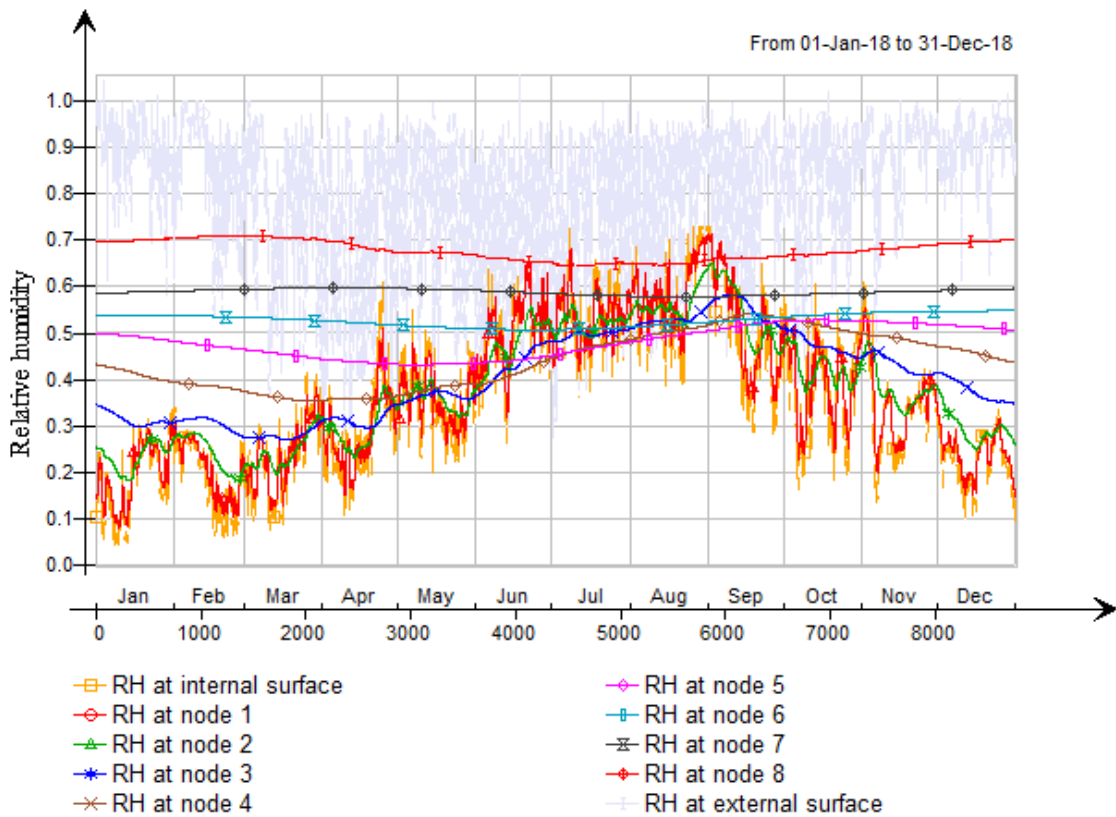
Figure 2.12: RH in the concrete wall, evenly distributed from the inside, in the wall from the single-layer case with constant temperature

found for the Viking Ship Museum in her thesis. She found a change in RHS between 0 and 2.5% for the "Gokstad" exhibition room. Her findings showed, as in this study a low effect for taking the moisture buffering effect into account.

2.2.4 Conclusion for the validation tests of the HMwall model

Through the validation tests presented in this chapter, a conclusion for the HMwall model can be made. To prevent misunderstanding, the three EQUA tests are done by EQUA, while the moisture buffering test is carried out as a part of this thesis.

– The EQUA test 1 (against EN 15026) shows that the HMwall model is valid.

– The EQUA test 2 (against WUFI) shows that the HMwall model only is valid for concrete. EQUA describes the model to be valid for "mineral materials".

– The EQUA test 3 (against WUFI) shows that the HMwall model has some difficulties of how it handles the boundary conditions of the wall. Even so, the results are quite accurate and does not give any reason to imply that the HMwall model is wrong.

- The moisture buffering test shows that the model is not valid when implementing insulation, as the RHS increased. This confirms the limitations EQUA found in EQUA test 2.

- The moisture buffering test also shows that the effect from taking the moisture buffering effect of concrete into account is low. Even so, this finding does not imply that the HMwall model is not valid.

As a conclusion, HMwall model is not ready to be used for evaluating the moisture buffering effect in the Viking Ship Museum. The HMwall model is only valid for walls with materials that are "minerals" (as EQUA described it), and the walls in the museum must be implemented with insulation. Even if the Viking Ship Museum could have been simulated without insulation, the effectiveness from the moisture buffering effect of concrete is limited. By this conclusion, the HMwall model will not be implemented in the museum.

2.3 Validation of the PCM model

EQUA has, as for moisture buffering, had an add-in for PCM for some time. In the last version of IDA ICE (version 4.8, released January 2018), the PCM model was implemented in the standard user interface. This made it possible to easily add PCM between layers in the walls, roofs or slabs. EQUA states clearly that even though the PCM model has been added in the program, it is still a beta version, which implies that it should be used carefully due to lack of tests. During the review, EQUA was asked for validation tests of the PCM model, but they did not have any tests to share, as they had for the HMwall model. Even so, a validation done by Cornaro et al. (2017) has been found and will be presented. In addition, a validation has been carried out as a part of this thesis, based up on a hot box experiment by Cao et al. (2010).

2.3.1 Implementation of PCM in IDA ICE

When PCMs are added in IDA ICE, some extra parameters for the materials needs to be filled in, which can be seen in figure 2.13.

The biggest difference from a regular wall is the enthalpy coordinates that needs to be implemented. IDA ICE uses partial enthalpy and temperature coordinates to implement the correct change of enthalpy over the phase change. This makes it possible to implement information from different products (e.g. Rubitherm SP24

Name	Value	Unit	Description
N	17	items	Number of temperature coordinates
NM1	16.0	items	Number of partial enthalpies (N-1)
RHOSOL	1500.0	kg/m3	Layer density (solid)
CPSOL	2000.0	J/(kg K)	Layer specific heat (solid) (J/(kg K))
LAMBDASOL	0.6	W/(m ...	Layer heat conductivity (solid) (W/(m K))
CPLIQ	1400.0	J/(kg K)	Layer specific heat (liquid) (J/(kg K))
LAMBDALIQ	0.6	W/(m ...	Layer heat conductivity (liquid) W/(m K)
C0	1400.0	J/(kg K)	Specific heat during reversing (c0 <= min(cpSol, cpliq)) ...
TH[1:17]	{16.5 17.5 18.5 ...	°C	Temperatures at which melting/solidifying enthalpies ar...
DHDTMELT[1:16]	{2000.0 2000.0 ...	J/(kg K)	Partial enthalpies between temperature coordinates divi...
DHDTSOLID[1:16]	{4000.0 5000.0 ...	J/(kg K)	Partial enthalpies between temperature coordinates divi...

Figure 2.13: Parameters available to build the correct PCM, print screen from IDA ICE

which was presented in figure 1.18). When the temperature of the PCM changes, the partial enthalpy change specified for this exact temperature will be taken into account.

In schematic view in IDA ICE it is possible to find and log different variables of the PCM. The most interesting variables for this thesis are total enthalpy, temperature and "mode". IDA ICE defines five different "modes" for the PCM and they are as follows:

- Mode -2: solid phase

- Mode -1: solidifying phase

- Mode 0: reversing during melting/solidifying phase

- Mode 1: melting phase

- Mode 2: liquid phase

Mode -2 and 2 correspond to the times where the PCM is completely solid and liquid, respectively. During mode -1 (solidifying phase), the PCM is cooled down and follows the enthalpy coordinates as implemented. Similarly, during mode 1 (melting phase), the PCM follows the enthalpy coordinates for the melting phase. When the material is at mode 0, the PCM stay within a state where the material neither melts or solidifies. When the PCM is implemented in IDA ICE, the program requires a parameter for specific heat capacity "during reversing" (see figure 2.13). This is the heat capacity related to the hysteresis, which was described in chapter 1.3.2. When the material is between the melting and solidifying curve, IDA ICE handles the material with no phase change. This can be illustrated by modifying figure 1.19, as shown in figure 2.14.
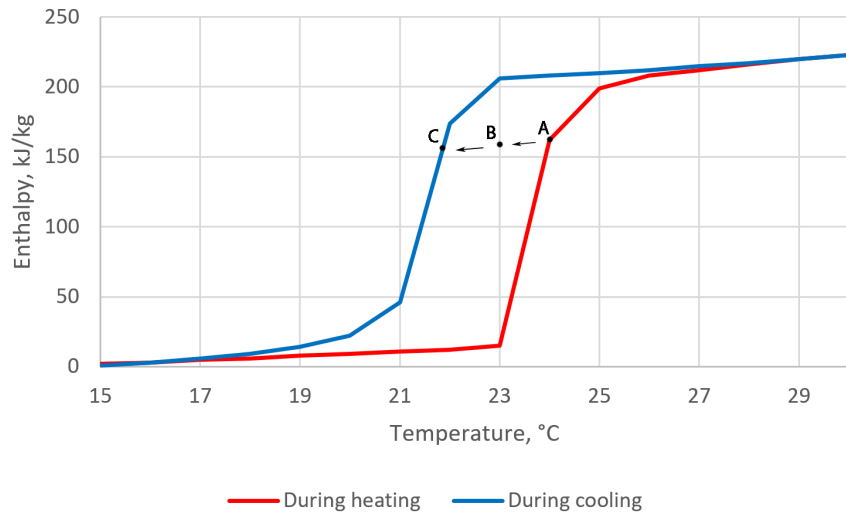
Figure 2.14: Illustration of how IDA ICE handles hysteresis

If a solid PCM is heated to 24°C (marked as "A") the change of enthalpy will follow the red line, and the PCM will be in mode 1 (melting phase). If the temperature starts to drop, the change in the enthalpy will follow a line specified by the specific heat capacity "during reversing". The PCM will then be in mode 0 (reversing during melting/solidifying phase). If the cooling stops at 23°C (marked as "B"), there will be no phase change, and no latent heat storage/release. The phase change will not be calculated for until the temperature and total enthalpy reaches the curve for cooling (marked as "C"). When reaching the blue line, the PCM will be in mode -1 (solidifying phase). These different modes can be tracked during the simulation in order to control whether the solidifying/melting happens at expected times.

2.3.2   Similar studies

There are numerous studies of PCM, both real tests and simulation, but most of the simulation tests found in literature lacks validation from real tests. Cornaro et al. (2017) performed a validation tests of the PCM model in IDA ICE by comparing it to real measures from Solar Test Boxes (STB). The boxes can be seen in figure 2.15.

Rubitherm SP21 PCM panes was implemented on the floor in one of the boxes, while the other box was used as a reference. Two different measurement campaigns were carried out, and both campaigns were then copied in IDA-ICE for comparison and validation. The results from the validation showed quite accurate results, as shown in figure 2.16. The results show that the experimental and simulated temperatures are overlapping most of the time. It can be seen that there are differences in the temperature curves when comparing the two campaigns. This is due to different

Figure 2.15: Images of the STB used in the validation by Cornaro et al. (2017)

climate conditions when the different campaigns were carried out. Cornaro et al. (2017) comments that the deviations that can be seen during night time in the second campaign (fig. 2.16b) could be due to lack of information about the PCM in such low temperatures.

(a) First measuring campaign

(b) Second measuring campaign
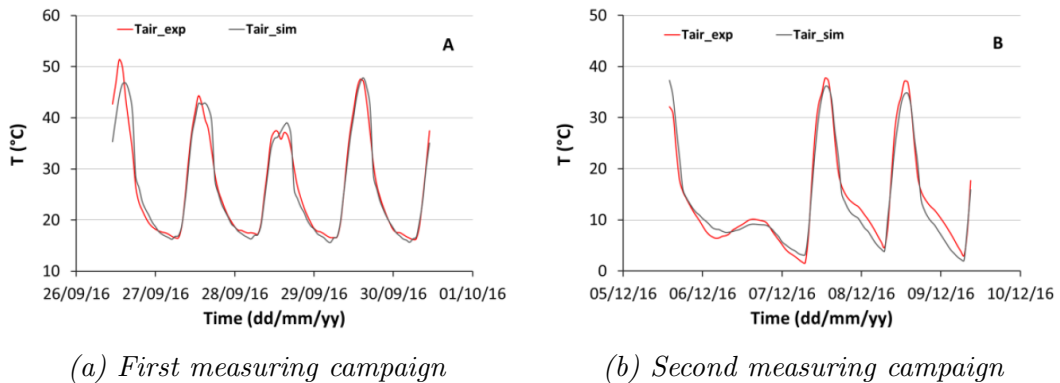
Figure 2.16: Measured (Tair_exp) and simulated (Tair_sim) air temperatures from STB validation tests (Cornaro et al., 2017)

Cornaro et al. (2017) calculated the root mean square error (RMSE) and the normalized RMSE (NMRSE) for two different simulation periods. The result can be seen in table 2.6. The RMSE and NRMSE shows that there are no more deviations between experimental and simulated results when PCM is implemented. When looking at the second campaign, the RMSE and NRMSE are actually decreasing when the PCM is implemented. These results show that IDA ICE is handling models with PCM just as good as models without PCM.

The results give no reason to conclude that IDA ICE handles PCM wrong.

Table 2.6: Simulation results for PCM in STB, simulated with IDA ICE (Cornaro et al., 2017)

x	Ref box		PCM box	
Campaign	RMSE (°C)	NRMSE (%)	RMSE (°C)	NRMSE (%)
26-29/09/16	1.78	4.1	1.57	5.0
05-12/12/16	2.50	5.2	1.83	5.1

2.3.3 Validation by hot box experiment

In addition to the validation by Cornaro et al. (2017), a validation has been carried out as a part of this thesis. In 2008 Cao Sunliang performed a hot box experiment as a part of his thesis at NTNU. This experiment has been the baseline for the validation carried out in this thesis. The concept of the hot box is to evaluate the heat flow through a specific building part and can be seen in figure 2.17.
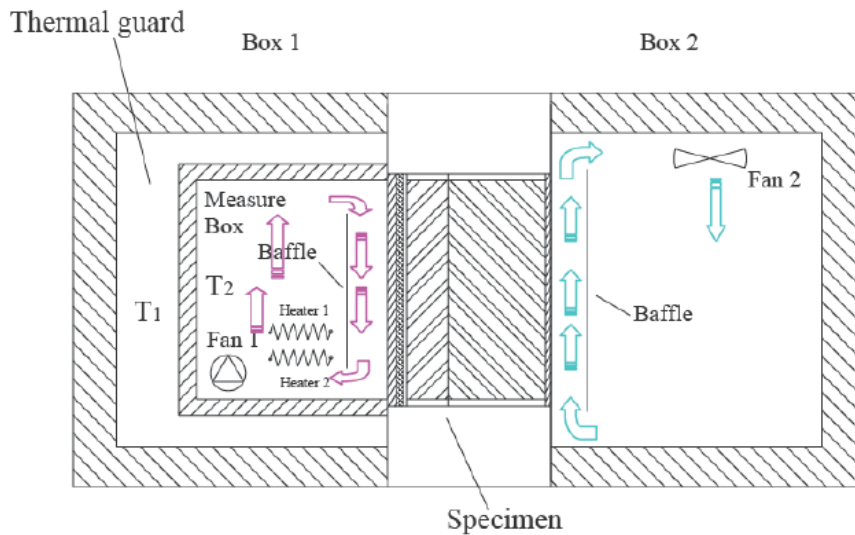
Figure 2.17: Schematic view of the hot box used in the experiment (Cao et al., 2010)

Box 1 exists of an outer and an inner box, where the outer part is used to control that the heat flow out of the measuring box can be neglected. This is done by assuring that T_1 and T_2 are equal, and as a result, the walls can be seen as adiabatic. The inner part of box 1, named as the measure box, exists of two heaters, a fan, a baffle and a wall facing box 2. Box 2 is constantly cold, resulting in a heat flow through the tested wall, described as "specimen" in figure 2.17. The baffles used in the two boxes are used to reduce the radiative heat flow from the heaters/coolers and to give an evenly distributed air flow over the tested wall. Heater 1 is used to assure that the temperature in the measuring box stays above 20°C, while heater 2 is used

to provide additional heating in order to generate the results. The fan within the measuring box is used to increase the convective heat flow. As the fan is placed entirely within the box, all the energy used is assumed to be converted to heat.

The tested wall is built up as seen in figure 2.18. The PCM used is the DuPont^{TM} Energain® PCM panel. Some of the most important thermal parameters are listed in table 2.7.

(a) With PCM *(b) Without PCM*
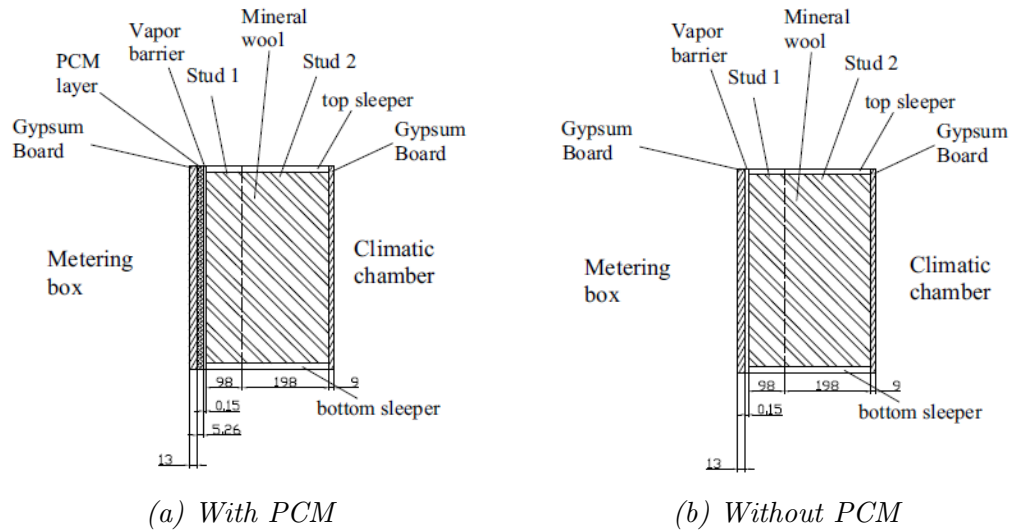
Figure 2.18: Cross section of the tested wall in the hot box (Cao et al., 2010)

Table 2.7: Some of the thermal parameters of DuPont^{TM} Energain® PCM panels (Cao, 2010)

Parameter	Value
Melting point	21.7°C
Latent heat storage capacity	>70 kJ/kg
Total heat storage capacity (from 14°C to 30°C)	>170 kJ/kg
Thermal conductivity in solid phase	0.18 W/mK
Thermal conductivity in liquid phase	0.14 W/mK

DuPont has been contacted in order to receive extender information about the PCM panels, but due to the fact that Energain® was discontinued in 2016, the information could not be shared. As a result, the information for the PCM panels is only found from Cao et al. (2010) and Cao (2010). The enthalpy change of the PCM panels was calculated by Cao (2010). The hysteresis of the PCM panels was neglected, so that the change of enthalpy was equal both during heating and cooling. The partial changes of enthalpy are shown in figure 2.19

The experiment was executed in two groups of five days. The first five days the hot
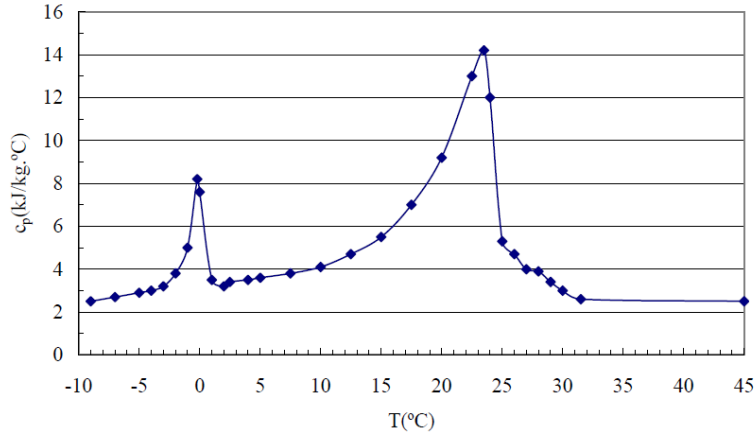
Figure 2.19: The calculated values for enthalpy change of DuPont^{TM} Energain$^{®}$ PCM panels (Cao, 2010)

box without PCM was measured with different effect of the fan and heater every day, as seen in table 2.8.

Table 2.8: Test procedure from the hot box experiment (Cao et al., 2010)

The air velocity during the heating procedure (m/s)	With or without PCM layer	Power of heater 2 (W)	Power of fan 1 (W)	The total heating powers of heater 2 and fan 1
0.4	without	0.00	90.59	90.59
0.3	without	24.62	66.65	91.27
0.2	without	61.86	29.55	91.41
0.1	without	80.90	9.86	90.76
0.0	without	91.16	0.00	91.16
0.4	with	0.00	90.59	90.59
0.3	with	24.52	67.54	92.06
0.2	with	61.79	30.33	92.12
0.1	with	80.90	9.79	90.69
0.0	with	91.22	0.00	91.22

The air temperature from these measures can be seen as a dark blue dotted line in figure 2.20. The results showed that the highest temperature was measured when the fan was turned off and the convection towards the tested wall was only driven by natural convection. During the second test group, the PCM was implemented and the same procedure was used to test for five days. The pink dotted line in figure 2.20

show the air temperature when the PCM was implemented. The results show that the air temperature was decreased by about 2° with the PCM. The exact measured data have been received for the validation.
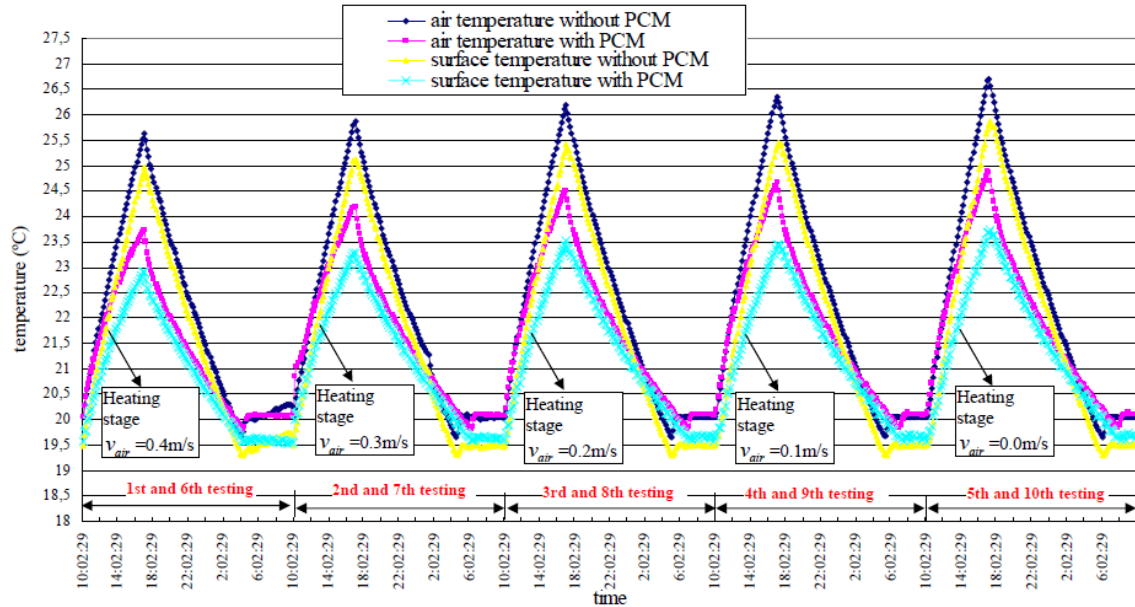
Figure 2.20: Results from the hot box experiment (Cao et al., 2010)

Build-up of the validation model

The model built in IDA ICE is made in order to represent the hot box used in the experiment by Cao et al. (2010). As IDA ICE do not have an option to give an air velocity within the room, only the simulation where the fan was turned off was used. It is possible to find the convective heat loss/gain to the wall, but it would be a problem to compare to the experiment. The initial thought was to build the entire system of the hot box, but due to functions in IDA ICE, this was not necessary. The walls surrounding the measuring box could be implemented as adiabatic, resulting in no heat loss through the walls. The tested wall between the measuring box and the cold box could be implemented as a wall facing a constant temperature of -20°C, which would result in just a single zone model: the measuring box itself. The model was built and calibrated, but issues occurred when the PCM was implemented. The model was struggling to handle the PCM in a wall facing a constant temperature. As a result, the cold box was added, with a cooling system providing a constant temperature of -20°C. The geometry of the model can be seen in figure 2.21.

Cao (2010) calculated the thermal resistance of the tested wall both with and without PCM and found it to be 7.53 m^2K/W and 7.50 m^2K/W respectively. A thermal resistance of 7.53 m^2K/W (i.e. the wall without PCM) equals a U-value of 0.1328
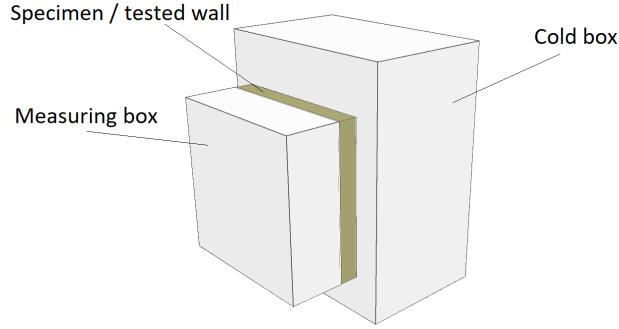
Figure 2.21: Illustration of the hot box in IDA ICE with two zones

W/m^2K which was implemented into the model in IDA ICE. The HVAC-system was removed from the model, along with all internal gains, thermal mass, leakages and domestic hot water. Two heaters were implemented, as for the hot box experiment. Heater 1 was implemented as an ideal heater controlled by the ambient air temperature in order to keep the temperature above 20°C. The second heater was implemented as an ideal heater with a schedule to control the unit. As for the hot box experiment, heater 2 was turned on from 10:00 till 17:00. A summary of the functions of the heating units can be seen in table 2.9.

Table 2.9: Information about the heaters in the model

Unit	Function
Heater 1	Keep temperature above 20.0°C
Heater 2	Heat the zone with a given effect from 10:00-17:00 every day

After all the information about the geometry, thermal properties of the materials and the heaters was implemented, the model was calibrated. The average air temperature from the measured experimental data was compared to the mean air temperature measured in IDA ICE.

When the model was calibrated and found representative for the experiment without PCM, the PCM was implemented and the results was compared. An illustration of the PCM implemented in the wall can be seen in figure 2.22.

The quantitative estimation of the validation has in addition to visual comparison been done by the following indices, where T_{ei} and T_{si} are the experimental and simulated temperatures at time step i respectively:

– Maximum temperature difference in accordance to equation 2.1

$$\Delta T_{max} = max(|T_s - T_e|) \tag{2.1}$$

47
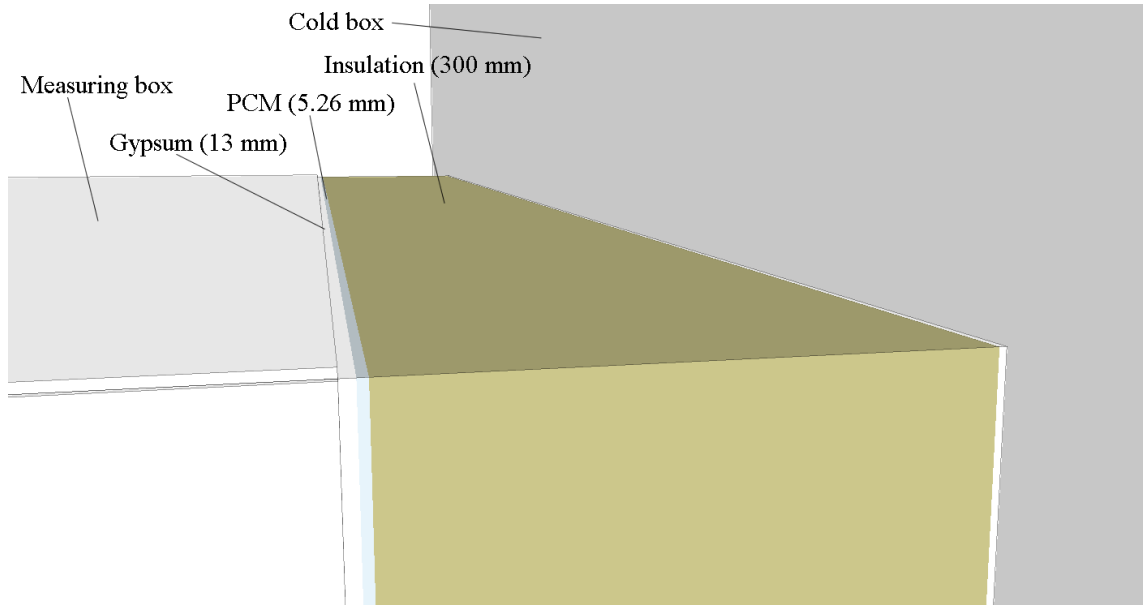
Figure 2.22: The layers in the wall, when implemented in IDA ICE

- Average temperature difference in accordance to equation 2.2

$$|\Delta T| = \frac{1}{n} \cdot \sum_{i=1}^{n} |T_{si} - T_{ei}| \qquad (2.2)$$

- Root mean square error (RMSE, [°C]) in accordance to equation 2.3

$$RMSE = \sqrt{\frac{1}{n} \cdot \sum_{i=1}^{n} (T_{si} - T_{ei})^2} \qquad (2.3)$$

- Normalized root mean square error (NRMSE, [%]) in accordance to equation 2.4

$$NRMSE = \sqrt{\frac{1}{n} \cdot \sum_{i=1}^{n} (\frac{T_{si} - T_{ei}}{T_{ei}})^2} \qquad (2.4)$$

Calibration of the model

Even though most of the surfaces are calculated as adiabatic with no heat loss, there will be heat storage in the building parts. These building parts, and their thermal mass was used to calibrate the model along with adjustments of heater 2. The measured data from the simulation without PCM, and with no fan was used for the calibration. Heater 2 was implemented with an effect of 91.16 W (as described in table 2.8) running from 10:00 till 17:00 during the day.

The calibration was done in three steps:

1. Adjust the thermal mass surrounding the measuring box

2. Adjust the properties of heater 2

3. Readjust the thermal mass

Before any detailed results was extracted from IDA ICE, the thermal mass was used to get the correct peak temperature. According to the experimental results from the hot box without PCM, the peak temperature was found to be 26.59°C. The same temperature was achieved in IDA ICE, and the comparison of the air temperatures can be seen in figure 2.23.
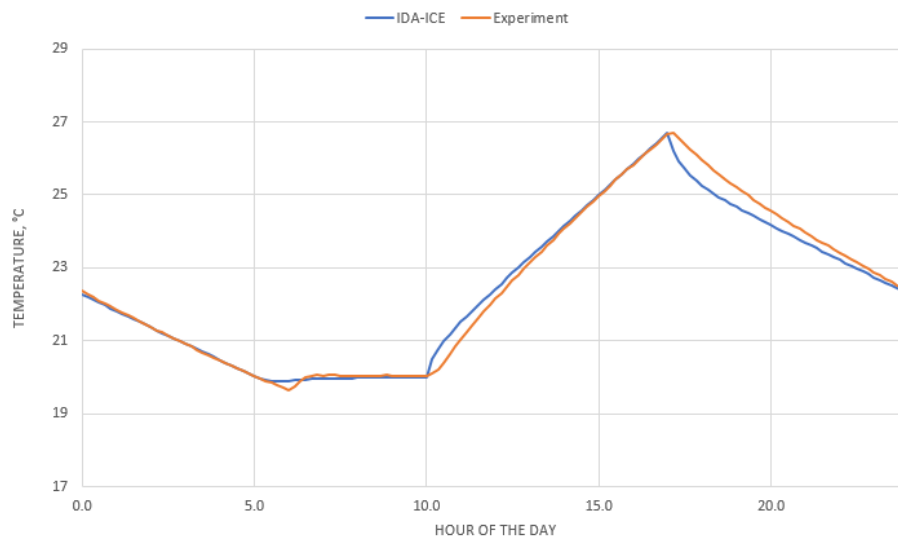
Figure 2.23: Temperature as a function of time in the calibration, only adjusted for thermal mass

The results show that the heater implemented in IDA ICE reacted much faster than the heater in the experiment. As a result, the temperature increased much faster at 10:00, and decreased much faster at 17:00. By changing the schedule of heater 2 so that it used about 1 hour to reach max power and again an hour to cool down, the results in figure 2.24 was achieved.

The change of temperature harmonized much better with the measured results from the hot box, but the maximum temperature was not reached. It was also noticed that the gradient of the temperature curve during the cooling period was different in both figure 2.23 and figure 2.24. This was understood as too much thermal mass in the simulation. By adjusting the thermal mass once more, the results in figure 2.25 was achieved.

The results in figure 2.25 are visually evaluated as accurate and gave results of the indices as described in table 2.10.
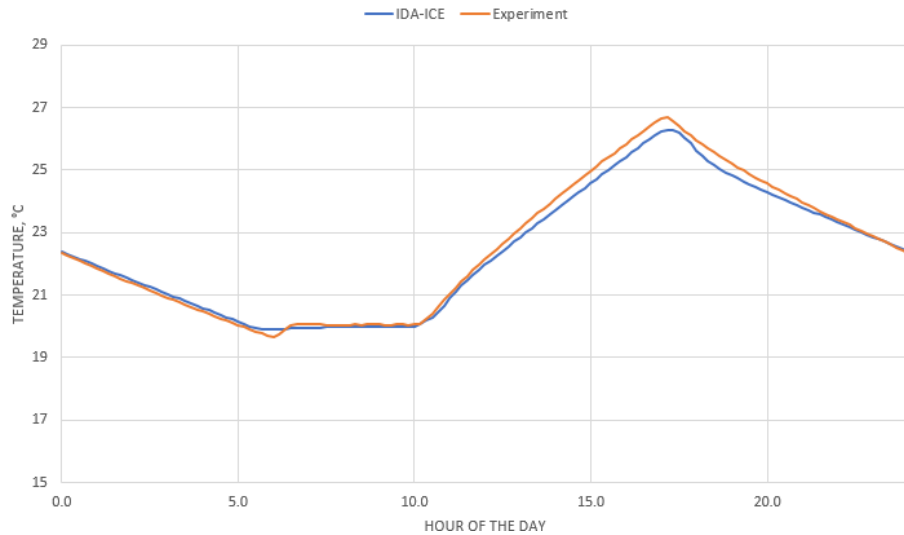
Figure 2.24: Temperature as a function of time in the calibration, adjusted schedule for heater 2
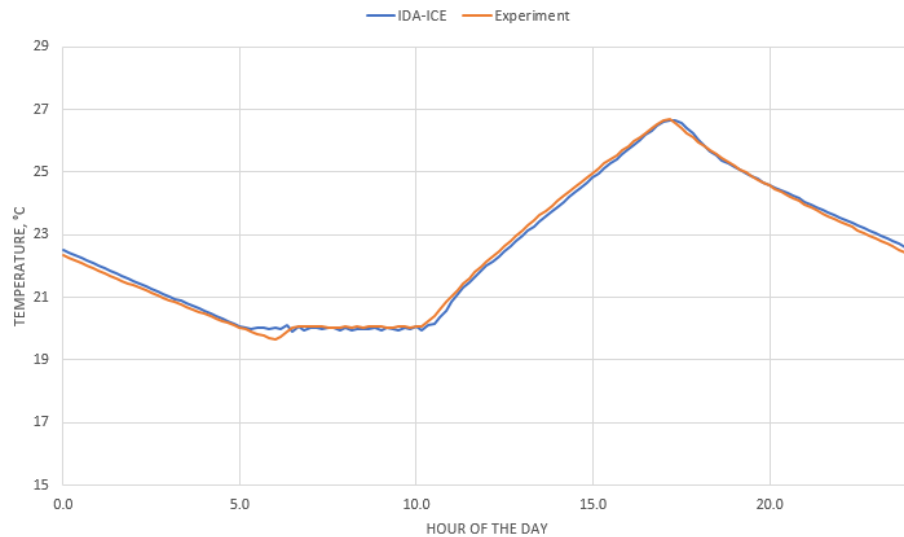
Figure 2.25: Temperature as a function of time in the calibration, adjusted for schedule and thermal mass

After the calibration, PCM was implemented into the model as for the hot box experiment. The PCM was added with a thickness of 5.25 mm as earlier presented in figure 2.18, and with the properties as described by Cao et al. (2010).

Results and discussion of the validation

After the PCM model was implemented in IDA ICE, the results for the temperature were as shown in figure 2.26.

The results in figure 2.26 shows accurate results during the heating, but some de-

Table 2.10: Results of the indices from the calibration

Indices	Value
ΔT_{max}	0.39°C
$|\Delta T|$	0.12°C
RMSE	0.13°C
NRMSE	0.61%
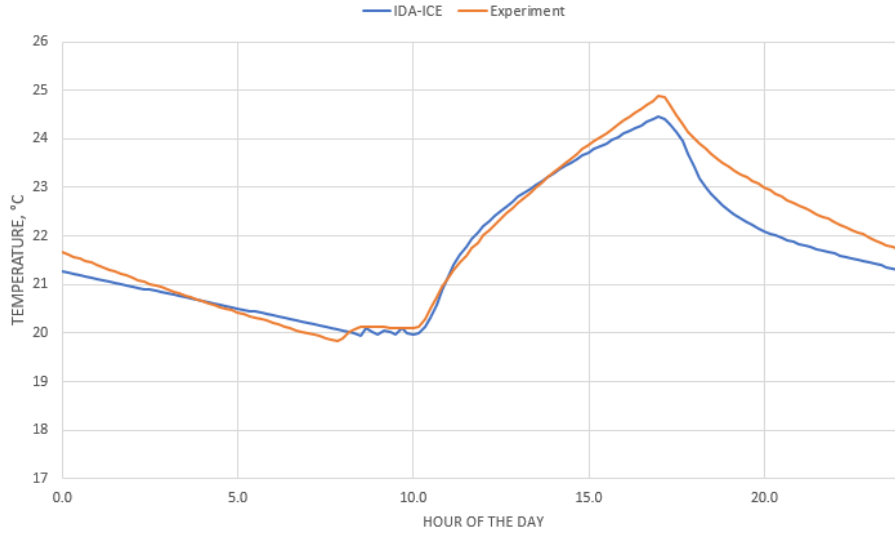
Figure 2.26: Validation of the implementation of PCM in IDA ICE

viation during the cooling period. The indices are calculated as presented in table 2.11.

Table 2.11: Results of the indices from the hot-box validation of PCM

Indices	Value
ΔT_{max}	0.92°C
$|\Delta T|$	0.31°C
RMSE	0.41°C
NRMSE	1.80%

According to I. ASHRAE (2017), a model can be considered to be calibrated if RMSE are lower than 30% when hourly data are used and 15% when monthly data are used. The RMSE found in this validation is 1.8%, which are far below the criteria by I. ASHRAE (2017). Even though the results are quite accurate, the deviation in the cooling process is of interest. As described in 1.3.2, most PCMs have different partial enthalpy change at different temperatures for heating and cooling. The hysteresis for this test is neglected, and due to the lack of information from DuPont about the panels, it is hard to know it if was reasonable to neglect or not.

51

As figure 2.26 shows, the temperature drops more rapidly in the simulation than in the hot box experiment. This could be to wrong distribution of the partial enthalpy change during cooling in the simulation. When controlling the enthalpy change of the PCM in the simulation, as shown in figure 2.27, it is clearly that the PCM model in IDA ICE absorb and release energy as implemented.
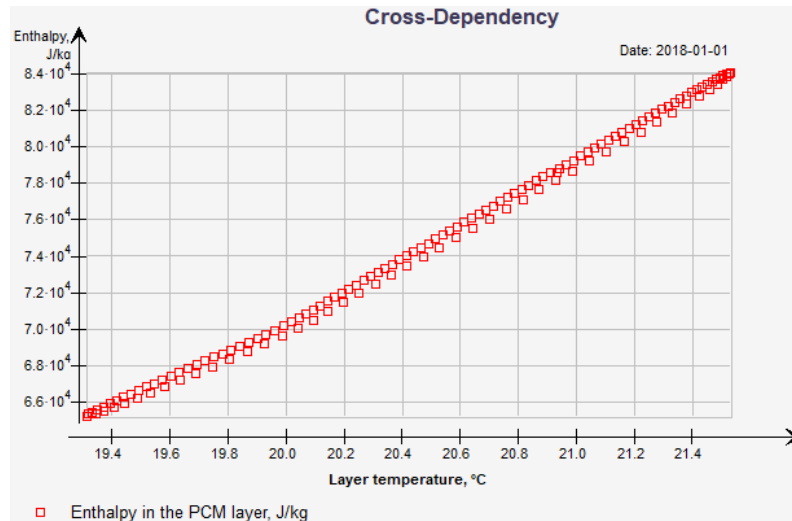
Figure 2.27: Enthalpy in PCM layer as a function of temperature, print screen from IDA ICE

Figure 2.27 also shows that the PCM layer only achieve a peak temperature at about 21.6°C. The peak change in the enthalpy is, according to figure 2.19, at about 24°C. This implies that the PCM don't reach complete melting and that the effect of the PCM probably would be even higher if it was heated more. This can also be seen by logging the different modes of the PCM. The log of the different modes can be seen in figure 2.28. The figure shows that the PCM only reaches mode "1", which implies that it is melting. If the PCM had melted completely, the PCM should reach mode "2".

These findings do not explain why there are differences between the experiment and the simulation, but they give some information of how the PCM has reacted to the increased temperature. Without having access to more detailed information about the DuPont PCM panels, it is hard to make a conclusion of the deviation during cooling. It would be interesting to perform another hot box experiment with a more detailed described PCM, and within a setting where the PCM reached complete melting. Even so, the results, both by visual comparison and by the indices are shown to be quite accurate enough in accordance to I. ASHRAE (2017).
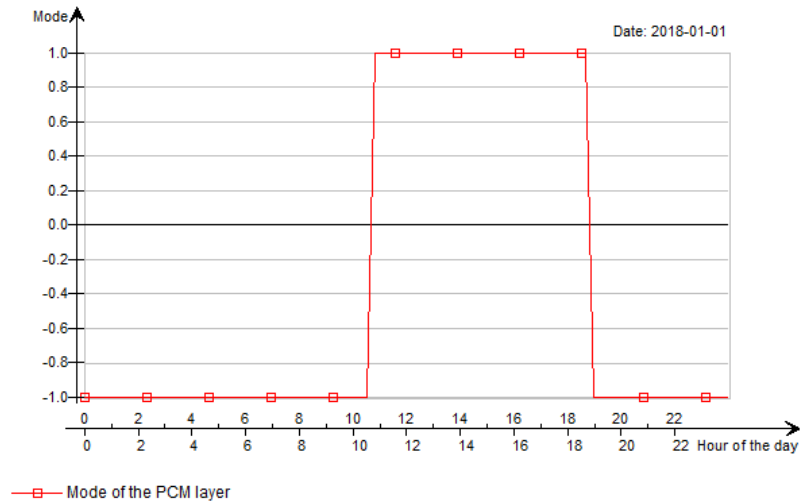
Figure 2.28: The different modes of the PCM during the simulation of the hot box, print screen from IDA ICE

2.3.4 Conclusion for the validation tests of the PCM model

Through the validation tests in this chapter, a conclusion for the PCM model can be made.

– The validation by Cornaro et al. (2017) shows that the PCM model in IDA ICE is accurate. Even though this test is not enough to state that the entire PCM model is valid, the results does not invalidate the model.

– Through the hot box validation, the PCM model was found to be very precise during the heating of the PCM. Some deviation was found during the cooling period, which can be due to lack of information about the DuPont^{TM} Energain® PCM panels.

– During the hot box validation, the behavior of the PCM was investigated and found to be behaving as expected. The PCM is both melting and solidifying, and the PCM is proven to be storing energy.

As a conclusion, the PCM model in IDA ICE is proven to be valid for representing real measurements of PCM. These results do not give any reason to doubt that IDA ICE handles PCM in a correct way. The PCM model will therefore be used for further investigation of how it can affect the indoor environment in the Viking Ship Museum. Even so, the PCM model is still in beta level in IDA ICE and should be used carefully.

2.4 Single zone case study of PCM

As shown in chapter 2.2 the HMwall model was found to have limitations in the validity, and the effectiveness from moisture buffering for concrete was found low. The moisture buffering will therefore not be used for further investigation of the Viking Ship Museum. The single zone case study described in this chapter therefore only focus on how PCM can stabilize the indoor temperature in the "Gokstad" exhibition room. It has been a great focus on achieving the exact same energy consumption for all cases, so that the only factor that affected the indoor environment is the implementation of PCM. To do so, all other parameters have been made either constant, scheduled or dependent on outdoor conditions. It is important to understand that the temperatures achieved in this study may be too high or too low, but the focus is the stabilization (e.g. fluctuations) of temperature.

2.4.1 The model

The geometric model in IDA ICE was received from Rebecca Lundqvist, but some changes was done before the simulations was executed. Lundqvist (2018) used an external software to build the model, and then imported it to IDA ICE. As a result, the geometry of the building was unchangeable. Even so, it was possible to extract the zones and merge them together. This is illustrated in figure 2.29 and was done in order to focus on one single zone, and to reduce the potential risk of errors.
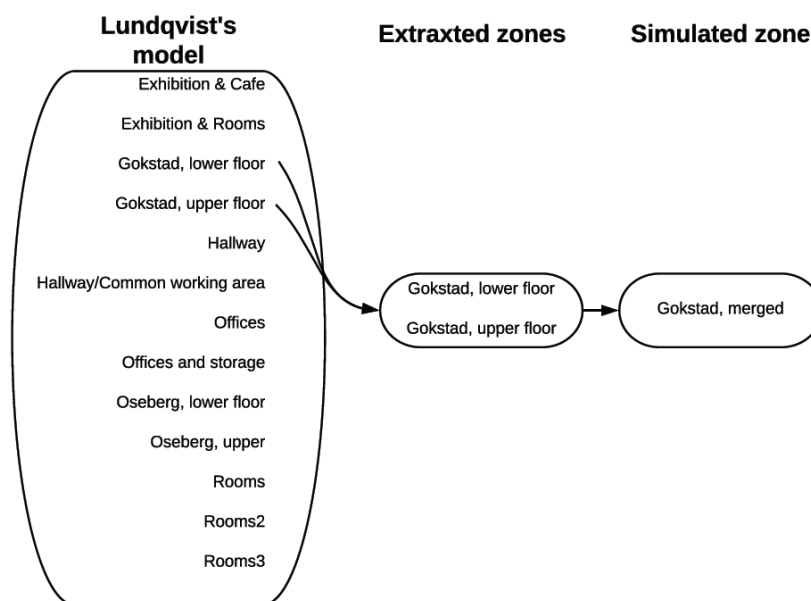
Figure 2.29: The process of changing Lundqvist's model to a single zone.

The geometry of the model before and after the extraction can be seen in figure 2.30.

(a) The museum model from Lundqvist

(b) The "Gokstad" exhibition room
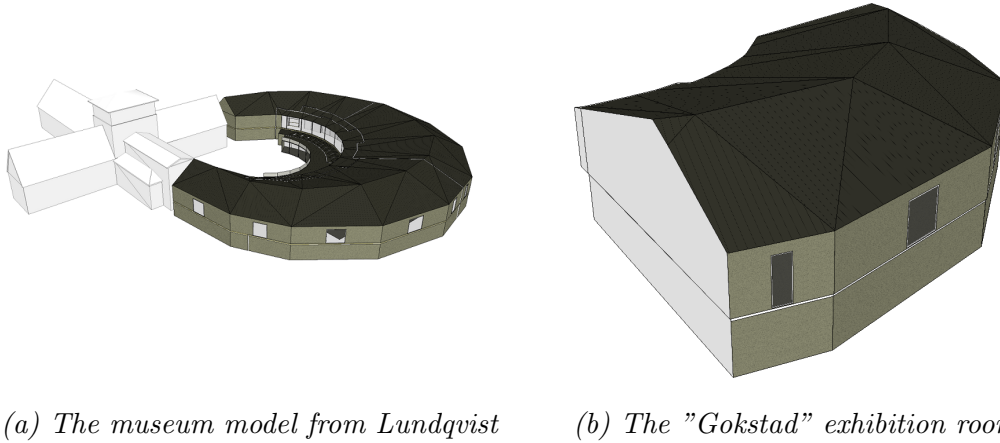
Figure 2.30: The geometry of the IDA ICE models in the single zone case study

Lundqvist (2018) received some preliminary data from Hjellnes Consult for some of the building parts and internal gains. Values from NS 3031 was used for the equipment and lighting, which are given as W/m^2. The area used for these values are the gross area of the building, which in many cases are larger than the floor area. When the zone was made, the area given in the model was based on the floor area but was changed to $2250m^2$ according to information from Hjellnes Consult. Some of the parameters given from Hjellnes Consult are shown in table 2.12.

Table 2.12: Input parameters to the IDA ICE model

U-values	Value	
External walls	$0.12W/m^2K$	
Roof	$0.08W/m^2K$	
Slab on ground	$0.08W/m^2K$	
Window and doors	$0.80W/m^2K$	
Other parameters	**Value**	
Leakage	0,6 ohm	
Thermal bridges	$0.03W/m^2K$	
Internal gains	**Museum open**	**Museum closed**
Equipment	$1.0W/m^2$	$0.0W/m^2$
Light	$8.0W/m^2$	$4.0W/m^2$

All of the external building parts have been implemented as concrete with external insulation, while the internal building parts are only concrete. The thickness and conductivity of the insulation has been modified in order to meet the demands in table 2.12.

The occupancy in the new museum is for now not known, as the museum is expected to have more visitors after the new museum has been made. Hjellnes Consult has predicted a total amount of 650 people in the "Gokstad" exhibition room, with an expected distribution as shown in figure 2.31.
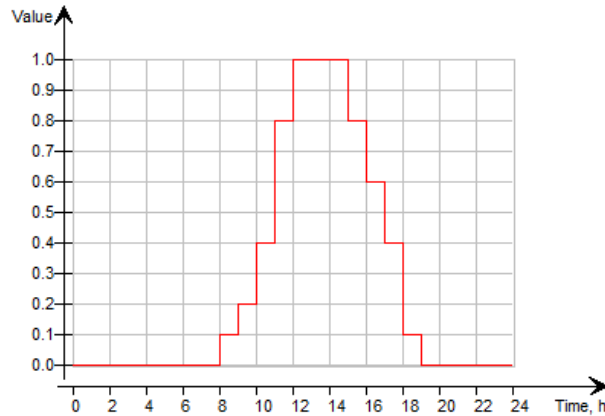
Figure 2.31: Expected distribution of the occupancy in the "Gokstad" exhibition room, print screen from IDA ICE

Distribution of hot water was not described by Hjellnes consult but was implemented as $10kWh/(m^2 \cdot year)$, as described in NS3031.

The demands for the indoor environment, as described by Hjellnes Consult are:

1. Overall temperate range during a year: 16-25°C

2. Overall RH range during a year: 35-65%

3. RH range during summer (May 1st - Sept 30th): 55% ±10% (45-65%)

4. RH range during winter (Oct 1st - Apr 31st): 45% ±10% (35-55%)

Some fluctuations of temperature and RH are accepted, but not more than 5% fluctuation of RH within 24 hours.

As technical installations as heating, cooling and ventilation of modern buildings are based on sensors and thermostats that provides signals and adjust the effects, they had to be modified. The technical installations were made constant so that PCM was the only change that could affect the indoor environment.

The ventilation system was described by Hjellnes Consult to be as high as $15m^3/m^2h$ for the exhibition rooms. This high value was used due to high thermal load from the occupants and large fluctuation in humidity from the occupants. The passive house standard (NS 3017) describes an air flow at $6m^3/m^2h$ for cultural buildings. For this study, to see the effect of PCM, $6m^3/m^2h$ has been used. The ventilation has been implemented as a CAV-system (Constant Air Volume), with a scheduled

temperature. The temperature of the provided air is 12°C when the museum is closed, and 20°C when the museum is open. The schedule can be seen in figure 2.32. Even though the ventilation system is controlled to provide constant temperatures, there are no cooling coils in the system. As a result, the provided air will not be lower than the external temperature. The heat recovery was also turned off to assure that the energy consumed was related to only external factors. By scheduling the system like this, dissimilarities between the simulations was removed and at the same time provide a temperature range possible to achieve results from.
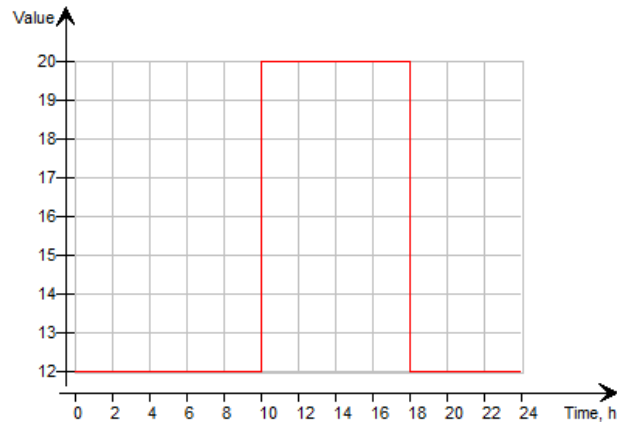
Figure 2.32: The schedule for the ventilation temperatures, print screen from IDA ICE

The heating and cooling systems are hard to keep constant within a year, as there is much more heat loss in the winter than in the summer. A constant system would often result in overheating in the summer, and not enough heating in the winter. As the ventilation system provided air with given temperatures, it was possible to remove the heating and cooling units entirely in the summer without achieving temperatures that was unreasonable for the study. The simulation has been done from July 2nd till July 8th in 2018. The temperature range was found to be from 18.23-25.21°C within the simulated period. A more detailed view of the temperature in the simulated week can be seen in figure 2.33. In order to investigate the stabilization effect from PCM it was found sufficient to only carry out a summer simulation.

Even though the mean air temperature fluctuates several degrees, the wall will react much slower to the change of temperature, as proven in the hot box validation in chapter 2.3.3. IDA ICE has made it possible to log the wall temperatures, either as a surface temperature or within the wall. The surface temperatures for the simulated week are shown in figure 2.34. When evaluating the indoor environment, it is the mean air temperature that is compared, but the surface temperatures give information about which temperatures that are expected within the PCM when
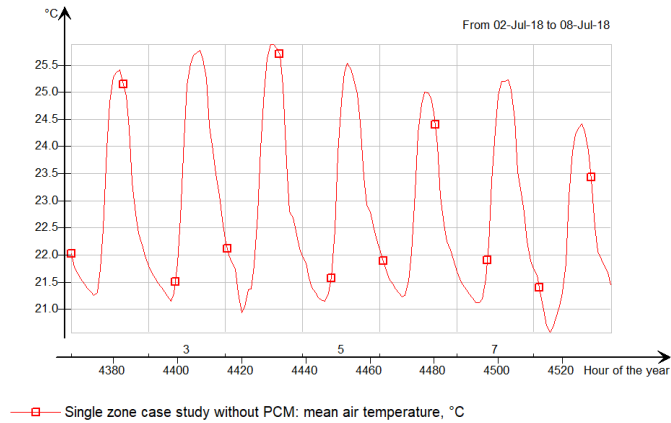
Figure 2.33: Results of the temperatures from the simulated week in the single zone case study without PCM implemented, print screen from IDA ICE

implemented. Figure 2.34 shows much less fluctuations in the temperature than the mean air temperatures shown in figure 2.33. The daily fluctuations of the mean air temperature are about 4°C, while the surface temperatures are at about 2°C
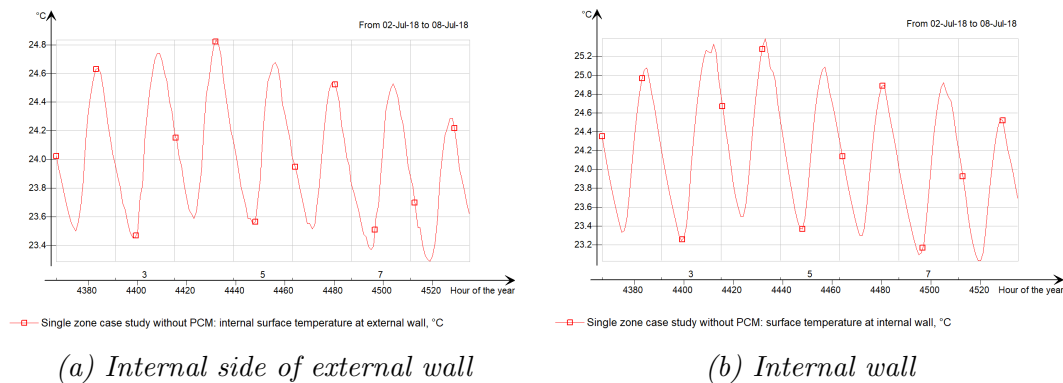
(a) Internal side of external wall

(b) Internal wall

Figure 2.34: Surface temperature at an external and an internal wall in the single zone case study without PCM, print screen from IDA ICE

2.4.2 Selecting PCM

As described in chapter 1.3.2, there are several different PCMs available for implementation in a building. Rubitherm is one of the manufacturers that provides detailed description of their PCMs, and their database has therefore been chosen as the source for selecting PCM. There are five different properties evaluated for selecting PCM for this exact building, which are listed below.

– Type of PCM

– Melting temperature

– Total change of enthalpy

– Level of hysteresis

– The gradient of the change in enthalpy

Rubitherm Technologies GmbH (n.d.[d]) provides several different PCM products, varying from general PCM to specific products. The RT-LINE and SP-LINE, which are organic and inorganic PCM, respectively, was the two general PCM products relevant for this study. The RT-LINE has equal melting and solidifying temperatures, while the SP-LINE has some degree of hysteresis. The conductivity of the material is, as described in chapter 1.3.2, an important factor when selecting PCM. With a low conductivity, the PCM may not absorb and release the energy as fast as wanted. The RT-LINE has a conductivity of 0.2 W/mK, while the SP-LINE has a conductivity of 0.6 W/mK. The SP-LINE is based on these values preferred, due to higher conductivity. Rubitherm states that these PCMs can be produced at almost all temperatures. Even though the RT-LINE could give the wanted effect in the museum, organic PCMs are flammable (see table 1.1) and will therefore not be used further in this study. The usage of flammable PCMs are seen as unaccepted for a museum. As a result, the SP-LINE has been used further.

The mean air temperature range found from the simulations without PCM reach a temperature between 25 and 26°C. When looking at the detailed temperatures in figure 2.33 it is possible to focus on the fluctuations that occurs most frequently. The fluctuations usually stay within a temperature range between 21.3-25.0°C.

All of the Rubitherm PCMs in the SP-LINE can be modified to have a melting temperature from -21°C till 70°C. Even though all the PCMs can be adjusted, Rubitherm provides recommended temperature range for the different products. As a result, PCMs that lies within a temperature range expected to find in a building are evaluated, with the possibility to be adjusted some degrees. This adjustment will be described later.

Rubitherm Technologies GmbH (n.d.[c]) provides variation of total enthalpy change for their PCMs. The total enthalpy change of the PCM in the SP-LINE lies between 150-330kJ/kg. With a high level of enthalpy change, more energy can be stored. The PCM listed with melting temperatures within the expectancy in a building has a total enthalpy change from 170-200kJ/kg. These PCMs can be seen in table 2.13.

A summary of the gradient and hysteresis of the different PCMs can be seen in table 2.14. The gradient (i.e. how fast the PCM melts and solidify) can be seen by looking at the peak partial enthalpy change. With a low peak partial enthalpy change, the PCM melts at a temperature range over several degrees, while a high peak partial enthalpy change implies that the PCM mainly melts at a specific temperature. The

Table 2.13: PCMs from the SP-LINE with a melting temperature suitable for buildings (Rubitherm Technologies GmbH, n.d.[c])

Product	Melting temperature	Total enthalpy change
SP 21 EK	21 <> 23°C	170 kJ/kg
SP 24 E	24 <> 25°C	180 kJ/kg
SP 25 E2	24 <> 26°C	180 kJ/kg
SP 26 E	25 <> 27°C	180 kJ/kg
SP 29 Eu	29 <> 31°C	200 kJ/kg

level of hysteresis is in table 2.14 described by the temperature difference between the main peak for melting and solidification.

Table 2.14: Gradient and level of hysteresis of the PCMs in the SP-LINE (Rubitherm Technologies GmbH, n.d.[c])

Product	Peak partial enthalpy changes		Level of hysteresis
	Melting	Solidification	
SP 21 EK	49 kJ/kg	71 kJ/kg	1°C
SP 24 E	147 kJ/kg	128 kJ/kg	2°C
SP 25 E2	50 kJ/kg	71 kJ/kg	2°C
SP 26 E	109 kJ/kg	96 kJ/kg	1°C
SP 29 Eu	106 kJ/kg	61 kJ/kg	2°C

A steep gradient has been considered to be an advantage in order place a desired maximum temperature in the building, while a more distributed enthalpy change can be an advantage when the building reaches different peak temperatures every day. The level of hysteresis selected depends on the temperature fluctuations within the building. If the temperature only varies between 22 and 24°C, it could be desirable to select a PCM with low level of hysteresis. By doing this, the PCM can store the heat at 23°C and release it immediately when the temperature drops. A higher level of hysteresis can be an advantage when the temperature fluctuations are dimensioned to be higher (e.g. night time cooling). With a temperature fluctuation between 20 and 25°C, the PCM can store the heat at 24°C and release it when the temperature drops to 22°C.

Rubitherm SP 26 E has been selected for this study. A steep gradient for the enthalpy change has been seen as an advantage to see the effect from PCM isolated. Even though there are some temperature fluctuations within the building, it has been concluded to have a lower level of hysteresis. This conclusion is mainly based on the surface temperatures shown in figure 2.34. The surface temperature of the

walls is fluctuating much less than the mean air temperature. The partial enthalpy change for Rubitherm SP 26 E can be seen in figure 2.35.
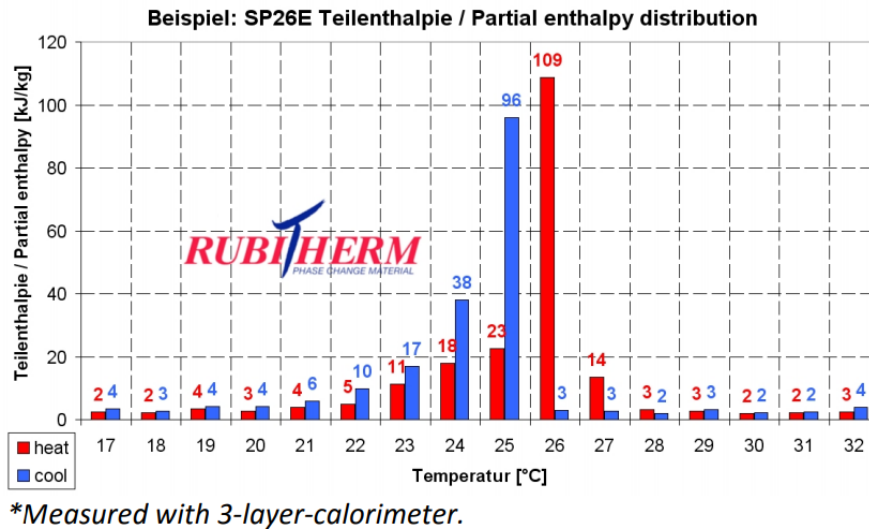
Figure 2.35: *Partial enthalpy change of Rubitherm SP26 (Rubitherm Technologies GmbH, n.d.[b])*

2.4.3   Adjusting the PCM

As seen in figure 2.35, the peak partial enthalpy change for heating is at 26°C and for cooling at 25°C. The fluctuations of the surface temperature in the summer are from 23-25°C (according to figure 2.34). When trying to evaluate which melting and solidifying temperatures that gave best result for the case, if was found necessary to do simulations of seven PCMs with different properties. The seven different PCMs implemented in IDA ICE are presented in table 2.15. The PCMs are described by HXXCXX, where "HXX" and "CXX" presents the temperature for the peak enthalpy change during heating and cooling. With this system, H25C24 describes a PCM with peak partial enthalpy change during heating at 25°C and during cooling at 24°C.

As described earlier in this chapter, there are PCMs available without hysteresis. It was found necessary for the study to modify one PCM instead of using several different PCMs with different change in enthalpy. By modifying one PCM the effect from the hysteresis is easier to see. PCM H25C24 and H24C23 are implemented with hysteresis, while the rest are implemented without hysteresis and melting temperatures varying from 21-25°C. Even though the simulated PCMs are modified, they are representative as there are many PCMs that have similar properties.

Table 2.15: Data for the two PCM tests after modification

PCM	Total enthalpy change	Peak melting temperature	Peak solidifying temperature	Hysteresis
H25C24	183 kJ/kg	25°C	24°C	1°C
H24C23	183 kJ/kg	24°C	23°C	1°C
H25C25	183 kJ/kg	25°C	25°C	0°C
H24C24	183 kJ/kg	24°C	24°C	0°C
H23C23	183 kJ/kg	23°C	23°C	0°C
H22C22	183 kJ/kg	22°C	22°C	0°C
H21C21	183 kJ/kg	21°C	21°C	0°C

2.4.4   Implementation of the PCM in the model

When PCM was implemented in the model, it could have been done in several ways. PCM can be found in slabs, walls, roofs, or implemented in internal objects. For this study, 5.26 mm of PCM is implemented internally at the external walls and at the internal walls. The thickness of the PCM is the same as used in the hot box experiment described in chapter 2.3. This results in about 1500 m^2 of PCM, which may seem like an unreasonably large area. When including the possibility to implement PCM in the internal floor (about $1200 m^2$), roof (conservative calculated flat to be about 1200 m^2), internal slabs or to implement PCM as internal glazing walls, the area seems a bit more realistic. An example of PCM as an internal wall can be seen in figure 2.36, which is a product by GLASSX AG with Rubitherm PCM inside. This study is not to investigate where to locate the PCM within the building, as exact placement for the museum artifacts and architectural details within the buildings are not known. For this study, the amount of PCM in external and internal walls have been used equally for all simulated PCM cases.

Rubitherm SP 26 E is given with 16 temperature coordinates (from 17 till 32°C) as seen in figure 2.35. By adding all the temperature coordinates into IDA ICE, the program will assume the melting process is ongoing at 31 degrees, while it can be considered to reach complete melting around 27°C. Rubitherm Technologies GmbH (n.d.[b]) give a specific heat capacity at $2kJ/kg{\cdot}K$ for the PCM, which can be recognized from the enthalpy changes at low and high temperatures in figure 2.35. It has therefore been chosen to just add the 7 temperature coordinates where the partial enthalpy change is remarkably higher than $2kJ/kg{\cdot}K$. In addition, the total change of enthalpy during heating and cooling are not equal. IDA ICE requires that the total change of enthalpy is exact the same during heating and cooling. As a

Figure 2.36: Picture of GLASSXstore, a PCM wall for internal use (GLASSX AG, 2005)

result, some of the partial enthalpy changes are modified to give equal results.

The seven different PCMs simulated in the study are shown in figure 2.37-2.43. After all the seven PCMs was implemented in the single zone model, the total energy consumption was compared to make sure the only change in the model was a direct result of the PCMs. The energy consumption was found equal and the results can be seen in chapter 3.2.
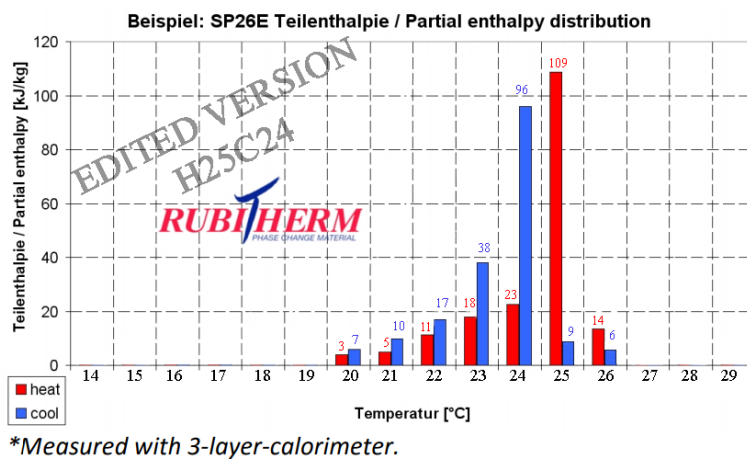
Figure 2.37: Partial enthalpy change of H25C24 after modification for this study

63
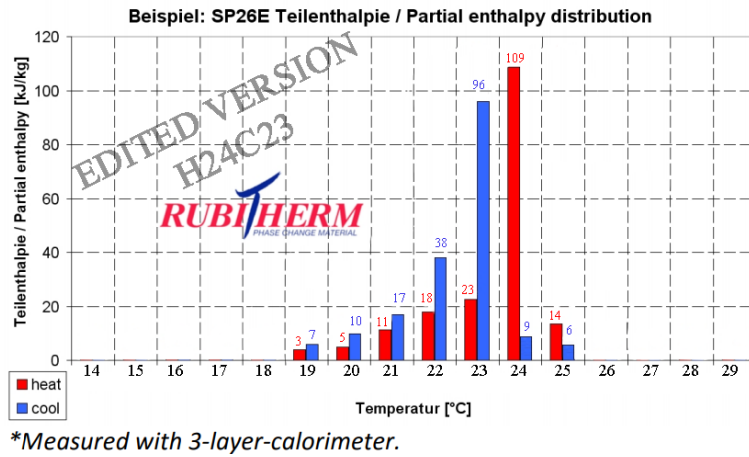
Figure 2.38: Partial enthalpy change of H24C23 after modification for this study
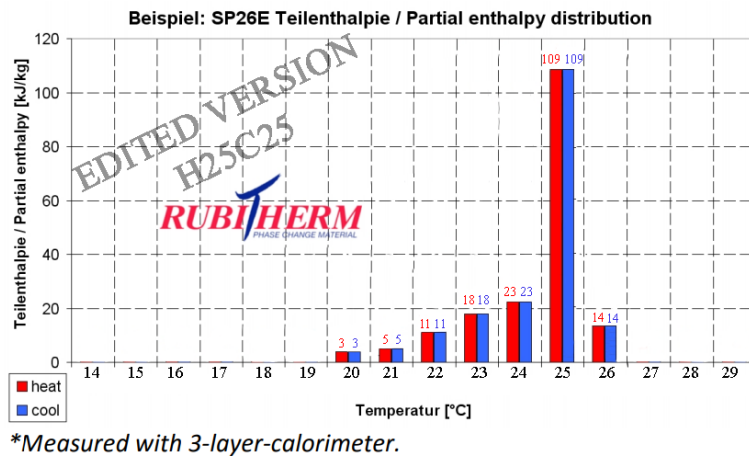
Figure 2.39: Partial enthalpy change of H25C25 after modification for this study
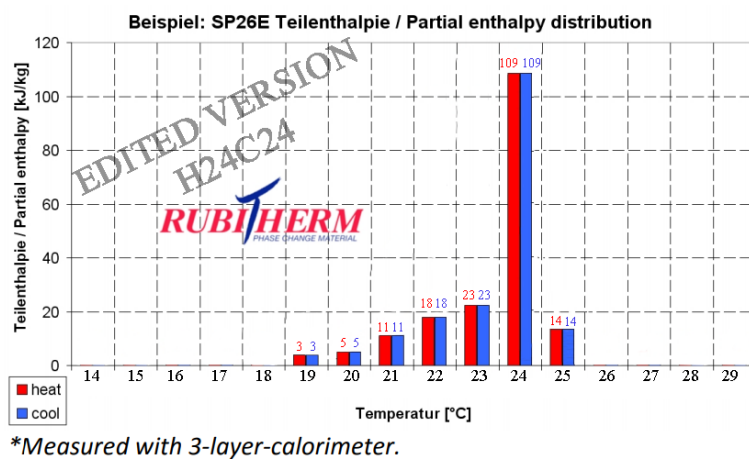
Figure 2.40: Partial enthalpy change of H24C24 after modification for this study
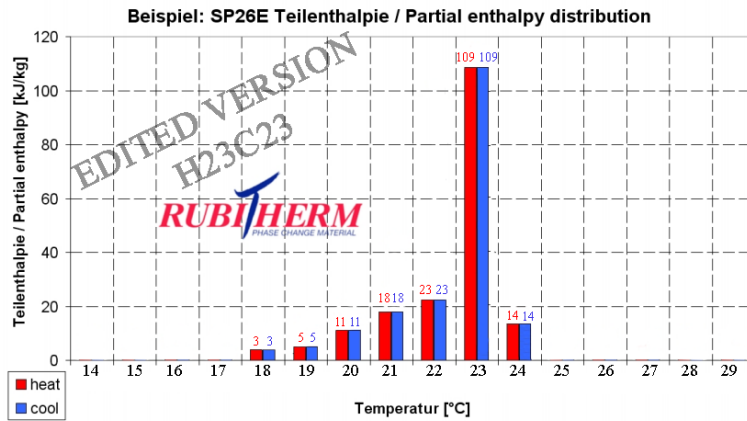
Figure 2.41: *Partial enthalpy change of H23C23 after modification for this study*
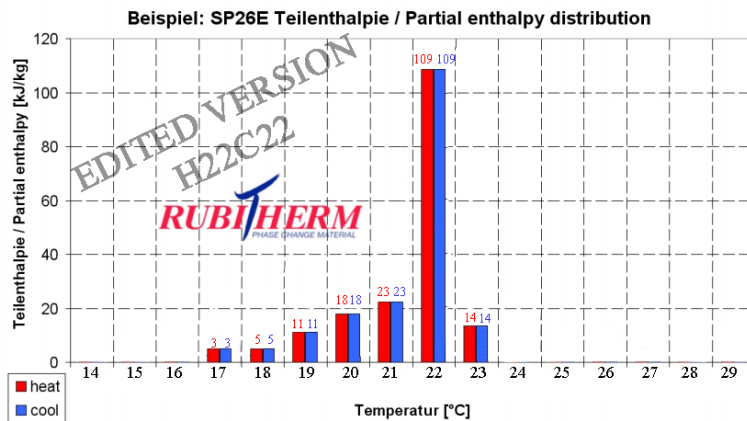
Figure 2.42: *Partial enthalpy change of H22C22 after modification for this study*
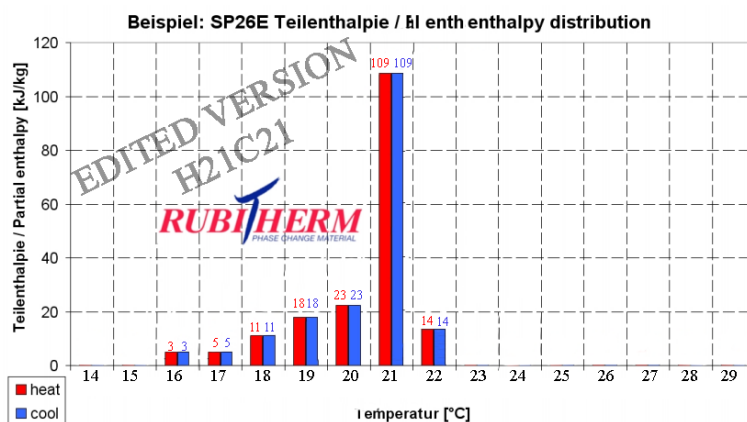
Figure 2.43: *Partial enthalpy change of H21C21 after modification for this study*

2.5   Whole building case study with PCM

The whole building simulations described in this chapter are a study of how PCM affects the indoor environment, energy consumption and peak energy demand in the museum. The PCM is implemented in the "Gokstad" exhibition room, but in difference to the single zone simulation, the zone will now interfere with the rest of the building. The HVAC systems now are sensor controlled, which makes it possible to study the effect on the energy consumption and peak energy demand. When studying the indoor environment, only the temperatures in the "Gokstad" exhibition room are presented. Some of the other zones may be reaching uncomfortably high or low temperatures, but this study is only focusing on the "Gokstad" exhibition room.

Parallel with this study, Tor Atle Skramdal has been studying how the ventilation system can stabilize the indoor environment. A model of the museum with sensor-controlled ventilation systems has been received from him for investigation. It is important to state that the ventilation systems are not complete at this stage. During Skramdal's study he found that the air flow rate had to be high to reduce the risk for overheating. In order to decrease the cost for both implementation and operate the ventilation systems, the air flow rate should be as low as possible, but still provide enough fresh air. By taking the implementation of PCM into account, the fluctuations could possibly be stabilized. A flowchart of how the model have been built can be seen in figure 2.44.
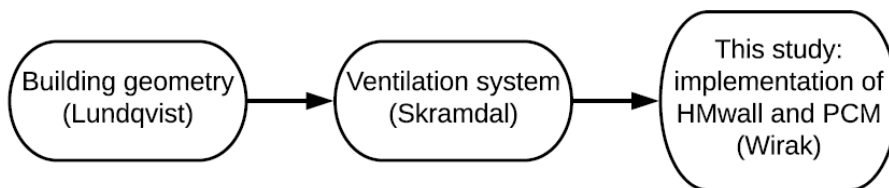
Figure 2.44: The process of modifying the museum model

2.5.1   The model

The model received from Skramdal was implemented with three different ventilation systems. The most advanced system was controlling the air in the exhibition rooms, while two more standard balanced systems with heat recovery controlled the air in the other rooms (e.g. hallway, office, etc.). The ventilation system for the exhibition rooms are shown in figure 2.45. The system consists of a heat recovery wheel, a

desiccant wheel, two heaters, one cooler and a humidifier. In addition, the rooms had water radiators for heating.
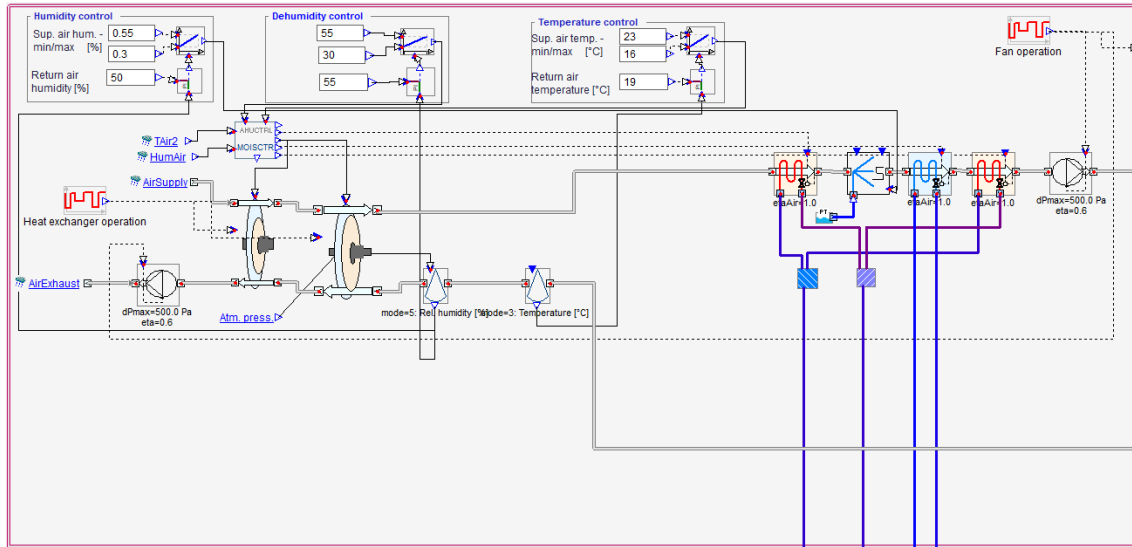
Figure 2.45: Overview of the ventilation system in the exhibition rooms, given from Tor Atle Skramdal

The ventilation system used for this study has an constant air flow rate at $6m^3/m^2$ in the entire museum. The main reason for choosing CAV system is to assure that the artifacts are provided with fresh air at all time.

In difference to the single zone study in chapter 2.4, the "Gokstad" exhibition room is now as two zones. This is the geometry from Lundqvist's model and it has not been changed in Skramdal's model. The slab between the zones is implemented with large openings to assure the air between the zones is mixed. The measured temperatures are taken from the lower part of the exhibition room, due to the fact that this is where both the main artifacts and occupants are.

The model was simulated for three different periods:

- **Summer Simulation:** From July 2nd till July 8th in 2018, to investigate the effect on the IAQ

- **Winter simulation:** From Jan 1st till Jan 7th in 2018, to investigate the effect on the IAQ

- **Entire year simulation:** The entire year of 2018, to find the energy consumption and peak energy demand

As presented in chapter 2.4, the surface temperature is expected to fluctuate less than the mean air temperature. Figure 2.46 shows the mean air temperature and surface temperature in the lower part of the exhibition room during a summer

simulation. The surface temperature is measured from the internal side of one of the external walls.
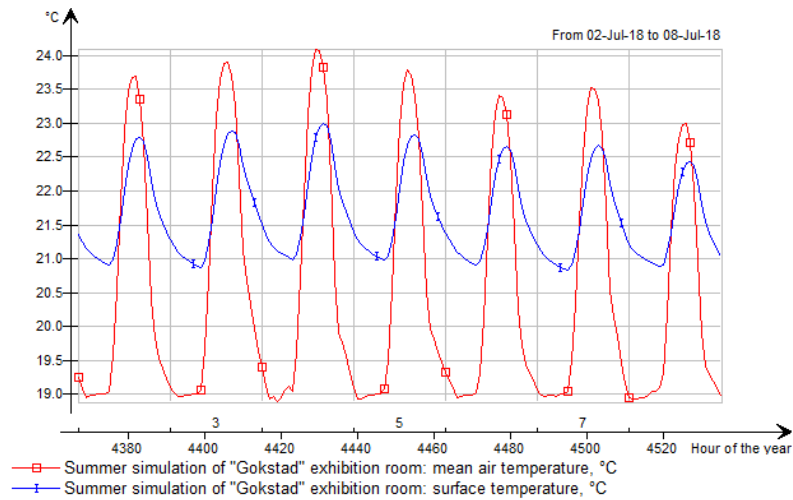
Figure 2.46: Measures temperatures during the summer simulation in the whole building case study without PCM

As seen in figure 2.46, the mean air temperature is fluctuating much more than the surface temperature. The mean air temperature is fluctuating about 5.0°C (from 19-24°C), while the surface temperature only fluctuates about 1.5°C (from 21-22.5°C). The mean air temperature and surface temperature from the winter simulations can be seen in figure 2.47.
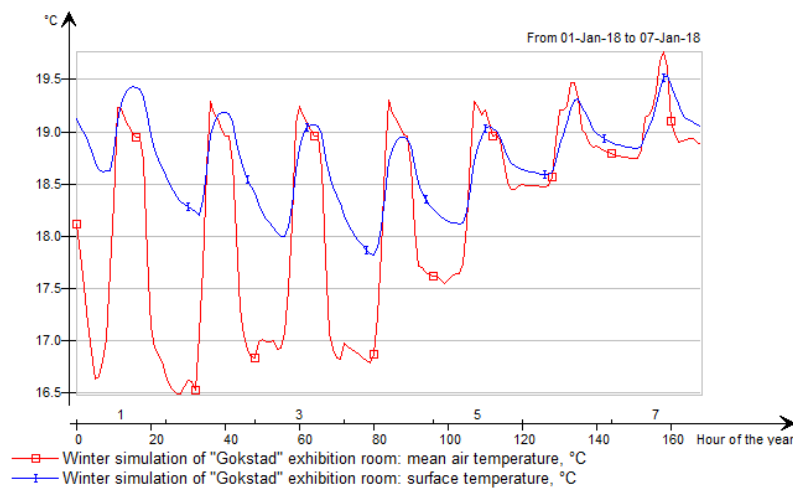
Figure 2.47: Measures temperatures during the winter simulation in the whole building case study without PCM

Figure 2.47 shows that the mean air temperature is fluctuating about 3.0°C (from 16.5-19.5°C). The results also show that the temperature is increasing during the week, which are due to higher external temperatures. The surface temperature is fluctuating about 2.0°C (from 17.5-19.5°C). When comparing the mean air and

surface temperatures in the winter simulation, one can see that the surface of the wall is reacting much slower to the increased temperature in the end of the simulated week. The Viking Ship Museum is designed with concrete (with high thermal mass), which delays the changes in the surface temperature. A summary of the measured temperatures both from the summer and winter simulations can be seen in table 2.16.

Table 2.16: Measures temperatures from the summer and winter simulations of the "Gokstad" exhibition room

Variable	"Gokstad" exhibition room
Summer: mean air temperature	19.0-24.0°C
Winter: mean air temperature	16.5-19.5°C
Summer: surface temperature	22.0-23.5°C
Winter: surface temperature	17.5-19.5°C

The main object when simulating the entire year is to find the effect on the energy consumption and peak energy demand when PCM is implemented. The zone has no coolers, except from cooling through ventilation, but there is a heater in both the upper and lower part of the exhibition room. There are no other zones connected to the air handling unit, which made it easy to find the energy consumed for HVAC. The energy for HVAC can be found from the following units:

- Heater in the lower part of the exhibition room

- Heater in the upper part of the exhibition room

- Heating through ventilation

- Cooling through ventilation

- Humidification through ventilation

- Fans in the ventilation

As the ventilation system uses constant air volume, the energy and peak energy demand for fans are the same for all the simulated cases. Even so, the energy for running the fans are included in order to compare the percentage difference of the energy consumption for HVAC between the models.

The energy consumption from the model before implementation of PCM can be seen in table 2.17.

Due to how the model has been built, it is hard to find the impact on the peak energy demand for the "Gokstad" exhibition room alone. All of the ventilation

Table 2.17: Delivered energy to "Gokstad" exhibition room, from the yearly
simulations without PCM in the whole building case study

Parameter	Value
Heating units	
Upper part	36 867.3 kWh
Lower part	35 588.9 kWh
Air handling unit	
Heating	126 745.0 kWh
Cooling	179 983.0 kWh
Humidification	184 512.0 kWh
Fans	39 195.0 kWh
Total energy	602 891.2 kWh
Specific energy	236.2 kWh/m^2

systems are connected to the same boilers, and as a result, the needed effect for the
boilers are for the entire building. The system had to be made different in order to
find the reduction of the peak energy demand for the "Gokstad" exhibition room
only. As the model was received without modification of either the ventilation or
the heating and cooling systems, the peak energy demand presented further is for
the entire museum. The peak energy demand before the implementation of PCM
can be seen in table 2.18.

Table 2.18: Peak energy demand from the yearly simulations in the whole building
case study, before implementation of PCM

Parameter	Peak effect
Electric cooling	114.7 kW
HVAC aux	127.7 kW
Fuel heating	651.9 kW

The "electric cooling" is the electricity used for cooling in the ventilation system.
The "HVAC aux" gives the peak effect for running all the ventilation systems (e.g.
fans etc.) but does not include the effect for heating and cooling through the venti-
lation. The effect for "fuel heating" is both the heating through ventilation and the
heating units placed in the museum.

2.5.2 Selecting PCM

The findings from the single zone study in chapter 2.4 have been used when choosing PCM for the whole building case study. These results are presented in chapter 3.2, and it is recommended to read though these results in order to understand the selection of PCM done for the whole building case study.

Even though the HVAC systems in this case are controlled by sensors and adjusted for the museum, the temperatures found from the summer simulations are comparable. The findings for both the mean air and surface temperature presented in table 2.16 are about 1°C lower than the measured temperatures in the single zone study in chapter 2.4 without PCM. Even though none of the PCMs implemented in the single zone case study in chapter 2.4 gave any stabilization effect, two of the PCMs (H22C22 and H21C21) managed to reduce the average mean air temperature by more than 1°C. The same PCMs also was shown to be storing the highest amount of energy during the simulated week. For the case study of the entire museum in this chapter, both H22C22 and H21C21 are chosen to investigate. It has also been seen as an option to perform simulations of other PCMs if the results from H22C22 and H21C21 turned out to indicate that other PCMs was better suited.

3 — Results

3.1 Brief

This thesis consists of three different main steps, which have been presented through the different parts of chapter 2.

1. Validate the HMwall and PCM models in IDA ICE

2. Evaluate the stabilization potential of moisture buffering and PCM in a single zone model

3. Evaluate the impact on the indoor environment, energy consumption and peak energy demand by implementing moisture buffering walls and PCM in the Viking Ship Museum

During the validation of the HMwall model in chapter 2.2 the model was found not valid for simulation when the building parts consisted of other materials than concrete (or "minerals" as EQUA described it). Even by running models which consisted of concrete only, the moisture buffering effect was shown to be ineffective. As a result, the HMwall model was not further used in this thesis. Therefore, this chapter will not present any results for moisture buffering in the Viking Ship Museum.

In the validation of the PCM model in chapter 2.3, the PCM was found to be valid and has therefore also been used to evaluate how PCM can affect the Viking Ship Museum. The results presented further on in this chapter are related to the single zone study (chapter 2.4) and the whole building case study (chapter 2.5).

3.2 Results for the single zone case study

The effect on the mean air temperature within the "Gokstad" exhibition room by implementing PCM can be seen in figure 3.1. The blue line in the figure is the result from the model without PCM, while the other lines represents PCMs as described in the figure. It is clearly that all of the PCMs reduced the peak temperatures in the zone, but the changes in the fluctuations are not clear from the figure.
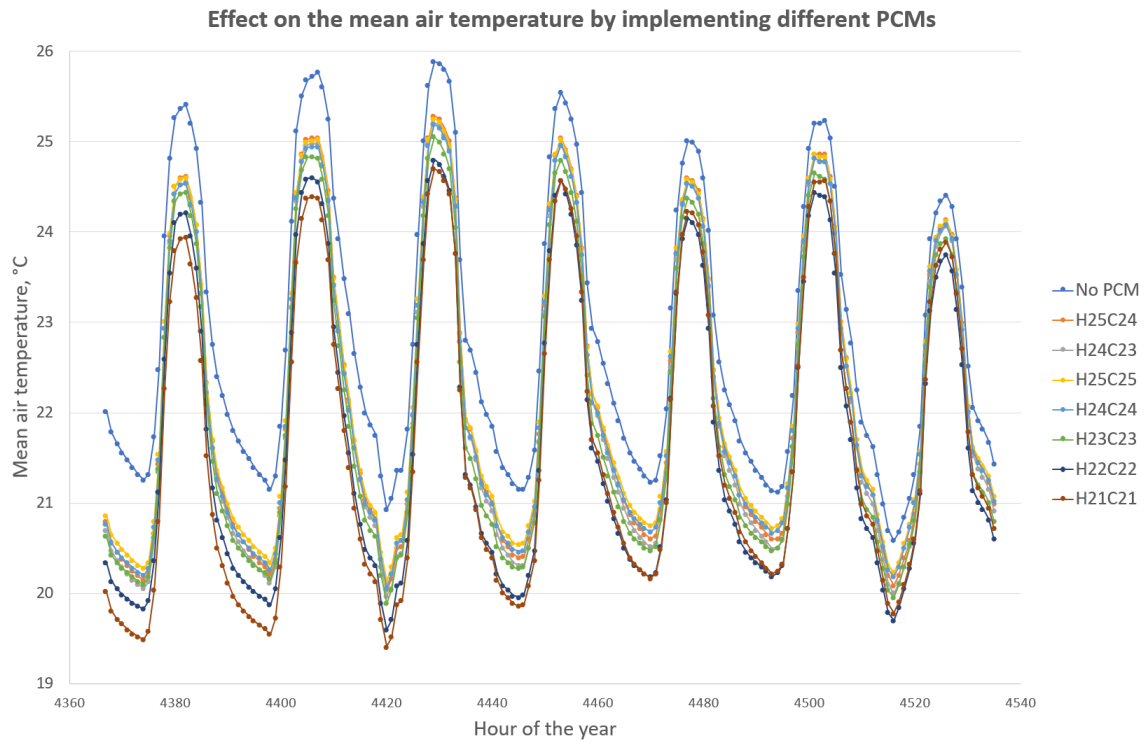
Figure 3.1: Simulation results of how PCM affected the mean air temperature in the single zone model

To find the distribution of the temperatures, box-plots has been made. The box-plot for the different models can be seen in figure 3.2.
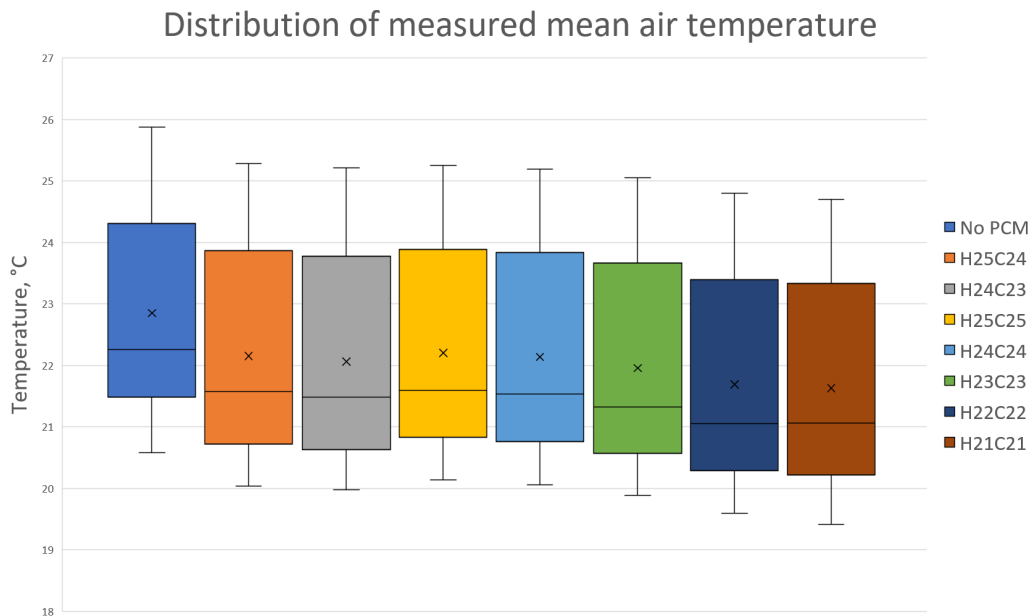
Figure 3.2: Distribution of the measured mean air temperature in the different models in the single zone case study

The solid colors in the box-plots represent the measured values between first and

third quartiles (i.e. 50% of the values). The "x" represents the average temperature and the line crossing the solid colors are the median. The thin upper and lower lines indicate the maximum and minimum values. The box-plot in figure 3.2 shows that the PCM affects the mean air temperature, but that the distribution is somehow similar for all the cases. When studying the exact measured temperatures, $\overline{T}$, $\Delta\overline{T}$, ΔT, TS and ΔTS can be evaluated. The results can be seen in table 3.1.

- $\overline{\boldsymbol{T}}$: Average mean air temperature [°C]

- $\boldsymbol{\Delta\overline{T}}$: Change in average temperature related to the case without PCM[°C]

- $\boldsymbol{\Delta T}$: Total change in mean air temperature $(T_{max} - T_{min})$ [°C]

- $\boldsymbol{TS}$: temperature stabilization index $(TS = \sum_{i=1}^{n} |\overline{T} - T_i|)$ [-]

- $\boldsymbol{\Delta TS}$: Change in TS related to the case without PCM [%]

Table 3.1: Effect on the measured mean air temperature by implementing PCM

PCM	$\overline{T}$	$\Delta\overline{T}$	ΔT	TS	ΔTS
No PCM	22.85°C	-	5.30°C	233.68	-
H25C24	22.15°C	-0.70°C	5.25°C	246.77	+5.60%
H24C23	22.07°C	-0.79°C	5.24°C	247.68	+5.99%
H25C25	22.21°C	-0.64°C	5.12°C	239.55	+2.52%
H24C24	22.14°C	-0.71°C	5.13°C	240.16	+2.78%
H23C23	21.96°C	-0.89°C	5.16°C	242.32	+3.70%
H22C22	21.69°C	-1.16°C	5.21°C	244.94	+4.82%
H21C21	21.63°C	-1.22°C	5.28°C	249.04	+6.57%

As seen in table 3.1, none of the implemented PCMs manage to reduce the fluctuations of the mean air temperature within the zone, as ΔTS is positive for all cases. According to these results, the fluctuations are actually increasing when PCM is implemented. The results show that the average temperature is reduced for all cases by implementing PCM. All of the PCMs reduced the average mean air temperature by 0.64°C or more, and two of the PCMs (H22C22 and H21C21) reduced the mean air temperature by more than 1°C.

In addition to the measured mean air temperature, the enthalpy and modes of the different PCMs have been tracked. The activity of all the PCMs can be seen in table 3.2.

- **H**: Measured enthalpy range of the PCM [kJ/kg]

- $\boldsymbol{\Delta H}$: Change in enthalpy [kJ/kg]

- **T**: Measured temperature range in the PCM [°C]

- **ΔT**: Change in temperature [°C]

- **Modes**: The modes of the PCM during the simulated period

Table 3.2: Data of how the PCMs have been acting in the simulations

PCM	H	ΔH	T	ΔT	Modes
H25C24	58-78 kJ/kg	20 kJ/kg	21.6-23.6°C	2.0°C	-1, 0, 1
H24C23	70-96 kJ/kg	26 kJ/kg	21.4-23.5°C	2.1°C	0, 1
H25C25	51-74 kJ/kg	23 kJ/kg	21.8-23.4°C	1.6°C	-1, 1
H24C24	62-91 kJ/kg	29 kJ/kg	21.8-23.3°C	1.6°C	-1, 1
H23C23	75-120 kJ/kg	45 kJ/kg	21.7-22.8°C	1.1°C	-1, 1
H22C22	90-180 kJ/kg	90 kJ/kg	21.5-22.3°C	0.8°C	-1, 1
H21C21	130-215 kJ/kg	85 kJ/kg	20.8-23.0°C	2.2°C	-1, 1, 2

The results in table 3.2 shows that the PCMs with low melting/solidifying temperature reaches a higher layer enthalpy. The PCMs implemented have the potential to store 183 kJ/kg, but none of the implemented PCMs managed to reach this potential. The highest change of enthalpy can be seen by H22C22, where the change was $90kJ/kg$. This is about half of the potential in the PCM. The general trend in the results are that if the PCMs are storing a great amount of energy, the temperature fluctuations within the material are decreased. This is not the case for H21C21, which is due to the fact that it is reaching mode 2 (i.e. completely melted) and therefore not going through a phase change any more. When the PCM reaches complete melting, the material is storing much less energy, and the temperature will increase faster.

By looking at the modes of the PCM along with the enthalpy of the layer, it is possible to track where on the enthalpy curve the PCMs are acting. Only H21C21 reaches complete melting (i.e. mode 2), while the rest of the PCMs are acting in mode -1 (solidifying), 0 (between melting and solidifying curve) or 1 (melting). A summary of where the PCMs without hysteresis are acting can be seen in figure 3.3.

By looking closer at one of the PCMs with hysteresis, it is possible to see how IDA ICE handles the hysteresis. The layer enthalpy of H25C24 can be seen in figure 3.4. The contour of the enthalpy curve can be seen in the figure, where "A" show the curve during heating and "B" show the curve during cooling. It is also clear that the PCM is handled with a constant heat capacity between the curves, marked as "C".
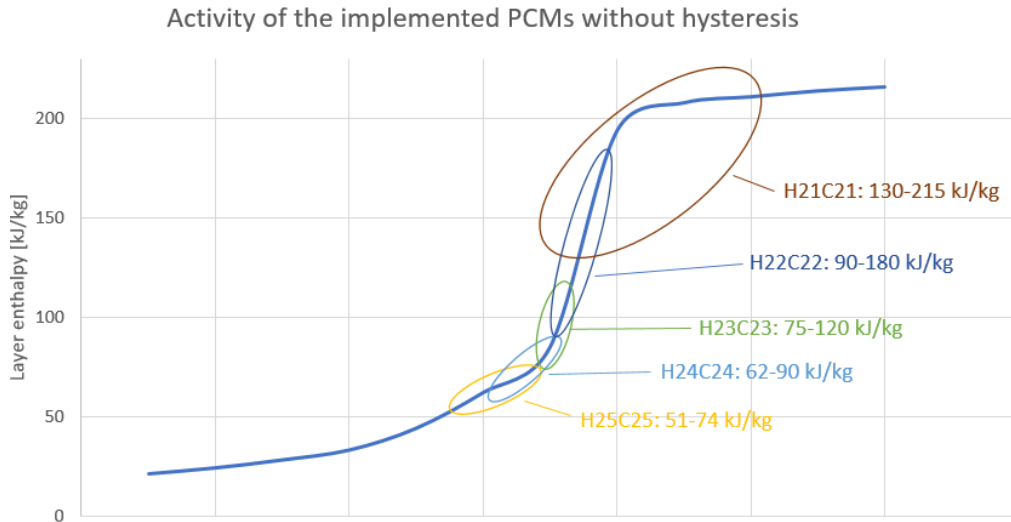
Figure 3.3: Illustration of where on the enthalpy curve the PCMs are acting in the simulated week
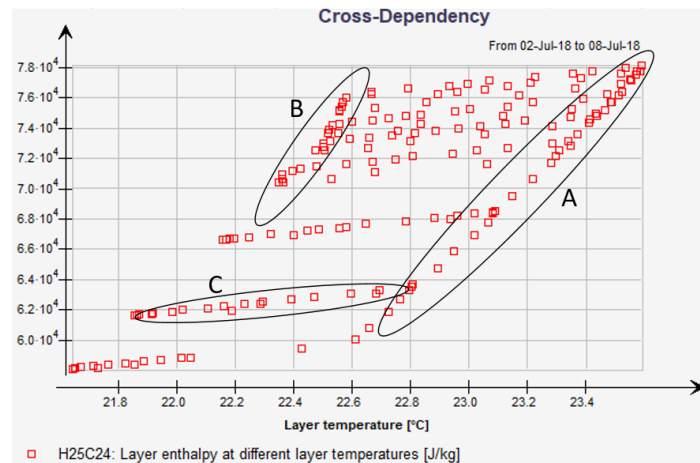
Figure 3.4: Layer enthalpy of PCM H25C24 as a function of temperature, dependent on the measured layer temperature

3.3 Results for the whole building case study

The whole building case study has been carried out with three different simulation periods, as described in chapter 2.5. This chapter will go through the results from each of the simulated periods.

Summer simulations

The effect on the mean air temperature from the summer simulations in the whole building case study can be seen in figure 3.5.
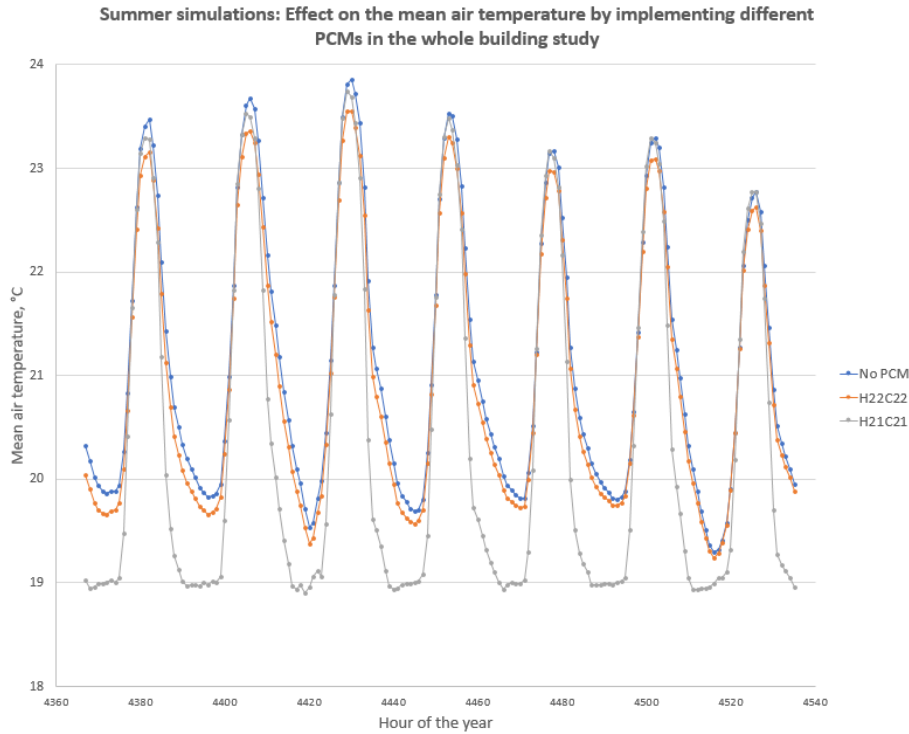
Figure 3.5: Simulation results of how PCM affected the mean air temperature during the summer simulations in the in whole building case study

The results found in these simulations are quite different from the single zone simulations in chapter 3.2. PCM H22C22 lowers the temperature both at nighttime and daytime compared to the case without PCM. PCM H21C21 on the other hand reduces the temperature at nighttime much more, but during daytime the temperature is about the same as for the case without PCM. It is clear by just looking at the temperature curves that H21C21 increases the fluctuations, while it is harder to evaluate the changes in fluctuations when implementing H22C22. Box-plots have been made from the results and can be seen in figure 3.6.

The box-plots show that H22C22 both reduced the average temperature and that the distribution is slightly decreased. H21C21 on the other hand has reduced the average temperature even more but has a more distributed result. The box-plot of H21C21 also shows that 50% of the measured temperatures are below 19.5°C. Temperatures this low is almost not measured at all in the case without PCM or with H22C22.

The measured temperatures have been exported and the same indices that was used for the single zone simulation presented in chapter 3.2 have been calculated. The results are shown in table 3.3.

- $\overline{T}$: Average mean air temperature [°C]
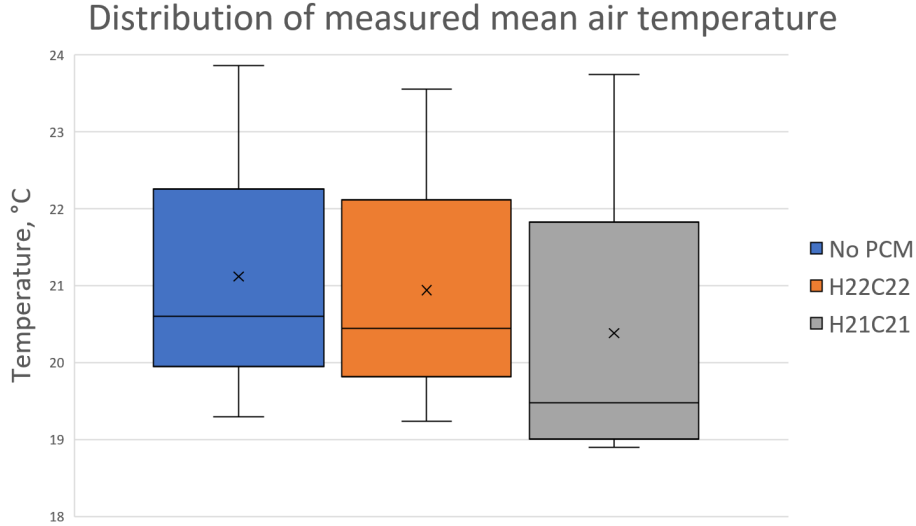
Figure 3.6: Distribution of the measured temperatures during the summer simulations in the whole building case study

- $\boldsymbol{\Delta \overline{T}}$: Change in average temperature related to the case without PCM[°C]

- $\boldsymbol{\Delta T}$: Total change in mean air temperature $(T_{max} - T_{min})$ [°C]

- $\boldsymbol{TS}$: temperature stabilization index $(TS = \sum_{i=1}^{n} |\overline{T} - T_i|)$ [-]

- $\boldsymbol{\Delta TS}$: Change in TS related to the case without PCM [%]

Table 3.3: Effect on the mean air temperature from the summer simulation in the whole building study

PCM	$\overline{T}$	$\boldsymbol{\Delta \overline{T}}$	$\boldsymbol{\Delta T}$	$\boldsymbol{TS}$	$\boldsymbol{\Delta TS}$
No PCM	21.12°C	-	4.65°C	195.11	-
H22C22	20.94°C	-0.18°C	4.32°C	190.12	-2.56%
H21C21	20.38°C	-0.73°C	4.84°C	248.13	27.18%

The indices confirm what has been shown in the temperature curves: that H21C21 increases the fluctuations. The changes in TS are 27.18%, which implies quite much more fluctuations. Both PCMs reduces the average mean air temperature $(\Delta \overline{T})$, while H22C22 also managed to reduce the fluctuations. The change in TS was found to be -2.56% when H22C22 was implemented, which is the highest reduction found during this thesis.

Winter simulations

The measured mean air temperatures from the winter simulations can be seen in figure 3.7
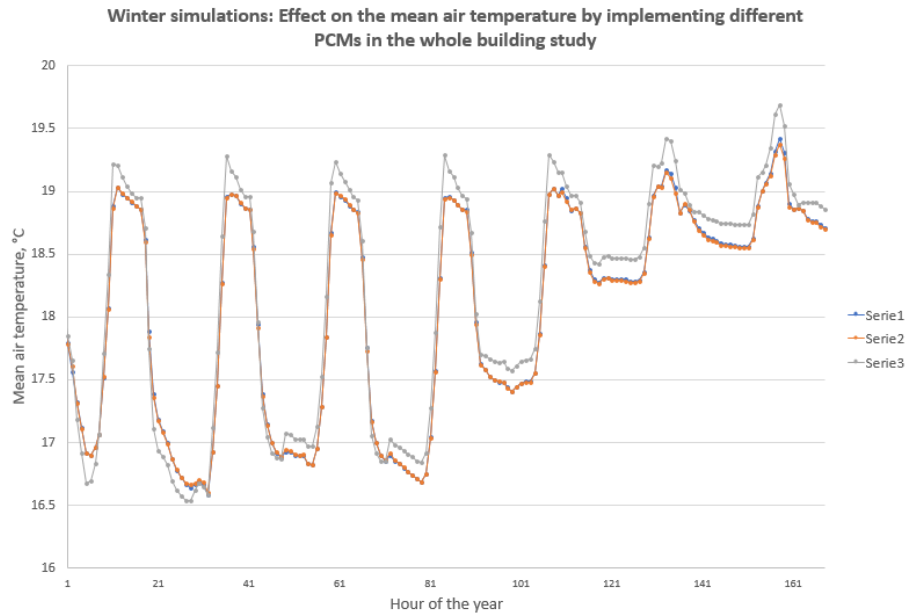
Figure 3.7: Simulation results of how PCM affected the mean air temperature during the winter simulations in the in whole building study

The figure shows that when H22C22 was implemented, the mean air temperature was almost not changed at all, as the lines are overlapping most of the time. H21C21 on the other hand gave increased fluctuations in the beginning of the week, as there are lower temperatures at nighttime and higher temperatures during daytime. In the end of the week, the mean air temperatures for all cases have increased, but there is no clear stabilization effect. Box-plots have been made for these results and are presented in figure 3.8.
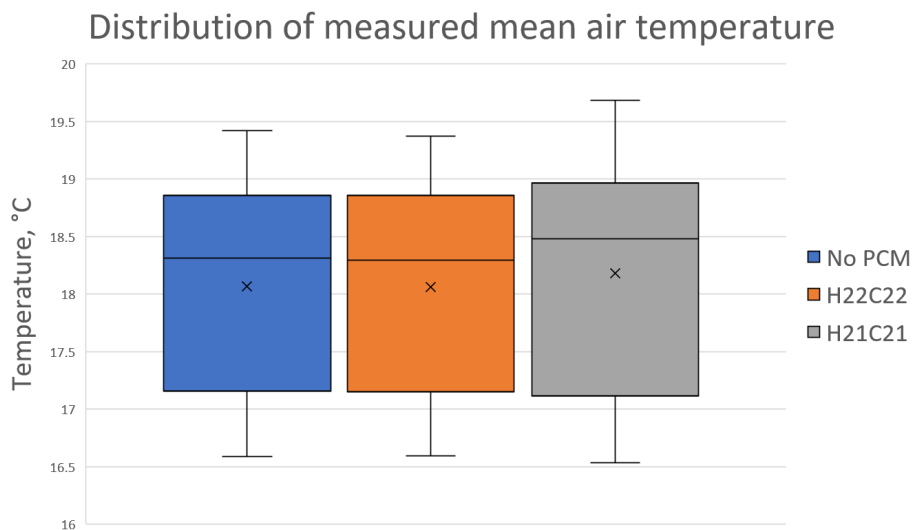
Figure 3.8: Distribution of the measured temperatures during the winter simulations in the whole building case study

The box-plots show that the distribution of temperature is somehow the same for the

case with H22C22 and the case without PCM. A small reduction of the maximum values can be seen, but the results are quite similar. When looking at the distribution of the mean air temperature from the case with H21C21, one can see that the fluctuations are increased. For quantification, the indices for the results are shown in table 3.4. The indices show a lower effect than for the summer simulations. The implementation of H22C22 reduces TS with 0.55%, while H21C21 increased TS with 7.74%.

Table 3.4: Effect on the mean air temperature from the winter simulation in the whole building study

PCM	$\overline{T}$	$\Delta\overline{T}$	ΔT	TS	ΔTS
No PCM	18.07°C	-	2.83°C	132.45	-
H22C22	18.06°C	-0.01°C	2.78°C	131.72	-0.55%
H21C21	18.18°C	0.12°C	3.15°C	142.71	7.74%

Whole year simulations

The results for the total energy consumption for all three cases can be seen in table 3.5.

Table 3.5: Delivered energy results from the yearly simulations

Parameter	Without PCM	H22C22	H21C21
Heating units			
Upper part	36 867.3 kWh	36 114.4 kWh	36 338.0 kWh
Lower part	35 588.9 kWh	35 579.2 kWh	35 464.3 kWh
Air handling unit			
Heating	126 745.0 kWh	126 754.0 kWh	126 689.0 kWh
Cooling	179 983.0 kWh	179 560.0 kWh	179 757.0 kWh
Humidification	184 512.0 kWh	184 083.0 kWh	184 279.0 kWh
Fans	39 195.0 kWh	39 195.0 kWh	39 195.0 kWh
Total energy	602 891.2 kWh	601 285.6 kWh	601 732.4 kWh
Total change	-	-1 605.6 kWh	-1 158.8 kWh
Percentage change	-	-0.27%	-0.19%
Specific energy	236.2 kWh/m^2	235.5 kWh/m^2	235.7 kWh/m^2

The results presented in table 3.5 shows that both PCMs managed to reduce the delivered energy to the exhibition room. The highest reduction is from the imple-

mentation of H22C22, where the total energy consumption was reduced by 1605.6 kWh, a reduction of 0.27%.

The results for peak energy demand (in figure 3.6) shows no reduction in either electric cooling or HVAC aux. The results for fuel heating shows a reduction of 0.06% when H22C22 was implemented, and a reduction of 0.26% with H21C21. It is important to remember that this is the reduction for the entire museum, and not the "Gokstad" exhibition room alone. When relating these results to the energy consumption presented in table 3.5, one can see that H22C22 managed to reduce the energy consumption the most, while H21C21 managed to reduce the peak energy demand the most.

Table 3.6: Peak energy demand from the yearly simulations

Parameter	Without PCM	H22C22	H21C21
Electric cooling	114.7 kW	114.7 kW	114.7 kW
Change	-	0%	0%
HVAC aux	127.7 kW	127.7 kW	127.7 kW
Change	-	0%	0%
Fuel heating	651.9 kW	651.5 kW	650.2 kW
Change	-	-0.06%	-0.26%

When looking further into how the PCM has been behaving throughout the year, the total enthalpy can be presented. Notice that it is the fluctuation of enthalpy that implies that the PCM has been active (i.e. absorbed and released energy). The enthalpy of H22C22 can be seen in figure 3.9.
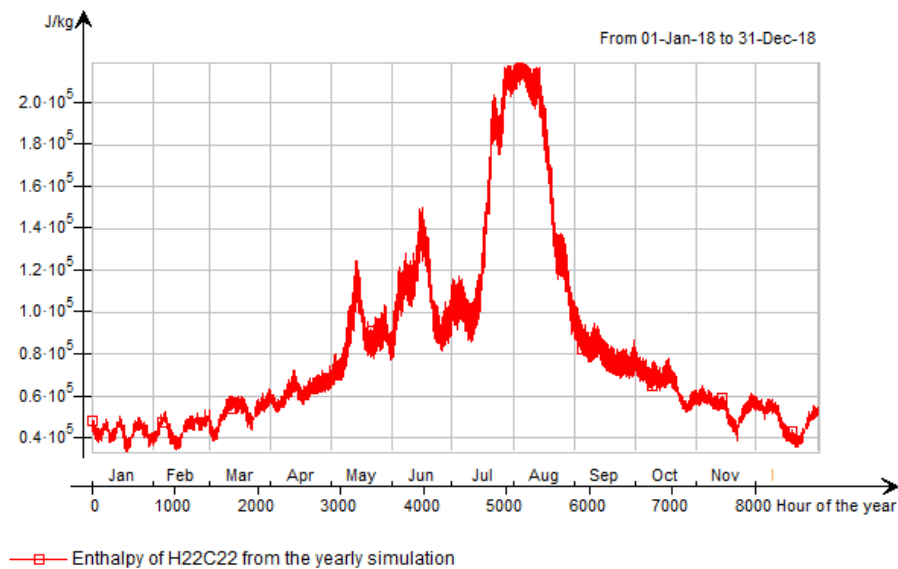
Figure 3.9: Results of the enthalpy of H22C22 from the whole building case study

81

The results in figure 3.9 shows that the enthalpy of H22C22 during the whole year simulation are fluctuating most during the early summer (May/June). One can see that the PCM only absorbs a limited amount of energy during the winter, and that the PCM does not release the energy around July/August. The results were exported with a time step of 1 hour, and the change of enthalpy during one day (24 hours) was found. During 24 hours, the highest change of enthalpy was found at July 19th to be 28.40 kJ/kg, which is 15.5% of the total enthalpy in the PCM. The average change was at 11.09 kJ/kg, which is 6.1% of the potential. The potential change in enthalpy for the PCM is 183 kJ/kg.

The enthalpy of H21C21 during the whole year simulation can be seen in figure 3.10.
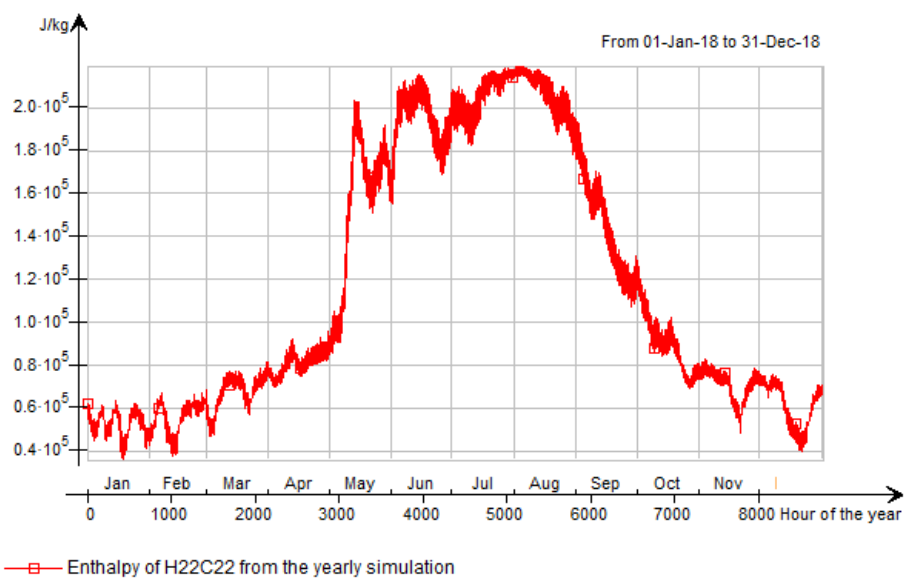
Figure 3.10: Results of the enthalpy of H21C21 from the whole building case study

Figure 3.10 shows that H21C21 stores the energy over a longer period in the summer than H22C22. The PCM is melting (i.e. absorbing energy) in May but does not solidify again before September/October. There are some more fluctuations in the winter for H21C21 than H22C22, but as for H22C22, the potential of the PCM is only used through parts of the year. When looking at the change of enthalpy during one day (24 hours), it was found an average of 11.07 kJ/kg, which is 6.0% of the potential of 183 kJ/kg. The highest change of enthalpy within 24 hours was found May 10th to be 29.28 kJ/kg, which is 16.0% of the potential of the PCM.

The results presented in this chapter shows that the PCMs are both storing and releasing energy. It can be seen some effect on the indoor environment, energy consumption and peak energy demand after the implementation of PCM. These results will be discussed further in chapter 4

4 — Discussion

4.1 Brief

In this chapter, the results from the validation, single zone study and the whole building case study are presented. The discussion is divided in to three parts, in order to discuss the three research questions developed for this thesis

1. Does IDA ICE provide valid models for simulating the effects of moisture buffering and PCM?

2. Can moisture buffering and PCM improve the indoor environment in the Viking Ship Museum?

3. Can moisture buffering and PCM reduce the total energy consumption and peak energy demands for HVAC in the Viking Ship Museum?

4.2 Validation

The validation described and carried out in this thesis has been done in order to evaluate whether IDA ICE provides valid models for simulating moisture buffering and PCM. The results, discussion and conclusion of the validation test have been important to understand whether the moisture buffering and PCM could be investigated further for the museum. This has been presented in chapter 2.2 and 2.3. In order to prevent repetition of the discussion presented earlier, this chapter will discuss a more overall outcome of the validation, instead of the validation tests in details.

HMwall model

Even if a model has been proven to be valid through tests and simulations, there can be limitations of the validity. The HMwall model was shown to be valid in some cases, but not for all. EQUA found it to be valid for "mineral materials", which implies that some simulation of the museum could have been carried out. The concrete shell of the museum could potentially have been simulated to investigate the potential moisture buffering effect. The main reason for not carry out such

simulations were due to the low moisture buffering effect found from the simulations of concrete alone. In addition, when simulating materials as insulation, the HMwall model had to be given information about the material that made no sense for the material. This does not invalidate the model in itself but gives the user a feeling that the software handles the material in a wrong way.

PCM model

The PCM model in IDA ICE was through the validation by Cornaro et al. (2017) and the hot box simulations carried out in this thesis found to be valid in both cases. One of the biggest uncertainties when simulating PCM is how to handle the hysteresis. When the PCM stays between the heating and cooling curves, the PCM tends to both melt and solidify at the same time. This makes it necessary to make some simplifications in the models. IDA ICE uses a constant heat capacity in their models, which implies the program handles the PCM to neither melt or solidify at all in this state. In the validation by Cornaro et al. (2017), PCM with hysteresis was used, and the results was proven to be accurate. Even though this implies validity, the temperature in the tested boxes fluctuated with about 30°C within 24 hours. With such high temperature fluctuations, the PCM will constantly be absorbing or releasing energy, and the PCM will not stay between the heating and cooling curves. There are no reasons, based on these results, to invalidate how the PCM model in IDA ICE handles hysteresis, but there are neither any models for now that validates how it is handled.

4.3   Stabilization effect

The stabilization effect of moisture buffering and PCM on the indoor environment can be discussed based on three different simulations carried out in this thesis. As the HMwall model was found invalid for simulations of the Viking Ship Museum with insulation, only the moisture buffering validation test can be used for discussion of moisture buffering. For PCM, the single zone study in chapter 2.4 and the whole building case study in chapter 2.5 can be discussed.

Moisture buffering

All of the results from the moisture buffering validation test showed some impact on the RH when taking moisture buffer into account, but the effect was low. As

described in figure 1.11 in chapter 1.3.1, concrete is not a building material that absorb and release a lot of moisture, compared to for instance spruce boards. Even so, it was assumed that the impact on the indoor environment was higher. None of the simulated cases showed significant changes of either RH fluctuations, RH_{max} or RH_{min}. In Rebecca Lundqvist's thesis, she also found comparable results when she implemented the HMwall model. Similarities between Lundqvist's results and the results found in this thesis are not enough to verify the users and both users could potentially do the same blunders when making the models. Even so, the model made for the study was built by guidance of a similar model received from EQUA, so there should not be any reason to doubt that the HMwall model is implemented correctly. The material parameters were found from Masea, n.d., which provides parameters for WUFI and is a trusted source of information.

PCM

The single zone case study of PCM showed that when PCM was implemented in a model with constant HVAC systems, it was possible to achieve some effect on the indoor environment. The PCMs managed to reduce the average mean air temperature with 0.64-1.22°C, but the fluctuations increased for all cases. This effect is related to the conductivity of the material. All of the PCMs are implemented internally on the concrete, i.e. the implementation results in less exposed concrete. The concrete implemented in IDA ICE had a conductivity of 1.7 W/mK, while the PCM had a conductivity of 0.6 W/mK. This implies that the heat is transferred faster into concrete than into PCM. As a result, small fluctuations in the mean air temperature will be absorbed faster by concrete than PCM.

When looking at the whole building case study, it was expected that the implementation of PCM had a lower effect on the average mean air temperature than in the single zone test. The HVAC systems were now sensor-controlled, so there were other parameters than the PCM in itself that affected the results. This can be illustrated as in figure 4.1. By implementing a ventilation system that is not sensor controlled, the grey line in figure 4.1 could be achieved, even though the temperature in the zone is far below the set point for max temperatures. If the ventilation system was sensor controlled, the effect from the ventilation system would be adjusted to just lower the temperature to be right below the set point temperature.

The effect on the average mean air temperature by implementing PCM was lower in the whole building case study than for the single zone case study, but H22C22 managed to reduce the fluctuations in the zone. None of the PCMs managed to achieve this effect in the single zone case study, but H22C22 managed to do it for

Illustration of how PCM and ventilation interfere

Legend:
- No PCM or ventilation
- With PCM, no ventilation
- With PCM and CAV ventilation
- Setpoint maximum temperature
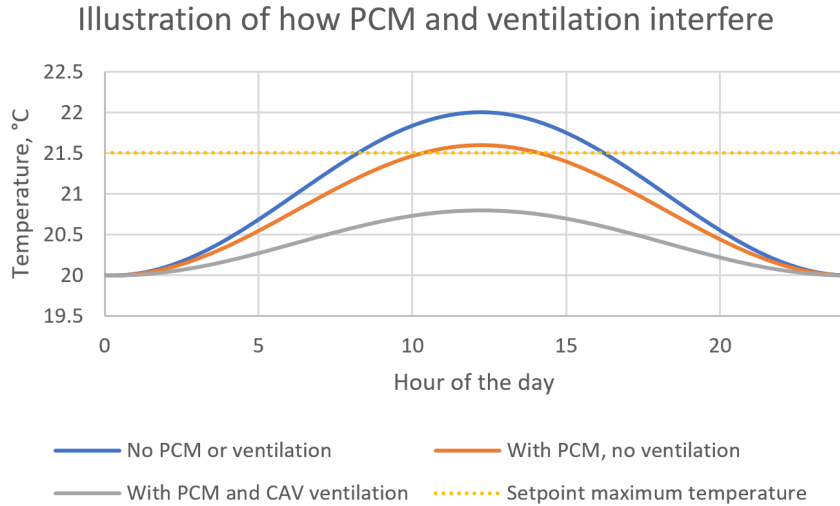
Figure 4.1: Illustration of how PCM and ventilation interfere

both the summer and winter simulation. The reduction of TS was found to be 2.56%. H21C21 on the other hand increased the fluctuations both for the summer and winter simulation. As described in chapter 1.3.2, Goia et al. (2013) stated that wrong selection of melting points could affect the comfort in a negative way. The results found in the whole building case study confirms this statement.

When looking at the enthalpy of the PCMs during the whole year simulations in the whole building case study, one could see that the potential of the PCM was not used. Ideally, the PCMs should store a great amount of heat during the day when the temperature within the zone is high, and then release the energy when the temperature drops. Theoretically, the PCMs can store and release 183 kJ/kg, but none of the PCMs was near using this potential on a daily basis. The highest change of enthalpy during 24 hours for H22C22 was found to be 28.40 kJ/kg, which is only 15.5% of the potential. Similarly, H21C21 had a change of enthalpy of 29.28 kJ/kg during 24 hours, which is 16% of the potential of 183 kJ/kg. As an average, both PCMs had a daily change of enthalpy at about 6% of the potential. As described in chapter 1.3.2, Evola et al. (2013) found that the PCMs they tested used 45% of the potential. The results found in this thesis are even lower. An important difference between the study by Evola et al. (2013) and the case study in this thesis is the thermal conductivity of the PCM used. Evola et al. (2013) used a PCM with a conductivity of 2.7 W/mK, which is very high compared to conductivity described by for instance Jelle and Kalnæs (2017). The PCM used in the case study in this thesis had a conductivity of 0.6 W/mK, which also is high compared to what has described by Jelle and Kalnæs (2017), but much lower than 2.7 W/mK

There are several factors that can have affected why the effect from the implemen-

tation of PCM was so low.

1. The average temperature is much higher in the summer than in the winter

   – This makes the melting points of the PCM hard to adjust. It was seen from the enthalpy of H22C22 that the enthalpy of the layer was low during the whole winter. As a result, the PCM only melts in parts of the year.

2. The temperature fluctuations within the PCM are lower than the mean air temperature

   – Even though the mean air temperature fluctuates several degrees during 24 hours, the temperature within the PCM only fluctuates few degrees. The result is a lower use of the potential in the PCM layer.

3. The building without PCM has a lot of thermal mass in concrete

   – The PCM has from other studies shown to have a greater impact on light weight buildings. In this study, PCM has been compared to a heavy weight concrete building with high thermal mass. The high thermal mass from concrete stabilize the temperature fluctuations, so the effect from PCM is lower.

4. PCM has a lower conductivity than concrete

   – The implementation of PCM results in less exposed concrete. As concrete both has high thermal mass and high thermal conductivity (compared to PCM), it manages to respond faster than PCM to small changes in the mean air temperature.

5. High ventilation rate

   – Even though the ventilation rate of $6m^3/m^2$ is as described in NS3031 for historical buildings, the mean air temperature is highly dependent on the temperature of the ventilated air. If the PCM was implemented in a model with VAV ventilation, the reduction could possibly be higher. With high ventilation at all time (as for CAV systems), the temperature in the ventilated air will affect the mean air temperature in a large extend.

4.4 Energy consumption and peak energy demand

As the HMwall model was not investigated further, there are no results in this thesis that gives reason to discuss the moisture buffering effect on the energy consumption

and peak energy demand. The effect from implementing PCM on the energy consumption and peak energy demand can be discussed based on the results from the whole building case study.

The energy consumption is highly dependent on the indoor environment. If the PCM had managed to stabilize the indoor environment in a great extent, it would probably be reflected on the energy consumption. Many of the topics discussed in chapter 4.3 are therefore also relevant when discussing the energy consumption. This will not be repeated here.

As mentioned earlier, the ventilation system was not dimensioned completely when this study was carried out. The results found in this thesis is therefore not a final answer to how PCM can affect the energy consumption and peak energy demand in the Viking Ship Museum. Changes in the temperature, changes in the heating or cooling systems, changes in the ventilation system or night time cooling are some of the factors that will affect the effect of PCM. Based on the temperatures and the HVAC systems used in the model, it can be seen from the results that the energy consumption was reduced by less than 1% when PCM was implemented.

As described in chapter 1.3.2, Han and Taylor (2016) found a reduction of the energy consumption from 1.3-17.0% when PCM was added internally on a wall existed of gypsum, lightweight concrete, insulation and brick. In difference to the case study carried out in this thesis, the PCM was implemented on gypsum instead of heavyweight concrete. Concrete has a higher heat capacity than gypsum, i.e. the building had a higher thermal mass. It is therefore considered as reasonable that the implementation of PCM in this thesis had a lower impact than in the study by Han and Taylor (2016). Becker (2014) on the other hand found no improvement on the energy consumption by implementing PCM in a heavyweight building. Even though the reduction of the energy consumption in the Viking Ship Museum is low by implementing PCM, there has been found some effect.

When looking at the peak energy demand for the entire building, a reduction of 0.06% was found from the implementation of H22C22, and a reduction of 0.26% with H21C21. As mentioned earlier, this is the peak energy demand for the entire building, and not for the "Gokstad" exhibition room alone. As described in chapter 1.3.2, Halford and Boehm (2007) found a reduction of the peak cooling load of 11-15% in a heavy weight building by implementing PCM. The results found in this thesis showed no effect on the peak effect for cooling, as the reduction was found for heating.

5 — Conclusion

As presented in chapter 1.4, there are three research questions to be answered in this conclusion.

Does IDA ICE provide valid models for simulating the effects of moisture buffering and PCM?

IDA-ICE has developed models for simulating both moisture buffering (i.e. HMwall model) and PCM (i.e. PCM model). During the validations presented in this thesis, a conclusion for the validity has been made. Both from the validation of the HMwall model by EQUA AB and the validation carried out in this thesis, the HMwall model was found to only be valid when simulating mineral materials as concrete. The PCM model on the other hand was both by Cornaro et al. (2017) and the validation carried out in this thesis found to be valid.

Can moisture buffering and PCM improve the indoor environment in the Viking Ship Museum?

As the HMwall model was found invalid for simulating building components with other materials than concrete, the study of how moisture buffering can improve the indoor environment has not been carried out. During the validation of the HMwall model, the concrete walls was shown to only give a small dampening effect, but this has as mentioned not been investigated further.

Both from the single zone study and for the whole building case study, the PCM was shown to give some stabilization effect of the indoor environment. Due to the high thermal mass in the Viking Ship Museum, the additional stabilization effect of implementing PCM is low. The PCM implemented had low thermal conductivity compared to concrete and as a result, the daily fluctuations of the mean air temperature was not absorbed fast enough in the PCM. The simulated PCMs only used about 6% of the potential of the latent heat when looking at the energy absorbed and released during 24 hours. As a conclusion, the implementation of PCM in the "Gokstad" exhibition room has limited improvement the environment in the zone.

Can moisture buffering and PCM reduce the total energy consumption and peak energy demands for HVAC in the Viking Ship Museum?

From the whole building case study, the energy consumption was shown to be slightly reduced when implementing PCM. The reduction of the energy consumption for the HVAC systems was less than 1% for the "Gokstad" exhibition room, which are comparable to the results from Becker (2014). Becker (2014) found no reduction in the energy consumption by implementing PCM boards in a heavyweight building.

As the ventilation systems were all connected to the same boiler, it was not possible to find the peak energy demand for the "Gokstad" exhibition room alone. Even so, it was shown a small reduction in the peak energy demand for "fuel heating" when the whole building was investigated. The highest reduction for "fuel heating" was found to be as low as 0.26% for the PCMs implemented. Based on other research, as Halford and Boehm (2007), the reduction in peak energy demand found in this thesis is low.

As a conclusion, the implementation of PCM in the "Gokstad" exhibition room has almost no improvement on the energy use and peak energy demand.

6 — Further Work

The results presented in this thesis have focused in a great extent on how IDA ICE handles moisture buffering and PCM. As the HMwall model was found to have limitations in the validity, another software should be selected in order to investigate the potential of moisture buffering. The PCM model was found valid in this study, but there has still not been any validation of how the PCM model handles the hysteresis of PCM.

The PCM implemented in the Viking Ship Museum was implemented internally on the concrete surfaces and the results showed that the PCM does not use its potential. Further work should look into implementing PCM in surfaces with higher temperature fluctuations. This could for instance be in solar exposed surfaces, which reaches a higher temperature during daytime. There are several commercialized products that could have been investigated, as for instance GLASSX glazing systems.

There are several other techniques than moisture buffering and PCM that could have a greater impact on the indoor environment. This thesis has not been focusing on other techniques than the two mentioned, but new technologies as smart windows or ventilated double skin facades could for instance been investigated. EQUA has a built-in model for the ventilated double skin facade and are currently working on an add-in for simulating smart windows (e.g. electrochromic or photochromic). Both of these technologies could have an impact on the indoor environment, energy consumption and peak energy demand.

References

Abadie, Marc Olivier and Kátia Cordeiro Mendonça (2009). "Moisture performance of building materials: From material characterization to building simulation using the Moisture Buffer Value concept". In: *Building and Environment* 44.2, pp. 388–401. ISSN: 0360-1323. DOI: https://doi.org/10.1016/j.buildenv.2008.03.015. URL: http://www.sciencedirect.com/science/article/pii/S0360132308000528.

ASHRAE (2017). *ASHRAE Terminology*. webpage.

ASHRAE Technical Committee 9.8, Cecily M. et al. (2010). "Chapter 21 ASHRAE Handbook Applications 2007: Museums, Galleries, Archives and Libraries". In: American Society of Heating, Refrigerating and Air-Conditioning Engineers, Inc. Chap. 21, p. 23.

ASHRAE, Inc. (2017). *19.7 Model Calibration*. URL: https://app.knovel.com/hotlink/khtml/id:kt011GGJW1/ashrae-handbook-fundamentals/model-calibration.

Becker, Rachel (2014). "Improving thermal and energy performance of buildings in summer with internal phase change materials". In: *Journal of Building Physics* 37.3, pp. 296–324.

Bluyssen, Philomena M (2009). *The indoor environment handbook : how to make buildings healthy and comfortable*. eng. London ; Earthscan. ISBN: 9781849774611.

Britannica (n.d.). *Latent heat*. https://www.britannica.com/science/latent-heat. (Accessed on 12/13/2017).

Cao, Sunliang (2010). "State of the art thermal energy storage, solutions for high performance buildings". MA thesis. University of Jyväskylä.

Cao, Sunliang et al. (2010). "The effect of wall-integrated phase change material panels on the indoor air and wall temperature–hot box experiments". In: *Zero Emission Buildings*, pp. 15–26.

Cornaro, Cristina et al. (2017). "Validation of a PCM simulation tool in IDA ICE dynamic building simulation software using experimental data from Solar Test Boxes". In:

EQUA Simulation AB (n.d.[a]). "HMWALL model – Description and validation". Word-document received by email from EQUA.

– (n.d.[b]). *IDA ICE - Simulation Software*. https://www.equa.se/en/ida-ice. (Accessed on 05/07/2018).

European Commission (2014). *Taking stock of the Europe 2020 strategy for smart, sustainable and inclusive growth*. webdocument.

Eurostat (2017). *Europe 2020 indicators - climate change and energy.* webpage.

Evola, G., L. Marletta, and F. Sicurella (2013). "A methodology for investigating the effectiveness of PCM wallboards for summer thermal comfort in buildings". In: *Building and Environment* 59, pp. 517–527. ISSN: 0360-1323. DOI: https://doi.org/10.1016/j.buildenv.2012.09.021. URL: http://www.sciencedirect.com/science/article/pii/S0360132312002636.

Fleischer, Amy S. (2015). *Thermal energy storage using phase change materials : fundamentals and applications.* eng. SpringerBriefs in Thermal Engineering and Applied Science. Springer. ISBN: 3-319-20922-1.

Garathun, Mare Gisvold (2014). *Byggenæringen satser minst på forskning og utvikling.* https://www.tu.no/artikler/byggenaeringen-satser-minst-pa-forskning-og-utvikling/230277. (Accessed on 03/12/2018).

Geving, Stig (2017). "Evaluation of hygrothermal simulation results". NTNU presentation in course TBA4166.

GLASSX AG (2005). *GLASSXcrystal.* http://glassx.ch/fileadmin/_migrated/content_uploads/GLASSX_AG_products_e.pdf. (Accessed on 05/07/2018).

– (n.d.[a]). *GLASSX AG - References.* http://glassx.ch/index.php?id=571. (Accessed on 05/07/2018).

– (n.d.[b]). *GLASSX - phase change glazing in German TV (english subtitles).* https://www.youtube.com/watch?v=LGJCv8ZBb4A. (Accessed on 05/07/2018).

Goia, Francesco, Marco Perino, and Valentina Serra (2013). "Improving thermal comfort conditions by means of PCM glazing systems". In: *Energy and Buildings* 60, pp. 442–452. ISSN: 0378-7788. DOI: https://doi.org/10.1016/j.enbuild.2013.01.029. URL: http://www.sciencedirect.com/science/article/pii/S0378778813000601.

Halford, C.K. and R.F. Boehm (2007). "Modeling of phase change material peak load shifting". In: *Energy and Buildings* 39.3, pp. 298–305. ISSN: 0378-7788. DOI: https://doi.org/10.1016/j.enbuild.2006.07.005. URL: http://www.sciencedirect.com/science/article/pii/S0378778806001939.

Han, Yilong and John E. Taylor (2016). "Simulating the Inter-Building Effect on energy consumption from embedding phase change materials in building envelopes". In: *Sustainable Cities and Society* 27, pp. 287–295. ISSN: 2210-6707. DOI: https://doi.org/10.1016/j.scs.2016.03.001. URL: http://www.sciencedirect.com/science/article/pii/S2210670716300324.

Jelle, Bjørn Petter and Simen Edsjø Kalnæs (2017). "Cost-effective energy-efficient building retrofitting : materials, technologies, optimization and case studies". eng. In: ed. by Fernando Pacheco-Torgal et al. Woodhead Publishing series in civil and structural engineering. Woodheat Publishing. Chap. 3, pp. 57–118. ISBN: 0-08-101227-6.

Kalnæs, Simen Edsjø and Bjørn Petter Jelle (2015). "Phase change materials and products for building applications: A state-of-the-art review and future research opportunities". In: *Energy and Buildings* 94, pp. 150–176. ISSN: 0378-7788. DOI: https://doi.org/10.1016/j.enbuild.2015.02.023. URL: http://www.sciencedirect.com/science/article/pii/S0378778815001188.

Krus, M. and K. Sedlbauer (2008). *Mold Growth Prediction by Computational Simulation*. webdocument.

Künzel, Hartwig M (1995). "Simultaneous heat and moisture transport in building components". In: *One-and two-dimensional calculation using simple parameters. IRB-Verlag Stuttgart*.

Lundqvist, Rebecca Celine (2018). "Investigation of stabilizing the indoor environment using building technologies - A case study: Viking Age museum in Norway". eng. MA thesis. URL: http://hdl.handle.net/11250/2492003.

Masea (n.d.). *Materialdatensammlung für die energetische Altbausanierung*. webpage. URL: http://www.masea-ensan.de/.

OECD/IEA (2015). *Energy Technology Perspectives 2015*. eng. Paris: OECD Publishing ; International Energy Agency. ISBN: 9789264233423. URL: http://site.ebrary.com/id/11071758.

Pawar, Amit (n.d.). *Global Phase Change Materials Market by Product Category, Application and Specification, Forecast to 2022*. http://newshawktime.com/global-phase-change-materials-market-by-product-category-application-and-specification-forecast-to-2022/. (Accessed on 05/07/2018).

Peukuri, R (2003). "Moisture dunamics in building envelopes". PhD thesis. Techical University of Denmark.

Rathod, Manish K. and Jyotirmay Banerjee (2013). "Thermal stability of phase change materials used in latent heat energy storage systems: A review". In: *Renewable and Sustainable Energy Reviews* 18, pp. 246–258. ISSN: 1364-0321. DOI: https://doi.org/10.1016/j.rser.2012.10.022. URL: http://www.sciencedirect.com/science/article/pii/S1364032112005643.

Reardon, Chris (2013). *Thermal mass — YourHome*. http://www.yourhome.gov.au/passive-design/thermal-mass. (Accessed on 01/23/2018).

Rode, Carsten et al. (2005). *Moisture buffering of building materials*.

Rubitherm Technologies GmbH (n.d.[a]). *Data Sheet SP24E*. https://www.rubitherm.eu/media/products/datasheets/Techdata_-SP24E_EN_02062016.PDF. (Accessed on 05/01/2018).

– (n.d.[b]). *Data sheet SP26E*. https://www.rubitherm.eu/media/products/datasheets/Techdata_-SP26E_EN_02062016.PDF. (Accessed on 05/09/2018).

– (n.d.[c]). *PCM SP-LINE*. https://www.rubitherm.eu/en/index.php/productcategory/anorganische-pcm-sp. (Accessed on 05/08/2018).

– (n.d.[d]). *Products.* https://www.rubitherm.eu/en/productCategories.html. (Accessed on 05/08/2018).

Schröder, J and K Gawron (1981). "Latent heat storage". In: *International Journal of Energy Research* 5.2, pp. 103–109.

SINTEF Byggforsk (2005). *Byggforskserien 421.132 - Solstrålingsdata for energi- og effektberegninger.* webdocument.

Souayfane, Farah, Farouk Fardoun, and Pascal-Henry Biwole (2016). "Phase change materials (PCM) for cooling applications in buildings: A review". In: *Energy and Buildings* 129, pp. 396–431. ISSN: 0378-7788. DOI: https://doi.org/10.1016/j.enbuild.2016.04.006. URL: http://www.sciencedirect.com/science/article/pii/S0378778816302419.

Standard Norge (2007). *NS-EN 15026:2007 Hygrothermal performance of building components and building elements - Assessment of moisture transfer by numerical simulation.* (Accessed on 05/07/2018). URL: http://www.standard.no/no/Nettbutikk/produktkatalogen/Produktpresentasjon/?ProductID=626361.

– (2012). *NS-EN ISO 13788:2012: Hygrothermal performance of building components and building elements - Internal surface temperature to avoid critical surface humidity and interstitial condensation - Calculation methods.* (Accessed on 05/07/2018). URL: http://www.standard.no/no/Nettbutikk/produktkatalogen/Produktpresentasjon/?ProductID=626361.

Statsbygg (2017). *Vikingtidsmuseet, utvidelse og nybygg.* http://www.statsbygg.no/Prosjekter-og-eiendommer/Byggeprosjekter/Vikingtidsmuseet/. (Accessed on 01/31/2018).

– (n.d.). *Vikingtidsmuseet, utvidelse og nybygg.* http://www.statsbygg.no/Prosjekter-og-eiendommer/Byggeprosjekter/Vikingtidsmuseet/. (Accessed on 05/06/2018).

Tate (2016). *tate-ecocore-brochure-2016-web_0.pdf.* http://tateinc.com/sites/default/files/support-docs/tate-ecocore-brochure-2016-web_0.pdf. (Accessed on 03/13/2018).

Thomson, Garry (1986). *The museum environment.* eng. 2nd ed. Butterworth-Heinemann series in conservation and museology. London: Butterworth-Heinemann in association with the International Institute for Conservation of Historic and Artistic Works. ISBN: 0750612665.

Thue, Jan Vincent (2014). *Bygningsfysikk - grunnlag.*

UiO (n.d.[a]). *Om Vikingskipshuset.* http://www.khm.uio.no/om/tall-og-fakta/om-bygningene/vikingskipshuset.html. (Accessed on 05/06/2018).

– (n.d.[b]). *Tal og fakta.* http://www.khm.uio.no/om/tall-og-fakta/. (Accessed on 05/06/2018).

– (n.d.[c]). *The Viking Ship Museum.* http://www.khm.uio.no/besok-oss/vikingskipshuset/. (Accessed on 01/31/2018).

Zhu, Na, Zhenjun Ma, and Shengwei Wang (2009). "Dynamic characteristics and energy performance of buildings using phase change materials: A review". In: *Energy Conversion and Management* 50.12, pp. 3169–3181. ISSN: 0196-8904. DOI: https://doi.org/10.1016/j.enconman.2009.08.019. URL: http://www.sciencedirect.com/science/article/pii/S0196890409003239.